THE UNIVERSITY OF CALGARY

# Tectonic Evolution of the Precambrian Basement and Structural Analysis of the Western Canada Sedimentary Basin in Southern Alberta, From Seismic Reflection and Potential-Field Studies.

by

Sophie Lemieux, B.Sc.

A THESIS

SUBMITTED TO THE FACULTY OF GRADUATE STUDIES

IN PARTIAL FULFILLMENT OF THE REQUIREMENTS FOR THE

DEGREE OF MASTER OF SCIENCE

DEPARTMENT OF GEOLOGY AND GEOPHYSICS

CALGARY, ALBERTA

JANUARY, 2000

© Sophie Lemieux 2000

National Library of Canada
Acquisitions and Bibliographic Services
395 Wellington Street
Ottawa ON K1A 0N4
Canada

Bibliothèque nationale du Canada
Acquisitions et services bibliographiques
395, rue Wellington
Ottawa ON K1A 0N4
Canada

*Your file Votre référence*

*Our file Notre référence*

The author has granted a non-exclusive licence allowing the National Library of Canada to reproduce, loan, distribute or sell copies of this thesis in microform, paper or electronic formats.

L'auteur a accordé une licence non exclusive permettant à la Bibliothèque nationale du Canada de reproduire, prêter, distribuer ou vendre des copies de cette thèse sous la forme de microfiche/film, de reproduction sur papier ou sur format électronique.

The author retains ownership of the copyright in this thesis. Neither the thesis nor substantial extracts from it may be printed or otherwise reproduced without the author's permission.

L'auteur conserve la propriété du droit d'auteur qui protège cette thèse. Ni la thèse ni des extraits substantiels de celle-ci ne doivent être imprimés ou autrement reproduits sans son autorisation.

0-612-49633-3

Canada

## ABSTRACT

Deep seismic reflection profiling of the southern Alberta crystalline basement, namely the Archean Medicine Hat Block (MHB), is integrated with potential-field studies (bandpass filtering and gravity modeling) and published geochronological and surface geological data. Integration of these datasets has revealed that the crust is characterized by west- and southwest-dipping reflection fabrics, a layered lower crust and geometric cutoffs that are interpreted to be remnants of two episodes of continental collision in the Late Archean and Early Proterozoic. MHB potential-field fabrics are terminated to the north by anomalies associated with the Early Proterozoic Vulcan structure and to the east by those related to the Early Proterozoic Trans-Hudson orogen. MHB dipping basement fabrics are interpreted to have reactivated and controlled the positions of significant extensional faults within the Western Canada Sedimentary Basin in the Paleozoic and Mesozoic. Late Cretaceous to Paleocene(?) extensional faulting in the Phanerozoic strata occurs as far as 140 km east of the triangle zone and is interpreted to be associated with thrust loading during the Laramide orogeny.

# RÉSUMÉ

Le profil sismique profond du socle cristallin du sud de l'Alberta, nommé le bloc Archéen de Medicine Hat (BMH), a été intégré avec des études sur les champs de potentiel (filtrage de longueur d'onde et modélisation gravimétrique) et des données publiées de géochronologie et de cartes géologiques. L'intégration de ces données a révélé que la croûte terrestre est caractérisée par des réflecteurs à pendage ouest et sud-ouest, une croûte inférieure litée et des recoupements géométriques. Ces observations sont interprétées comme représentant les vestiges de deux périodes distinctes de collision continentale, durant l'Archéen supérieur et le Protérozoïque inférieur. Les fabriques des champs de potentiel du BMH se terminent au nord, le long des anomalies associées avec la structure de Vulcan du Protérozoïque inférieur, et à l'est, par celles associées avec l'orogénie de Trans-Hudson du Protérozoïque inférieur. Les fabriques inclinées du socle du BMH sont interprétées comme ayant réactivé et controllé le positionnement de failles d'extension majeures à l'intérieur du bassin sédimentaire de l'ouest du Canada durant le Paléozoïque et le Mésozoïque. La zone de failles normales du Crétacé supérieur au Paléocène(?) dans les strates Phanérozoïques s'étend jusqu'à 140 km à l'est de la zone triangulaire dans les plaines du sud de l'Alberta. Ce régime extensionnel est interpété comme étant associé avec l'emplacement des chevauchements durant l'orogénèse des Laramides.

Merci beaucoup à Normand Bégin
pour son aide avec la traduction

## ACKNOWLEDGEMENTS

First and foremost, I would like to thank the two people who acted as my supervisors and made this thesis possible, Gerry Ross and Fred Cook. I cannot thank Gerry enough for proposing this project, introducing me to Fred, and most importantly, for his continued support, enthusiasm and tremendous patience. Fred is thanked for his supervision, ideas and for giving me the opportunity to present my work at various conferences. Lithoprobe (NSERC), the Galloway family, the Province of Alberta and the Department of Geology and Geophysics are thanked for providing the funding during my couple of years in graduate school. Thanks to the Lithoprobe staff at the University of Calgary, especially Arie van der Velden, Kevin Hall and Rolf Maier for their patience in explaining the ITA Insight and Geosoft softwares, and for making the computers work. Without their support, I would still be trying to figure it out! Thanks to the software companies that have donated GMA Plus Modelling and QcData to the Department of Geology and Geophysics.

I want to thank my best friend and husband, Michael McDonough, for his tremendous support, love and companionship during the completion of this work. Deb Spratt is greatly thanked for the time she took to discuss basinal structures amongst other things, and for having read meticulously every word of my thesis, which improved it considerably. Arie van der Velden, Kevin Hall, Peter Gretener, Phil Simony, Darcie Greggs and Federico Krause are thanked for their discussions and ideas on various topics. Thanks to Steve Hiebert, Mark Cooper, Hugh Balkwill and Marian Warren who took the time to meet with me and discuss southern Alberta Plains geology.

My family and friends (you know who you are!) are thanked for their continued support, friendship and distractions in moments of stress! Last, but not least, I want to thank our two labradors, Mancha and Moca, for warming my feet and being my best companions while I was writing this thesis at home. They are wonderful creatures!

## TABLE OF CONTENTS


Title Page ..... i
Approval Page ..... ii
Abstract ..... iii
Résumé ..... iv
Acknowledgements ..... v
Table of Contents ..... vi
List of Figures ..... ix
List of Tables ..... xi

**CHAPTER 1. INTRODUCTION** 1
1.1 Introduction: Why southern Alberta as a study area? ..... 1
1.2 Objectives of the research ..... 1
1.3 Data and methods ..... 3
1.3.1 Introduction ..... 3
1.3.2 Seismic reflection data ..... 3
1.3.3 Potential-field data ..... 6
1.3.4 Other geophysical and geological data ..... 8
1.3.5 Methods ..... 9
1.4 Previous crustal and basinal studies in southern Alberta ..... 9
1.5 Basement domains nomenclature of southern Alberta ..... 10

**CHAPTER 2. GEOLOGICAL SETTING OF THE SOUTHERN ALBERTA PLAINS** 12
2.1 Southern Alberta crystalline basement ..... 12
2.1.1 Introduction ..... 12
2.1.2 Archean Medicine Hat Block ..... 12
2.1.3 Vulcan structure and Loverna Block ..... 14
2.1.4 Great Falls Tectonic Zone and Trans-Hudson orogen ..... 14
2.2 Geochronological signatures ..... 15
2.3 Western Canada Sedimentary Basin ..... 17
2.3.1 Stratigraphic and tectonic setting ..... 17
2.3.2 Structure ..... 20

**CHAPTER 3. CRUSTAL STUDIES OF THE MEDICINE HAT BLOCK** 27
3.1 Introduction ..... 27
3.2 Potential-field studies ..... 27
3.2.1 Introduction ..... 27
3.2.2 Wavelength filtering procedures ..... 29
3.2.3 Filtered total-field intensity magnetic maps ..... 32
3.2.4 Filtered Bouguer gravity maps ..... 35
3.2.5 Potential-field interpretations ..... 41
3.3 Internal crustal structure ..... 42
3.3.1 Introduction ..... 42
3.3.2 SALT seismic reflection observations ..... 42
3.3.3 COCORP seismic reflection observations ..... 44
3.3.4 Seismic reflection interpretations ..... 47
3.3.5 Reflection Moho ..... 49
3.3.6 Time-structure maps ..... 50
3.4 Gravity modeling of the Medicine Hat Block crust ..... 51
3.4.1 Introduction ..... 51
3.4.2 Seismic refraction results and densities ..... 53
3.4.3 Crustal density model and interpretations ..... 53

**CHAPTER 4. STRUCTURAL ANALYSIS OF THE WESTERN CANADA SEDIMENTARY BASIN IN SOUTHERN ALBERTA** 57
4.1 Introduction ..... 57
4.2 Regional stratigraphic correlation wells ..... 57
4.3 Seismic reflection observations ..... 59
4.3.1 Introduction ..... 59
4.3.2 Regional stratigraphic trends ..... 67
4.3.3 Basement fabrics ..... 67
4.4 Structural interpretation ..... 70
4.4.1 Seismic reflection expression of fault geometries ..... 70
4.4.2 Extensional faults and forced folding model ..... 79
4.4.3 Fault reactivations ..... 81
4.4.4 Surface expression of extensional faulting ..... 84

4.4.5 Basement influence on basinal structures ..... 85
4.5 Timing of extensional faulting ..... 87
4.6 Mechanisms of extensional faulting and structural inversion ..... 88

**CHAPTER 5. DISCUSSION** **91**
5.1 Relationship between seismic reflection fabrics and magnetic trends ..... 91
5.2 Significance of geochronological and seismic refraction studies to Medicine Hat Block crustal geometry ..... 93
5.3 Role of the Great Falls Tectonic Zone ..... 94
5.4 Tectonic evolution of the southern Alberta basement ..... 95
5.4.1 Introduction ..... 95
5.4.2 Archean ..... 95
5.4.3 Early Proterozoic ..... 95
5.5 Relationship of extensional faulting to Medicine Hat Block ..... 98

**CHAPTER 6. CONCLUSIONS** **100**

**REFERENCES** **102**

## LIST OF FIGURES


1. Regional tectonic setting of the Medicine Hat Block ..... 2
2. Basement domain map of southern Alberta ..... 4
3. Color-shaded magnetic anomaly map of the study area ..... 13
4. Stratigraphic column of southern Alberta Plains ..... 18
5. Geological map of the southern Alberta Plains ..... 21
6. Detailed geological map of the southern Alberta Plains ..... 23
7. Photograph of the Monarch Fault zone, southern Alberta ..... 26
8. Short-wavelength filtered gravity map (400-200/20-10 km) ..... 28
9. Block diagram illustrating a bandpass filter and power spectrum ..... 31
10. Short-wavelength filtered magnetic map (93.3-70/20-15 km) ..... 33
11. Short-wavelength filtered magnetic map (300-150/20-10 km) ..... 34
12. Long-wavelength filtered magnetic map (333.3-200/50-30 km) ..... 36
13. Long-wavelength filtered magnetic map (312.5-250/100-80 km) ..... 37
14. Low-pass filtered gravity map (>10-5 km) ..... 38
15. Long-wavelength filtered gravity map (750-600/200-160 km) ..... 39
16. Long-wavelength filtered gravity map (2000-1000/200-100 km) ..... 40
17. Regional composite SALT seismic reflection profile ..... 43
18. Crustal dipping reflectivity of the Medicine Hat Block ..... 45
19. Composite COCORP seismic reflection profile ..... 46
20. Seismic reflection profile of sill intrusions ..... 48
21. Time-structure maps ..... 52
22. North-south SAREX seismic refraction profile ..... 54
23. Crustal density model of the Medicine Hat Block ..... 55
24. Synthetic seismograms:
    - **(A)** Gulf Blood: 05-18-007-23W4 and Gulf et al. South Blood: 15-12-006-24W4 ..... 60
    - **(B)** Husky et al. Cranford: 16-20-008-18W4 ..... 61
    - **(C)** Home Yellow Lake: 01-36-009-13W4 ..... 62
25. SALT line 30 (VE=3:1) ..... 63
26. SALT line 29 (VE=3:1) ..... 64
27. SALT line 31 (VE=3:1) ..... 65

28. Concatenated shallow seismic reflection profile (VE=20:1) ..... 66
29. Basement structure contour map ..... 68
30. Geometric correlation of basement fabric and extensional fault ..... 69
31. Geometry of compressional Fault 1 ..... 71
32. Fault 1 on SALT line 30 ..... 72
33. Fault 2 on SALT line 30 ..... 73
34. Fault 3 on SALT line 30 ..... 74
35. Fault 4 on SALT line 30 ..... 75
36. Fault 5 on SALT line 31 ..... 76
37. Line diagram interpretation of fault geometries in time ..... 77
38. Schematic diagram of extensional forced folding ..... 80
39. Flattened seismic reflection profile on post-Milk River horizon ..... 82
40. Flattened seismic reflection profile on Livingstone horizon ..... 83
41. Aeromagnetic map of southern Alberta with superposed geology ..... 86
42. Mechanism for inversion of extensional faults ..... 89
43. Photograph of an inverted extensional fault, northwestern Montana ..... 90
44. Schematic block diagram of the Medicine Hat Block crustal structure ..... 92
45. Tectonic evolution model of the Medicine Hat Block crust ..... 96

## LIST OF TABLES


1. Lithoprobe SALT acquisition parameters ..... 6
2. Lithoprobe SALT processing parameters ..... 7
3. Reprocessing parameters for COCORP Montana data ..... 8
4. List of abbreviations ..... 11
5. Precambrian drillcore information ..... 16
6. Bandpass filtering parameters ..... 30
7. Crustal velocities with corresponding densities and lithologies ..... 53
8. Synthetic seismogram calculation and well log information ..... 58

# CHAPTER 1. INTRODUCTION

## 1.1 Introduction: Why southern Alberta as a study area?

The Western Canada Sedimentary Basin (WCSB) was deposited on crystalline rocks of the Canadian Shield after the Shield was assembled through prolonged lithospheric plate interactions in the Precambrian. Although most geological studies of the WCSB in southern Alberta have focused on the ca. 4 to 5 km of Phanerozoic sedimentary rocks of the basin in exploration for hydrocarbons, more than 40 km of cratonic rocks underlie the basinal strata, thus representing a huge (ca. 1 000 000 $km^2$ in Alberta and Saskatchewan alone; Figure 1) area of unexposed Shield. To study the sub-Phanerozoic cratonic rocks, Lithoprobe undertook a multidisciplinary study of the Alberta basement with various geological and geophysical contributions. A key component of this work was the acquisition of high-quality seismic reflection images, some of which are described in this thesis (e.g., Ross et al. 1995; Eaton et al. 1997).

In southern Alberta, the WCSB is underlain by a ca. 100 000 $km^2$ region of Archean granitic rocks, known as the Medicine Hat Block (MHB; Figure 1). The MHB is surrounded by Proterozoic deformed belts on the north and east, and the Mesozoic to Cenozoic Cordillera to the west. The MHB apparently influenced regional stratigraphic and structural patterns of the WCSB in southern Alberta throughout the Phanerozoic, but its internal structure, tectonic history, and relationship to surrounding regions have been largely unknown (Clowes 1997). The purpose of this thesis is to address the tectonic evolution of the Archean MHB, and its impact on the Phanerozoic WCSB of southern Alberta, spanning more than three billion years of geological history.

## 1.2 Objectives of the research

This research addresses questions and problems concerning the tectonic relationship between the MHB crust and adjacent crustal domains, and the possible influence of Precambrian basement structures on Phanerozoic structural and stratigraphic patterns of the WCSB. Two primary objectives of this research include: (1) establishing the internal structures and the three-dimensional crustal geometry of the MHB and to relate these structures to adjacent crustal domains of the buried western Canadian Shield; and (2) investigating the regional stratigraphic trends and structures of the WCSB in southern Alberta and how they are affected by the deep basement

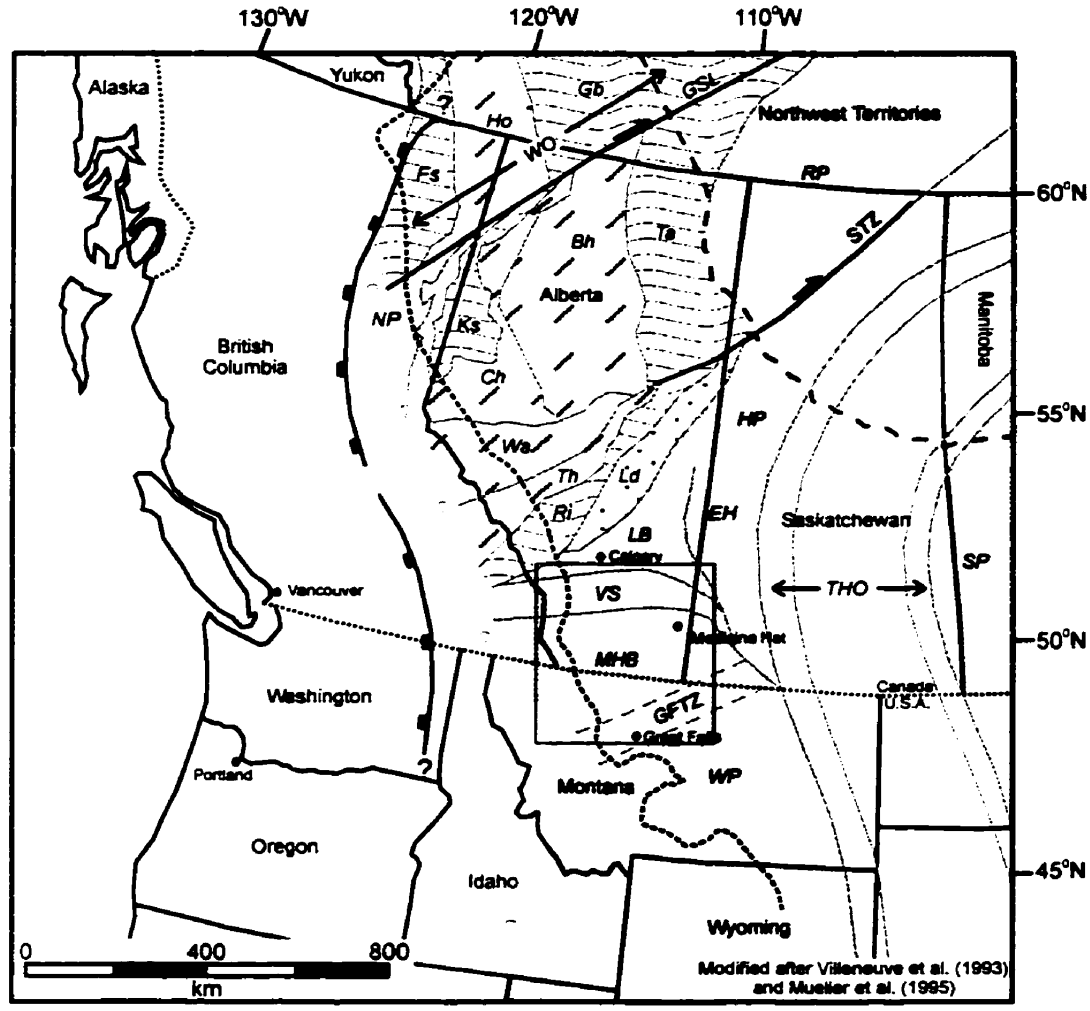


Archean provinces
HP: Hearne Province
MHB: Medicine Hat Block: study area
LB: Loverna Block
VS: Vulcan structure
EH: Eyehill High
WP: Wyoming Province
RP: Rae Province
SP: Superior Province
NP: Nova Province

2.0-1.8 Ga magmatic arcs
Ta: Taltson
Gb: Great Bear
Ri: Rimbey
Ks: Ksituan
Fs: Fort Simpson

GFTZ: Great Falls Tectonic Zone
THO: Paleoproterozoic Trans-Hudson orogen
WO: Paleoproterozoic Wopmay orogen

2.4-2.0 Ga accreted terranes
Ho: Hottah
Bh: Buffalo Head
Wa: Wabamun
Th: Thorsby
Ch: Chinchaga

Proterozoic metasedimentary terrane
Ld: Lacombe Domain

Exposed Precambrian Canadian Shield to east
Phanerozoic WCSB cover to west

Approximate eastern limit of Cordilleran deformation

West-facing Proterozoic crustal-scale ramp: reactivated in Mesozoic (Cook et al. 1991)

GSL: Paleoproterozoic Great Slave Lake Shear Zone
STZ: Paleoproterozoic Snowbird Tectonic Zone

Figure 1. Regional tectonic setting of the Archean MHB showing western North America basement domains with associated orogens, shear zones and tectonic zones (Villeneuve et al. 1993). Inset box illustrates location of Figure 2.

structures. Accordingly, this research leads to a better understanding of the geological processes involved in the continental assembly of the southern Alberta crust during the Precambrian, as well as, the influence that basement reactivation had on Phanerozoic sedimentary deposition.

## 1.3 Data and methods

### 1.3.1 Introduction

The principal data used in this research consist of Lithoprobe deep seismic reflection lines along a regional west-east transect that crosses the southern Alberta Plains from the eastern Foothills near Pincher Creek to approximately 24 km southwest of Medicine Hat (Figure 2). The seismic reflection images provide geometric constraints on the MHB crust, and establish a framework for the interpretation of other geophysical (potential-field and seismic refraction) and geological (geochronological) data presented in this study.

### 1.3.2 Seismic reflection data

The Lithoprobe Southern Alberta Lithospheric Transect (SALT) lines 29, 30 and 31 link to form a 287-km regional Vibroseis east-west transect recorded in 1995 to 18 s two-way time (twt), about 60 km depth for an average crustal velocity of 6.6 km/s (Buryanik et al. 1997). Two east-west lines (lines 30 and 31; 110 km and 140 km long, respectively) and an intersecting north-south line (line 29; 40 km long) provide regional coverage over an area of 15 000 $km^2$ with limited three-dimensional control (Figure 2). The data were recorded with a linear 20 s sweep from 10 to 80 Hz and a 12 s listening time. A group interval of 25 m (CDP interval of 12.5 m) and a 2 ms sample rate were used to allow high spatial resolution of shallow targets and 480 channels were deployed over a symmetrical split spread 12 km long. The migrated SALT lines were coherency filtered (this study) and plotted at the Lithoprobe Seismic Processing Facility at the University of Calgary. The Lithoprobe SALT dataset was acquired in summer 1995 by Pioneer Exploration Inc. on the behalf of Lithoprobe, the Geological Survey of Canada and eight industry partners, and the data were processed by Pulsonic Geophysical Ltd. A summary of the acquisition and processing parameters used for the SALT 95 survey is described in Tables 1 and 2.

Figure 2. (next page) Map of the tectonic domains of southern Alberta and northern Montana showing extent of Archean MHB and location of various data used in this research including: regional Lithoprobe SALT seismic reflection lines and COCORP seismic reflection Montana lines 3 and 4, stratigraphic correlation wells (S1 to S4), crustal xenolith sample sites, projection of dated drillcores penetrating the crystalline basement, and the regional SAREX seismic refraction line. The SALT seismic reflection dataset is located entirely within the MHB and extends from the Foothills of southwestern Alberta to the southeastern Alberta Plains. Projection information: (1) basement drillcores: W1: ~64 km to southeast; W2: ~31 km to southeast; W3: ~67 km to southeast; W4: ~33 km to southeast onto the eastern continuation of line 31; W5 is not projected as the north-trending linear magnetic fabrics are terminated to the north at the northwest-trending linear magnetic anomalies in this region (see Figure 3 in Chapter 2); and (2) xenolith sample sites: between 75 km to 105 km to northwest.

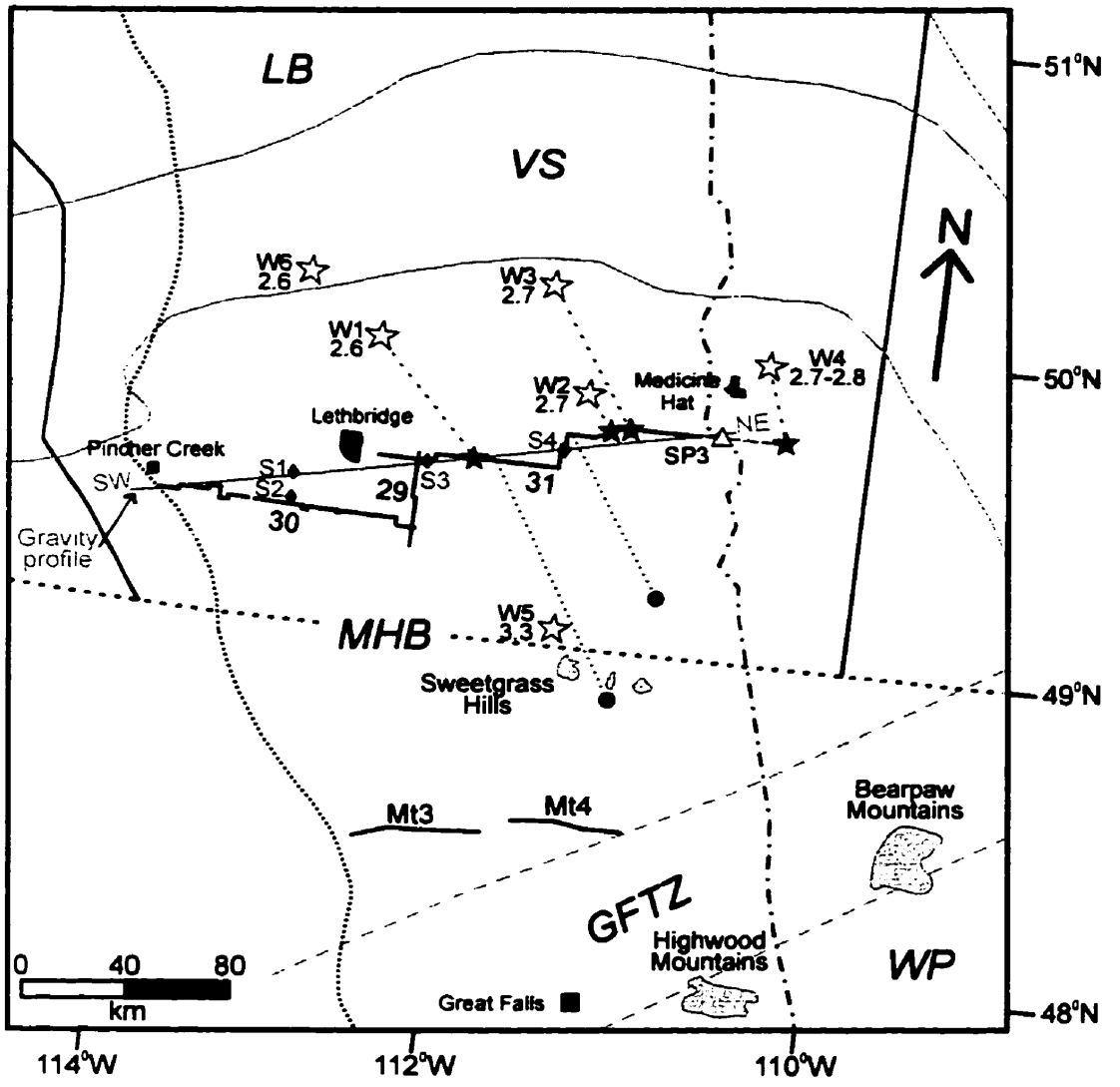


Basement domains:

- **LB** Loverna Block
- **VS** Vulcan structure
- **MHB** Medicine Hat Block
- **GFTZ** Great Falls Tectonic Zone
- **WP** Wyoming Province

\# Lithoprobe SALT seismic reflection lines

Mt COCORP Montana seismic reflection lines

SAREX/Deep Probe seismic refraction survey line (Buryanik et al. 1997; Henstock et al. 1998)

● Crustal xenolith sampling sites (Davis et al. 1995) projected along linear magnetic fabric of the Medicine Hat Block

☆ Dated drillcores penetrating the Precambrian basement: W1 to W6 (Villeneuve et al. 1993), U-Pb ages are in Ga

★ Projected drillcores onto seismic reflection lines along linear magnetic fabric of the Medicine Hat Block: W1 to W4

◆ Stratigraphic correlation wells: Synthetic seismograms S1 to S4

△ SP3: Shotpoint 3 on SAREX refraction line (Buryanik et al. 1997)

| ACQUISITION PARAMETERS | |
|---|---|
| Station interval | 25 m |
| Source type | Vibroseis |
| Source interval | 100 m |
| Receiver interval | 25 m |
| CDP interval (trace spacing) | 12.5 m |
| Number of CDP traces | 3239 (line 29); 8512 (line 30); 11169 (line 31) |
| Sample rate | 0.002 s |
| Number of channels per shot record | 480 plus 2 auxilaries that carry the sweep trace |
| Sweep frequency | 10 to 80 Hz linear |
| Sweep length | 20 s |
| Recording time (uncorrelated) | 32 s |
| Listening time | 12 s |
| Spread type: symmetric split spread | Traces: 1 240 241 480<br>Distance: 6050m 75m X 75m 6050m |
| Far offset | 6125 m |
| Fold | 60 |
| Format | SEGY |

Table 1. Lithoprobe SALT acquisition parameters (Eaton and Ross 1996).

The Consortium for Continental Reflection Profiling (COCORP) coherency filtered CDP stacks of Vibroseis Montana lines 3 and 4 were obtained by the Lithoprobe Seismic Reflection Facility at the University of Calgary, where they were subsequently reprocessed in order to improve crustal images (Table 3). The COCORP data consist of a 94-km west-east transect that cover the southern portion of the MHB (Figure 2), and were recorded to 16 s twt or about 53 km depth assuming an average crustal velocity of 6.6 km/s. The COCORP data were recorded with a linear 26 s sweep from 12 to 48 Hz and a 42 s listening time. A group interval of 100 m (CDP interval of 50 m) and a 8 ms sample rate were used, and 96 channels were deployed over a split spread of 9.6 km, resulting in less resolution compared to the Lithoprobe data.

### 1.3.3 Potential-field data

The potential-field data used in this research consist of 2-km gridded total-field intensity magnetic and 2-km gridded Bouguer gravity data that were obtained from the National Geophysical Database of the Geological Survey of Canada. The potential-field data extend from eastern British Columbia into Manitoba ($120^{0}$W to $100^{0}$W) and from

| PROCESSING PARAMETERS (from contractor) | |
|---|---|
| **Operations** | **Parameters** |
| Correlation | 18 s correlated trace length |
| Amplitude recovery | 500 ms AGC |
| Crooked line geometry | |
| Refraction statics | Two-layer solution: datum = 1200 m; weathering velocity = 610 m/s; replacement velocity = 2700 m/s |
| Deconvolution | Frequency domain, multiple design window, amplitude and phase spectrum prewhitening, zero-phase output |
| Spectral balance | Frequency domain, multi-gate design and application, zero-phase |
| Trace balance | Whole trace (single gate) |
| CDP gather | Using crooked line geometry |
| Velocity analysis | Interactive coherency spectra, every 120 CDP's (1.5 km) |
| Residual statics | Automatic surface-consistent statics, 300-3000 ms window (shallow resolution), maximum static = 20 ms |
| Normal moveout | |
| Mute | Offset (m): 195, 200, 1800, 6075, 12150<br>Time (ms): 0, 550, 1200, 4500, 7000 |
| CDP stack | 60 fold |
| Noise attenuation | Fx deconvolution with 30% addback |
| Bandpass filter | Zero-phase, frequency domain: 5-10-80-95 (0-2 s); 10-15-40-50 (3-5 s); 5-10-40-50 (6-12 s); 5-10-30-40 (16-18 s) |
| Migration | Wave equation ($45^0$ finite-difference algorithm) with 100% stacking velocities |
| Scaling | Multiple gate balance (0-3 s, 3-6 s, 6-18 s) |
| **PROCESSING PARAMETERS (this study)** | |
| **Operations** | **Parameters** |
| Decimation | 1/3 of traces kept; write one trace, skip two traces; trace spacing = 37.5 m |
| Coherency filter | Window size: 15 traces; aperture = 500 m; maximum slope = 8 ms/trace |
| Bias | Amplitude threshold: -200%; window 0-18 s |
| Plotting | Rasterize biased sections, variable area without wiggles, positive amplitudes only |

Table 2. Lithoprobe SALT processing parameters (from contractor; Eaton and Ross 1996; and this study).

central Alberta into Idaho and Wyoming ($52^0$N to $44^0$N). Data coverage was extended beyond the MHB in order to examine the potential-field relationship between the MHB anomalies and the surrounding basement regions.

| REPROCESSING PARAMETERS | |
|---|---|
| **Operations** | **Parameters** |
| Tape read | Reading SEGY unmigrated coherency filtered CDP stacks into IT&A |
| Tie Montana lines 3 and 4 | Number of traces: 1035 (line 3); 848 (line 4) with 400 traces between the lines and 500 traces padded at each end; trace spacing = 50 m |
| Coherency filter | Window size: 10 traces; aperture = 500 m; maximum slope = 13 ms/trace |
| Migration | Phase shift (time) migration; constant velocity = 5000 m/s; maximum frequency: 50 Hz at 0 s, 50 Hz at 4 s, 50 Hz at 16 s; maximum aperture: $90^0$ |
| Coherency filter | Window size: 10 traces; aperture = 500 m; maximum slope = 13 ms/trace |
| Bias | Amplitude threshold: -225%; window 0-16 s |
| Plotting | Rasterize biased sections, variable area without wiggles, positive amplitudes only |

Table 3. Reprocessing parameters for COCORP data.

### 1.3.4 Other geophysical and geological data

Other data are used in this study in conjunction with the seismic reflection and potential-field data. They include: (1) Deep Probe/SAREX seismic refraction data extending north-south across the eastern portion of the MHB (Buryanik et al. 1997; Henstock et al. 1998); (2) geochronological data from five petroleum industry drillcores penetrating the top portion of the Precambrian basement in southern Alberta (Villeneuve et al. 1993); (3) geochronological and geothermobarometric data for crustal xenoliths in Eocene dykes and sills from the Sweetgrass area of southern Alberta and northern Montana (Davis et al. 1995); (4) four stratigraphic correlation wells, from which synthetic seismograms were calculated in GMA Plus Modelling software; and (5) surface geological maps of the southern Alberta Plains (Irish 1967; Lebel 1996; Okulitch et al. 1996) acquired from the Geological Survey of Canada. Structure contour maps on the top of the Oldman River Formation are also used to determine regional Phanerozoic structural patterns of southern Alberta (Russell and Landes 1940). Magnetotelluric (electromagnetic) data were acquired for the most part in central Alberta (Boerner et al. 1995) and across the Great Falls Tectonic Zone (Boerner et al. 1998) with little to no emphasis on the MHB.

### 1.3.5 Methods

The crustal study of the southern Alberta basement consists mainly of the interpretation of new seismic reflection data to determine the internal structure of the MHB and the construction of time-structure maps from reasonably continuous crustal surfaces to resolve the three-dimensional crustal geometry. Analysis of potential-field data, especially wavelength filtering of total-field intensity magnetic and Bouguer gravity data, is conducted to extract long and short wavelength anomalies and to determine any relationships between potential-field anomaly trends and basement seismic reflection trends (Ulrych 1968; Hartman et al. 1971; Dobrin 1976; Kane and Godson 1985; Dobrin and Savit 1988). Seismic refraction data constrain the Mohorovicic (Moho) discontinuity depth and establish a crustal density model. Geochronological data (isotopic ages of rocks in drillcores penetrating the Precambrian basement and ages and geothermobarometry of xenoliths) provide age constraints on tectono-metamorphic events and timing of tectonic events involving the MHB.

The study of the Phanerozoic WCSB primarily includes the interpretation of the shallow portion (first 3 s twt) of the seismic reflection data to: (1) determine the locations and orientations of major faults; (2) investigate evidence for growth faulting, onlapping features, thinning and thickening patterns of strata; and (3) examine the influence of basement structures on sedimentation patterns. Synthetic seismograms are used to identify formation picks and to constrain ages of faulting and folding. Analysis of total-field magnetic data is conducted to determine any relationship between magnetic anomaly trends with shallow basement structures and faulting in the sedimentary sequence.

## 1.4 Previous crustal and basinal studies in southern Alberta

Previous crustal seismic studies in southern Alberta date back to the late 1960's when the first refraction survey provided the large-scale velocity structure of the southern Alberta crust (Kanasewich et al. 1969; Clowes and Kanasewich 1972). Their interpretation included a high angle offset of the upper crystalline crust and Moho, presently known as the Vulcan structure. A regional seismic reflection survey of the Canadian Rockies in the Crowsnest Pass area showed that the Precambrian basement continues under the thrust belt (Bally et al. 1966). In the 1990's, the Lithoprobe program and various industry partners acquired approximately 2718 km of deep seismic reflection

data in central Alberta, the Peace River Arch area and in southern Alberta, yielding crustal-scale images of the Alberta basement and the Phanerozoic strata (Ross et al. 1995; Eaton et al. 1997).

Geochronological studies of the Alberta basement were initiated in the late 1950's and early 1960's (Burwash 1957; Burwash et al. 1962). In the 1980's, development of high-precision U-Pb dating (Krogh 1982; Roddick et al. 1987) and the geological synthesis work of the exposed Canadian Shield by Hoffman (1988, 1989) have provided a regional kinematic and tectonic framework for the Canadian Shield that can be extended to the crystalline crust beneath the WCSB. Finally, the synthesis work of Ross et al. (1991) and Villeneuve et al. (1993) provided a regional crustal domain map of the Alberta basement based on drillcore dating and potential-field anomaly data.

The first geological studies of the sedimentary basin involved mapping of the southern Alberta Plains by Dawson (1875), Dawson and McConnell (1883), Dowling (1910) and Williams et al. (1930) and a substantial contribution on the stratigraphy and structure of the southern Alberta Plains was published by Russell and Landes (1940). This pioneering work set the stage for the beginning of an intensive search for petroleum in the 1930's (Russell and Landes 1940). More recent mapping of the southern Alberta Plains includes the work of Irish (1967), Lebel (1996) and Okulitch et al. (1996). In the 1980's and early 1990's, Beaumont (1981), Bond and Kominz (1984), Bond and Kominz (1991), Ross (1991) and Beaumont et al. (1993) studied subsidence mechanisms in the evolution of the WCSB throughout the Phanerozoic. Finally, the Geological Atlas of the WCSB (Mossop and Shetsen 1994) provides a complete overview of the Phanerozoic geological history and tectonic evolution of the WCSB.

## 1.5 Basement domains nomenclature of southern Alberta

Maps of the buried Alberta basement domains were constructed by Ross et al. (1991) and Villeneuve et al. (1993) using potential-field signatures (primarily magnetic and horizontal gravity gradient trends) and U-Pb zircon geochronology of samples from drillcores that penetrate into Precambrian crystalline rocks below the WCSB. The basement divisions can only pertain to the upper portion of the Alberta basement as potential-field anomalies outline the domain boundaries and dated samples from each domain establish ages of the rocks near the basement surface (Villeneuve et al. 1993). Some features, such as northeast-trending fault zones (e.g., Snowbird Tectonic Zone),

are correlated to outcrops in the exposed Canadian Shield to the east (Figure 1). Other features (e.g., MHB) are only known from their potential-field and geochronological signatures.

Such basement domain names as MHB, Loverna Block and Fort Simpson terrane imply a structural and tectonic significance to crustal regions that cannot be determined solely on the basis of potential-field analysis and dating of drillcore samples. The word "block" may imply that the southern Alberta basement is surrounded by high-angle faults that separate it from adjacent basement domains. This research will show that, in fact, the MHB is likely continuous to the south, and thus, is part of a larger Archean basement domain including the Wyoming Province. Therefore, in this study, the use of the word "block" does not imply any genetic or tectonic significance, but refers to basement domains defined on their internal geophysical character. Abbreviations used in the potential-field maps are listed in Table 4.

| BASEMENT DOMAINS | |
|---|---|
| LB | Loverna Block |
| EH | Eyehill High |
| VS | Vulcan structure |
| MHB | Medicine Hat Block |
| GFTZ | Great Falls Tectonic Zone |
| THO | Trans-Hudson orogen |
| WP | Wyoming Province |

Table 4. List of abbreviations used in the potential-field maps.

# CHAPTER 2. GEOLOGICAL SETTING OF THE SOUTHERN ALBERTA PLAINS

## 2.1 Southern Alberta crystalline basement

### 2.1.1 Introduction

The present configuration of the North American craton has been interpreted to have formed from accretionary events involving continent-continent and arc-continent collisions, beginning in the Archean (3.2 Ga) and culminating during the Early Proterozoic (~1.8 Ga) [Hoffman 1988; Ross and Stephenson 1989; Ross et al. 1991; Villeneuve et al. 1993]. Available U-Pb zircon and monazite dates recovered from five petroleum industry drillcores penetrating the top portion of the basement indicate that Archean (~2.6 to 3.3 Ga) crystalline basement is present beneath the Western Canada Sedimentary Basin (WCSB) in southern Alberta (Figure 2; Ross et al. 1991; Villeneuve et al. 1993). Because these samples are all Archean granitic gneisses and because they are all located within an aeromagnetically and gravimetrically distinct area, they have been interpreted to represent a coherent region of the Canadian Shield beneath the WCSB. This region is called the Medicine Hat Block (MHB; Ross et al. 1991; Villeneuve et al. 1993).

### 2.1.2 Archean Medicine Hat Block

The MHB is bounded on the east by the Early Proterozoic Trans-Hudson orogen as the MHB potential-field fabrics terminate against potential-field anomalies associated with the Trans-Hudson orogen. On the west, the MHB is buried beneath the Mesozoic and Cenozoic Cordillera. To the north and south, cross-cutting relationships between potential-field fabrics suggest that the MHB is bounded by two crustal discontinuities: (1) the Early Proterozoic Vulcan structure in the north, which forms the southern boundary of the Archean Hearne Province; and (2) the controversial Great Falls Tectonic Zone in the south (Figure 1; O'Neill and Lopez 1985; Villeneuve et al. 1993; Boerner et al. 1998). Recent potential-field and seismic reflection studies have revealed that the MHB may continue across the Great Falls Tectonic Zone into the Wyoming Province to the south (Figure 3), making the Vulcan structure the main Early Proterozoic collisional suture between the Hearne and Wyoming Provinces (Eaton et al. 1999). The magnetic signature of the MHB consists of prominent linear northwest- and north-trending

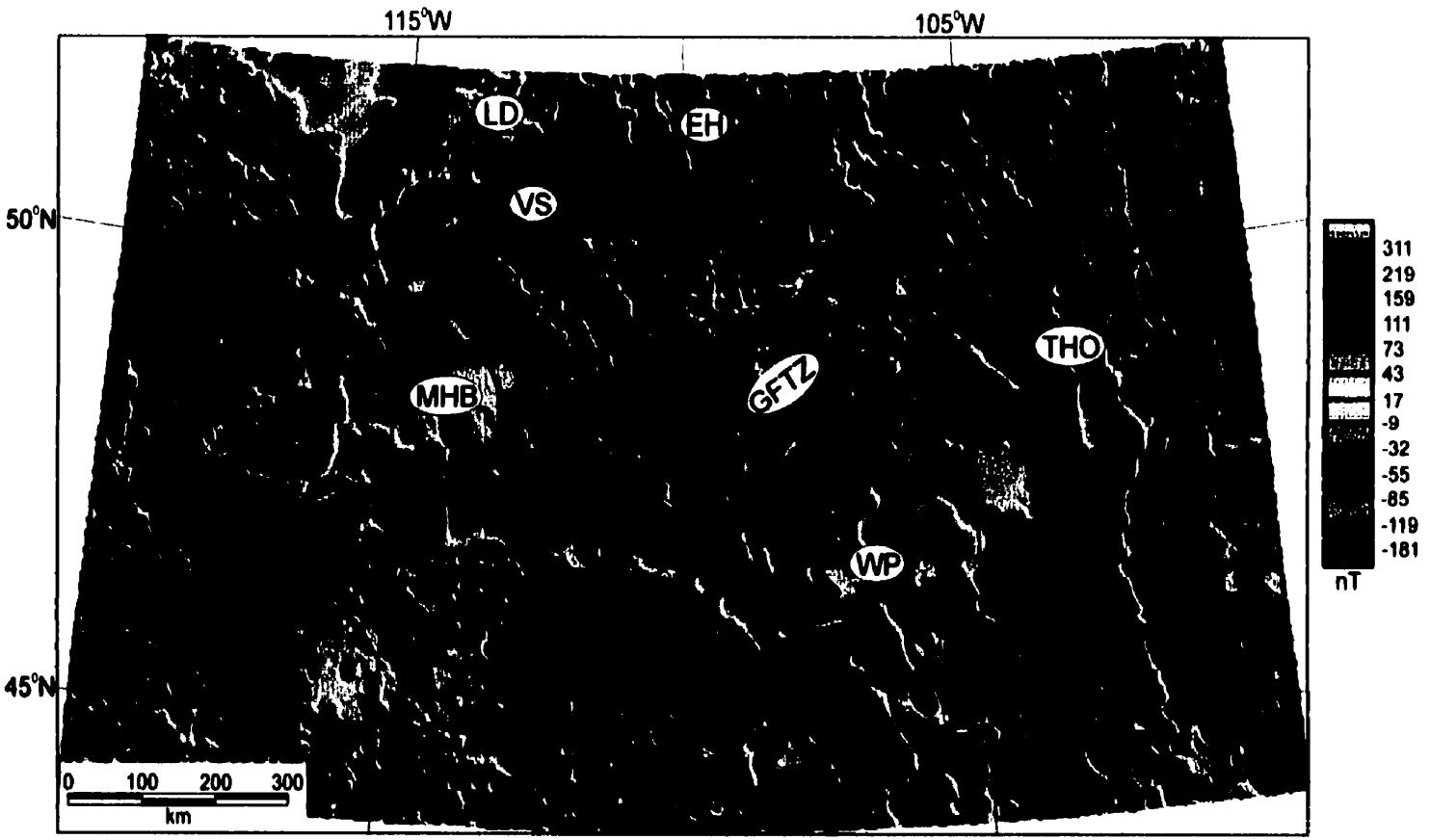


Figure 3. Color-shaded (azimuth = 239°) total-field intensity magnetic anomaly map showing predominant linear northwest- and north-trending fabrics that characterize the MHB. Arrows indicate continuity of MHB magnetic fabrics across the Great Falls Tectonic Zone. Locations of wells penetrating the Precambrian are indicated by stars and locations of xenolith sampling sites are indicated by circles. White lines show projection onto the SALT seismic reflection lines.

anomalies (Figure 3). This study will show that these anomalies can be correlated to crustal-scale northeast- and east-verging features (from geometric relationships observed on seismic reflection data) that are likely associated with significant crustal shortening of the southern Alberta basement in the Late Archean (from geochronological data).

### 2.1.3 Vulcan structure and Loverna Block

The MHB is characterized by linear north- and northwest-trending magnetic anomalies that terminate to the north against anomalies associated with the Vulcan structure (Figure 3). In contrast, the Vulcan structure is characterized by east-trending magnetic and gravity anomalies that extend for approximately 350 km across southern Alberta, separating the Loverna Block from the MHB. The Vulcan structure potential-field anomalies appear to merge with the magnetic fabrics associated with the Trans-Hudson orogen to the east (Figure 2; Villeneuve et al. 1993; Ross 1997).

The Vulcan structure has been variously interpreted using different geophysical datasets as a failed Precambrian rift (Kanasewich et al. 1969; seismic refraction), a collisional suture between the Hearne and Wyoming Provinces (Thomas et al. 1987; potential-field; Hoffman 1988), a north-dipping subduction zone (Ross et al. 1991; seismic reflection) and an intraplate collisional zone (Hoffman 1990). Recently, Eaton et al. (1999) interpreted the Vulcan structure as a relatively narrow (40 to 70 km) axial zone of continental collision that represents the south-dipping Hearne-Wyoming collisional suture, based on seismic reflection and new potential-field studies (gravity modeling across the Vulcan structure). North and east of the Vulcan structure, the Archean and Early Proterozoic Loverna Block and Archean Eyehill High (Figure 3) have preserved west-northwest verging contractional features, interpreted from seismic reflection data (Ross et al. 1995). These contractional features are associated with significant crustal shortening of the central Alberta basement at about 1.78-1.85 Ga, forming the East Alberta orogen (Ross et al. 1995). This deformation may be coeval with shortening in the adjacent Trans-Hudson orogen to the east (Figure 1; Ross et al. 1995).

### 2.1.4 Great Falls Tectonic Zone and Trans-Hudson orogen

The Great Falls Tectonic Zone is defined solely on the basis of surface geological mapping of supracrustal rocks and a correlative basement potential-field

signature. O'Neill and Lopez (1985) named the zone after recognizing a series of northeast-trending high-angle faults and shear zones displacing rocks of middle Proterozoic to early Tertiary age within the Idaho Batholith and adjacent regions in the Cordillera. The zone was then extrapolated to the northeast into the subsurface of Montana and southwestern Saskatchewan on the basis of similar northeast-trending patterns of Late Cretaceous to Early Tertiary dike swarms and igneous intrusions, depositional patterns of Phanerozoic strata, and linear gravity and magnetic anomalies (Figure 1; O'Neill and Lopez 1985).

The Great Falls Tectonic Zone has been considered the tectonic boundary between the Hearne and Wyoming Provinces, as the potential-field fabrics of the MHB and the Wyoming Province appear to terminate along the northeast-trending potential-field fabrics of the Great Falls Tectonic Zone (Figure 3; O'Neill and Lopez 1985; Villeneuve et al. 1993; Boerner et al. 1998). It was first interpreted as the Hearne-Wyoming Proterozoic suture (O'Neill and Lopez 1985), and more recently as a reactivated Archean(?) intracontinental shear zone (Boerner et al. 1998). One of the key elements of any interpretation is the continuity, or lack thereof, of MHB fabrics across the Great Falls Tectonic Zone. Thus, truncation of the MHB anomalies at the Great Falls Tectonic Zone would imply that the Great Falls Tectonic Zone postdates the MHB, and that the MHB and Wyoming Province were not necessarily part of the same tectonic lithosphere. Continuity of anomalies across the Great Falls Tectonic Zone could be interpreted with the MHB and Wyoming Province as tectonically coupled prior to the Great Falls Tectonic Zone. Potential-field studies may be a valuable tool to address this question depending on the extent to which potential-field anomalies can delineate subsurface geological trends. Nevertheless, the Great Falls Tectonic Zone magnetic fabric to the northeast appears to terminate at a high angle to the northwest-trending fabric of the 1.84 to 1.80 Ga western Trans-Hudson orogen (Figure 3). The Early Proterozoic Trans-Hudson orogen is characterized by curvilinear north- and northwest-trending magnetic fabrics that probably include accreted Proterozoic crust within the orogen and deformed Hearne Province crust of the western hinterland (Ross 1997).

## 2.2 Geochronological signatures

The eastern half of the MHB has been cored in five petroleum industry drillholes (Figure 2). U-Pb zircon dating indicates 2.61 to 3.28 Ga (Archean) crystallization ages

(Table 5; Villeneuve et al. 1993). The drillcores were projected onto the seismic reflection lines along the prominent northwest magnetic fabric of the MHB (Figures 2 and 3). To the north, Calstan Parkland sampled the Vulcan structure and gives a ca. 2.1 Ga (Early Proterozoic) titanite age, and a ca. 1.8 K-Ar biotite age from an Archean (2.6 Ga) garnet metabasite, suggesting a metamorphic/thermal event in the Early to Middle Proterozoic (Figure 2; Villeneuve et al. 1993). Sm-Nd isotopic data from selected MHB cores and Late Archean metasedimentary rocks from around the Wyoming Province yield depleted mantle model ages (indicates the time of separation from mantle) of 2.7 to 3.8 Ga. Therefore, extensive continental crust was present in the Wyoming Province and MHB by the Late Archean (Frost 1993; Mueller et al. 1993; Villeneuve et al. 1993; Carlson and Irving 1994).

| Well name | Location | Lithology | U-Pb zircon age |
|---|---|---|---|
| **W1 (MHB)** PCP Travers | 01-31-013-20W4 | Granodiorite gneiss | 2616 +36-23 Ma |
| **W2 (MHB)** BA et al. Grand Forks | 12-14-012-12W4 | Biotite quartz monzonite | 2721 +35-30 Ma |
| **W3 (MHB)** Imperial Calstan Lake Newell | 05-01-017-14W4 | Pegmatitic granitic gneiss | 2715 +41-23 Ma |
| **W4 (MHB)** PCP Medicine Hat | 12-19-014-04W4 | Granodiorite gneiss | 2.7 – 2.8 Ga |
| **W5 (MHB)** Home Pacific Knappen | 16-29-001-11W4 | Quartz diorite | 3278 +22-21 Ma |
| **W6 (VS)** Calstan Parkland | 04-12-015-27W4 | Garnet metabasite | 2627 +4-3 Ma |

Table 5. Precambrian drillcore information (Villeneuve et al. 1993).

In contrast, new U-Pb zircon analyses (1.85 Ga; Mueller et al. 1996) and $^{40}Ar$-$^{39}Ar$ analyses (1.72 Ga; Kovaric et al. 1996) document evidence for widespread Proterozoic thermal events in the Archean rocks of the northwestern Wyoming Province. North of the MHB, the Loverna Block and Rimbey granitic gneisses (Figure 1) give Archean to Early Proterozoic crystallization ages that range from 1.78 to 2.71 Ga (Villeneuve et al. 1993).

Crustal xenoliths entrained in Eocene mafic sills and dykes of the Sweet Grass

Hills igneous complex, some 90 to 115 km south of the seismic reflection transect are of three types: (1) low pressure tonalite gneisses from the upper crust (ca. 5 to 15 km depth), with 2.6 Ga ages (may represent crystallization or metamorphic ages) that correspond to ages and lithologies of the drillcores; (2) high pressure garnet-kyanite paragneisses from the lower crust (12.4 kbar or ~37 km) that have 1.81-1.75 Ga (Early Proterozoic) ages; and (3) high pressure mafic granulites from near the crust-mantle boundary (13.5 kbar or ~41 km) that have slightly younger Early Proterozoic ages of 1.75-1.70 Ga (Davis et al. 1995; Figure 2). The pressure to depth conversion uses an average of 3 kbar/km. The lower metamorphic grade xenoliths (tonalite gneisses) record exclusively Archean ages, but exhibit Proterozoic Pb loss in zircon and titanite, indicating an Early Proterozoic disturbance (Davis et al. 1995). Indeed, the K-Ar ages of the lower crustal rocks of the MHB were extensively reset between 1.85-1.70 Ga, at about the same time as the terminal collisional events in the Trans-Hudson orogen and the East Alberta orogen (Davis et al. 1995; Ross et al. 1995). Considerable Early Proterozoic thermal overprinting of the lower and upper crust is also evident for much of the Wyoming Province crust according to a number of studies throughout Montana (Collerson et al. 1988; Mueller et al. 1993; Davis et al. 1995; Boerner et al. 1998).

## 2.3 Western Canada Sedimentary Basin

### 2.3.1 Stratigraphic and tectonic setting

The WCSB comprises the Phanerozoic sedimentary rocks that overlie the crystalline Precambrian basement of the stable continental interior and extend westward into the Cordillera, where they were deformed from early Jurassic to Paleocene (Bally et al. 1966; Monger 1989). Erosion of the evolving thrust belt caused deposition of latest Jurassic through Tertiary foreland basin fill, forming the youngest strata of the WCSB (Monger 1989). In southern Alberta, seismic reflection data indicate that the WCSB thickens westward from approximately 3.1 to 6.5 km.

Current ideas on the WCSB evolution suggest three distinct phases of basin subsidence and related sedimentation during the Phanerozoic (Figure 4; Bond and Kominz 1984; Bond and Kominz 1991; Ross 1991; Beaumont et al. 1993). The first phase represents superposed rift and passive margin sequences that began in the latest Precambrian and terminated by Devonian time (Ross 1991). Subsidence mechanisms

Figure 4. (next page) Regional schematic stratigraphic column for the southern Alberta Plains, outlining the geological history and basin evolution in southern Alberta (Core Laboratories). Paleozoic strata mainly include carbonate rocks, whereas Mesozoic strata are composed of siliciclastic rocks. Abbreviations within the Cretaceous Colorado Group include: basal Colorado (basal col.); Second White Speckled Sandstone (SWSSS); Second White Speckled Shale (SWSSH); Medicine Hat (Med. Hat.); and First White Speckled Shale (FWSSH).

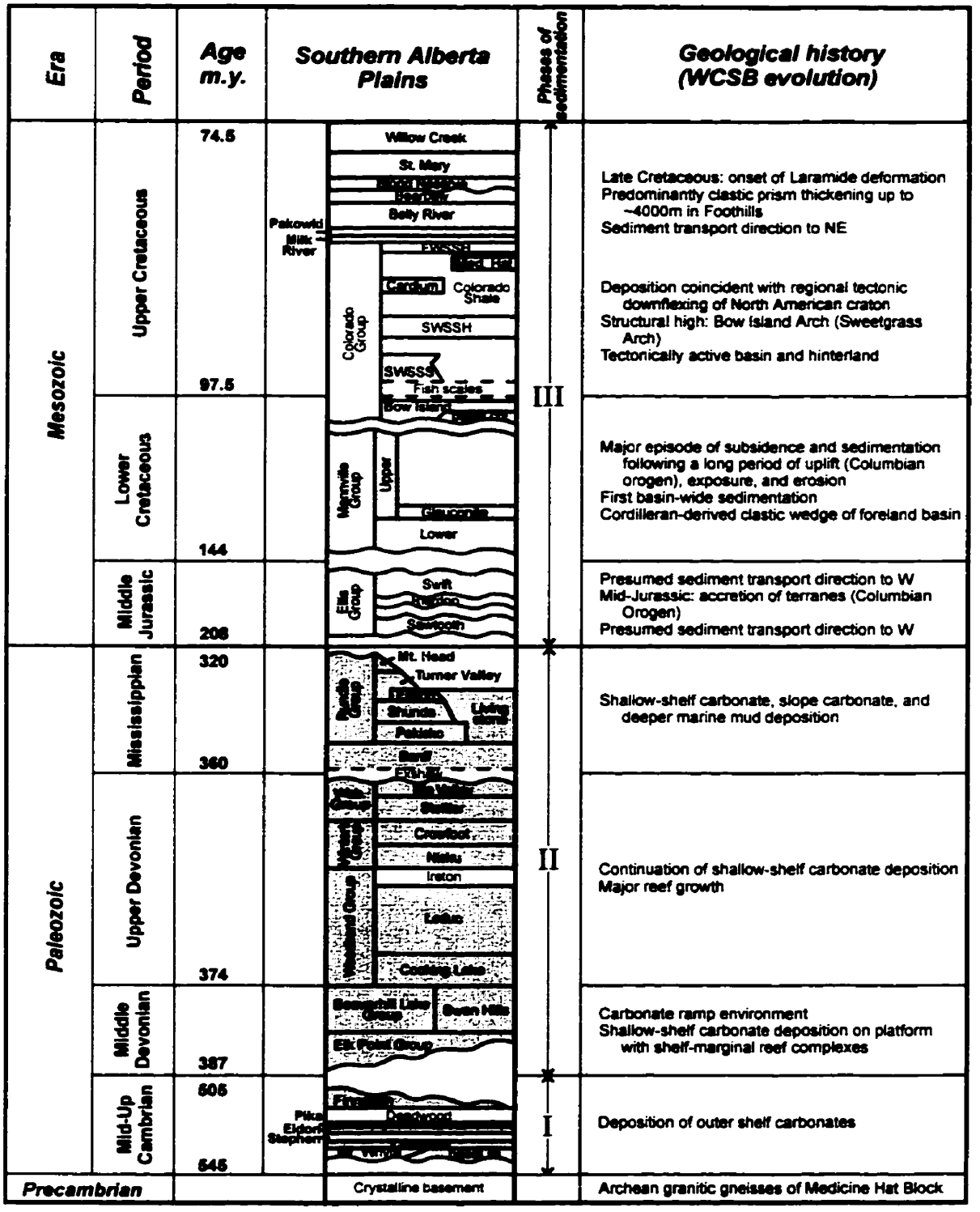
Era
Period
Age m.y.
Southern Alberta Plains
Phases of sedimentation
Geological history (WCSB evolution)
Mesozoic
Upper Cretaceous
74.5
97.5
Willow Creek
St. Mary
Belly River
Pakowki
Milk River
Colorado Group
Cardium
Colorado Shale
SWSSH
Fish scales
Bow Island
Late Cretaceous: onset of Laramide deformation
Predominantly clastic prism thickening up to ~4000m in Foothills
Sediment transport direction to NE
Deposition coincident with regional tectonic downflexing of North American craton
Structural high: Bow Island Arch (Sweetgrass Arch)
Tectonically active basin and hinterland
III
Lower Cretaceous
144
Mannville Group
Upper
Glauconite
Lower
Major episode of subsidence and sedimentation following a long period of uplift (Columbian orogen), exposure, and erosion
First basin-wide sedimentation
Cordilleran-derived clastic wedge of foreland basin
Middle Jurassic
208
Ellis Group
Swift
Rierdon
Sawtooth
Presumed sediment transport direction to W
Mid-Jurassic: accretion of terranes (Columbian Orogen)
Presumed sediment transport direction to W
Paleozoic
Mississippian
320
360
Mt. Head
Turner Valley
Shunda
Pekisko
Banff
Exshaw
Shallow-shelf carbonate, slope carbonate, and deeper marine mud deposition
Upper Devonian
374
Wabamun Group
Cairn
Crossfield
Nisku
Ireton
Leduc
Cooking Lake
Continuation of shallow-shelf carbonate deposition
Major reef growth
II
Middle Devonian
387
Beaverhill Lake Group
Swan Hills
Elk Point Group
Carbonate ramp environment
Shallow-shelf carbonate deposition on platform with shelf-marginal reef complexes
Mid-Up Cambrian
505
545
Pika
Elkton
Stephen
Deadwood
Deposition of outer shelf carbonates
I
Precambrian
Crystaline basement
Archean granitic gneisses of Medicine Hat Block
Shales
Sandstones/siltstones
Carbonates
After Stratigraphic Correlation Chart
Core Laboratories, Calgary

for the second phase of sedimentation from Devonian through Triassic time still are undetermined, as common subsidence mechanisms fail to produce observed subsidence curves (Bond and Kominz 1991; Beaumont et al. 1993). The first two phases of basin subsidence are represented by Paleozoic carbonate strata, and indicate a significant period of carbonate ramp, shallow-shelf carbonate, slope carbonate and reef deposition on the western margin of North America (Phases I and II; Figure 4). The third phase of basin subsidence, from Jurassic to Early Tertiary, was responsible for the creation of the foreland basin and resulted principally from flexural subsidence, related to tectonic loading during orogenic deformation (Beaumont et al. 1993). This last phase of subsidence is represented by Mesozoic to early Cenozoic siliciclastic strata of the Cordilleran-derived clastic wedge (Phase III; Figure 4).

Subsequent to Laramide orogenesis, extension-related magmatism occurred in the Sweetgrass Hills, Bearpaw Mountains and Highwood Mountains of the northern Montana Plains at about 50 to 54 Ma (Figure 2; Leckie 1989). Linear short wavelength, northwest-southeast-trending magnetic anomalies observed on a high-resolution aeromagnetic survey from southern Alberta have been interpreted as Eocene dykes associated with the Sweetgrass Hills intrusions (Figure 5; Ross et al. 1997).

### 2.3.2 Structure

The WCSB in southern Alberta is dominated by three major structural features: the Sweetgrass Arch, the Alberta Syncline, and the Cordilleran deformed belt (Lerand 1983). Near the 49$^{th}$ parallel, the Sweetgrass Arch exposes Upper Cretaceous Pakowki and Milk River strata in its core, and plunges northeastward, exposing Belly River Group strata over a wide area (Figure 5). The western flank of the Sweetgrass Arch is common with the eastern limb of the Alberta Syncline, which has Upper Cretaceous Bearpaw, Blood Reserve, St. Mary, Willow Creek, and Paleocene Porcupine Hills strata exposed in its core (Figure 5; Lerand 1983). Early geological mapping of the southern Alberta Plains revealed that three northwest-striking extensional faults are exposed in the Oldman River near Lethbridge (Townships 8 and 9, Ranges 21 and 22; Figure 6). Each has the southwest side downthrown from 18 to 31 m within strata of the Belly River Group (Russell and Landes 1940).

A series of five faults that disrupted most of the Phanerozoic sedimentary sequence (up into Upper Cretaceous strata) is imaged on the Lithoprobe SALT seismic

Figure 5. (next page) Geological map of the southern Alberta Plains (Lerand 1983) showing the distribution of extensional faults and of inversion structure on the SALT dataset, the Monarch Fault zone north of line 30, subsurface Eocene dykes, and the four stratigraphic correlation wells. Only uppermost Cretaceous and Early Tertiary (Paleocene) strata are present at the surface of the southern Alberta Plains. Inset box illustrates the location of Figure 6.

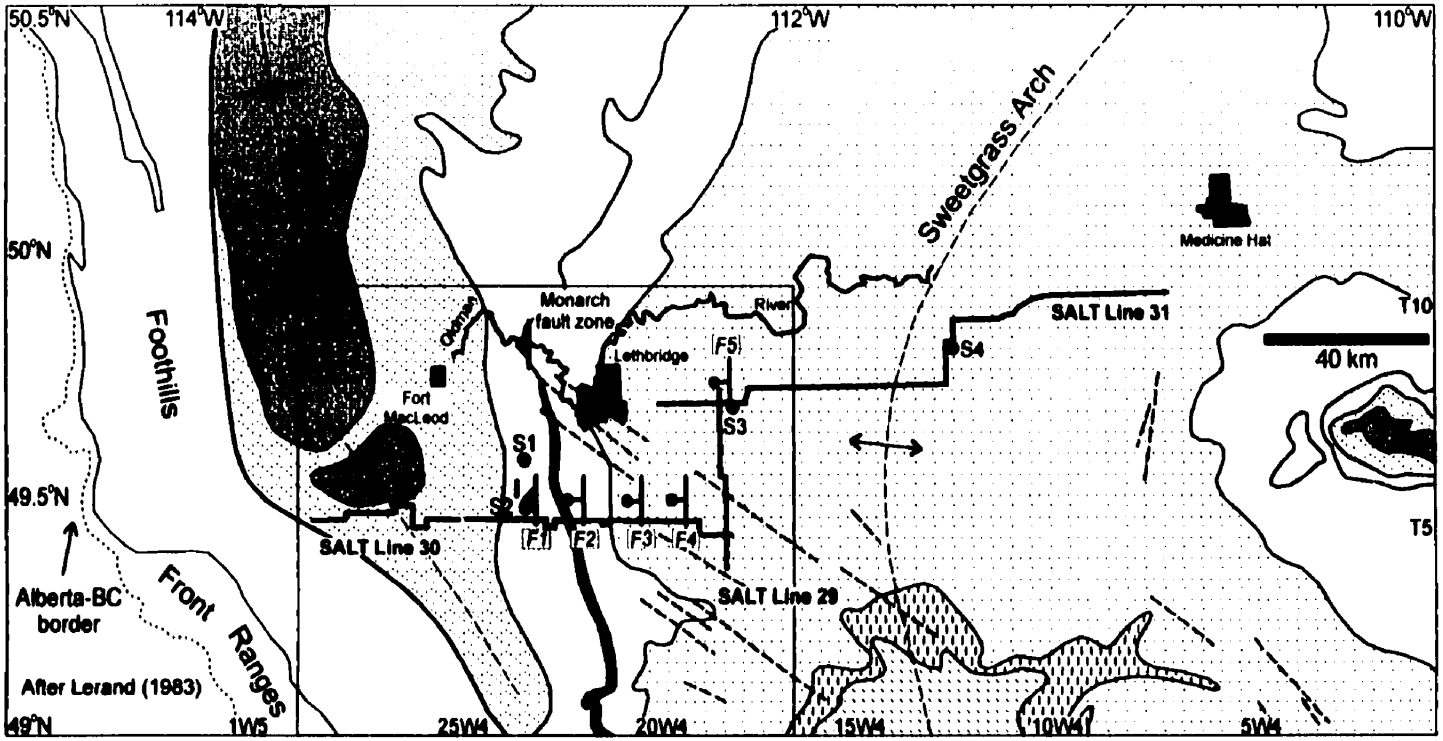


**Paleocene**

- Porcupine Hills Fm: sandstone and mudstone

**Paleocene/Upper Cretaceous**

- Willow Creek Fm: claystone and sandstone

**Upper Cretaceous**

- St. Mary River Fm: calcareous sandstone and mudstone
- Blood Reserve Fm: sandstone
- Bearpaw Fm: shale
- Belly River Gp: sandstone, siltstone, shale, and coal
- Pakowki Fm: shale and sandstone
- Milk River Gp: sandstone, shale, and claystone

- Wells:
  - S1: 05-18-007-23W4 (Gulf Blood)
  - S2: 15-12-006-24W4 (Gulf et al. South Blood)
  - S3: 16-20-008-18W4 (Husky et al. Cranford)
  - S4: 01-36-009-13W4 (Home Yellow Lake)
- Compressional fault
- Compressional fault - inversion structure
- Extensional fault
- Subsurface Eocene dykes (Ross et al. 1997)

Figure 6. (next page) Detailed geological map of southern Alberta (Irish 1967) showing distribution of faults on the SALT dataset (F1 to F5), along the Oldman River (Russell and Landes 1940; Hiebert 1992), east of the Fort MacLeod region (Wright et al. 1994) and from Shell proprietary seismic reflection data. Extensional faults outcropping in the Oldman River within the Lethbridge area offset Upper Cretaceous Belly River Group and Bearpaw Formation strata (Russell and Landes 1940). Fold patterns are taken from structure contour maps on top of the Oldman Formation (Russell and Landes 1940) and surface mapping (Lebel 1996). Dotted lines across faults represent an along-strike extrapolation of extensional faulting. S1 to S3 refer to three of the four wells described in Figures 2 and 5. The regional strike of extensional faulting appears to be northwest-southeast, which corresponds to the trend of magnetic fabrics characteristic of the MHB. Based on seismic reflection expression, F1 is presently a west-dipping compressional fault (net thrust offset observed) that inverted shortly after its down-to-the-west extensional fault development during Laramide deformation.

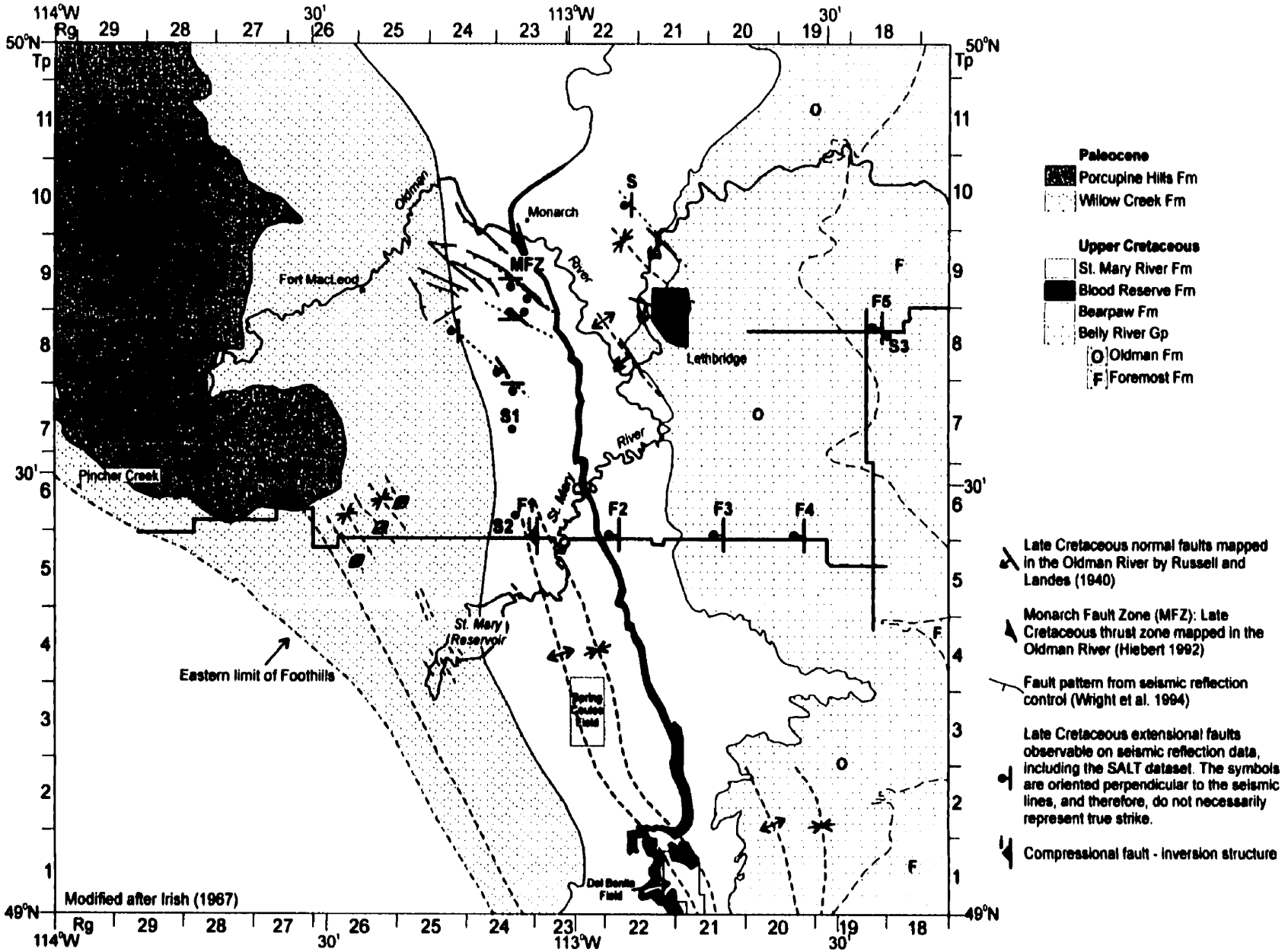
114°W
Rg 29 28 27 30' 26 25 24 23 113°W 22 21 20 19 30' 18
50°N
Tp 11 10 9 8 7 30' 6 5 4 3 2 1
49°N
Oldman
Monarch
MFZ
Fort MacLeod
Pincher Creek
Lethbridge
River
St. Mary
St. Mary Reservoir
Eastern limit of Foothills
Modified after Irish (1967)
S1
S2
S3
F1
F2
F3
F4
F5
Paleocene
Porcupine Hills Fm
Willow Creek Fm
Upper Cretaceous
St. Mary River Fm
Blood Reserve Fm
Bearpaw Fm
Belly River Gp
O Oldman Fm
F Foremost Fm
Late Cretaceous normal faults mapped in the Oldman River by Russell and Landes (1940)
Monarch Fault Zone (MFZ): Late Cretaceous thrust zone mapped in the Oldman River (Hiebert 1992)
Fault pattern from seismic reflection control (Wright et al. 1994)
Late Cretaceous extensional faults observable on seismic reflection data, including the SALT dataset. The symbols are oriented perpendicular to the seismic lines, and therefore, do not necessarily represent true strike.
Compressional fault - inversion structure

reflection dataset in southern Alberta, and forms the focus of the regional basinal study (Figures 5 and 6). Additional industry seismic reflection data in the vicinity of SALT line 30, and in the Fort MacLeod area, also exhibit extensional faulting of the sedimentary sequence (Figure 6; Wright et al. 1994).

Approximately 40 km north of SALT line 30, and 65 km east of the triangle zone, the Monarch fault zone crops out in the Oldman River (Figure 6). The zone strikes north-northwest-south-southeast, with a minimum width of 1.5 km across-strike, and is interpreted to represent an inverted extensional fault that has been partially localized by basement-controlled normal faulting, based on seismic reflection data in the area (Hiebert and Spratt 1996). The zone was first described in detail by Irish (1967) as an imbricate zone containing several high-angle east-dipping thrusts faults disturbing uppermost Bearpaw, Blood Reserve and lowermost St. Mary River strata. Hiebert (1992) further described the thrust style of the zone as bearing a remarkable resemblance to the deformational style across the apex of a conventional triangle zone, as a change in vergence is observed across the structure. However, two significant differences occur at the Monarch fault zone that are not typical of a conventional triangle zone: (1) steep ($50^0$ to $60^0$) east-dipping thrust faults; and (2) the absence of an upper detachment (Figure 7).

Figure 7. Photograph of the north-south exposure of the Monarch Fault Zone in the Oldman River, near the town of Monarch in southern Alberta. Upper Cretaceous strata of the St. Mary River Formation are steeply-dipping to the west and southwest at about 50° to 60°. Note the unconformity (dashed line) between the dipping Cretaceous strata and the Quaternary sediments in the upper portion of the exposure.

# CHAPTER 3. CRUSTAL STUDIES OF THE ARCHEAN MEDICINE HAT BLOCK

## 3.1 Introduction

The tectonic assembly of the western Canadian Shield was completed by about 1.78 Ga after a series of Archean terranes was amalgamated along Proterozoic orogenic belts. The largest of these are the Trans-Hudson and Wopmay orogens (Figure 1). The Trans-Hudson orogen extends south-north from Montana to northern Manitoba, and then northeastward through Hudson's Bay. The Wopmay orogen strikes north-south, extending from northeastern British Columbia to the Arctic Ocean. The region between these two Proterozoic belts includes, from north to south, the Archean Rae, Hearne, and Wyoming Provinces. The Rae Province is separated from the Hearne Province by the Snowbird Tectonic Zone, a major right lateral shear zone (Hanmer 1990). The tectonic relationship between the Hearne and Wyoming Provinces is not clear, as they underlie the Phanerozoic strata of the Western Canada Sedimentary Basin (WCSB). The region between the southern Hearne and northern Wyoming Provinces contains the Medicine Hat Block (MHB; Figure 2). The origin of the MHB and its relationship to the Hearne and Wyoming Provinces have been largely unknown.

## 3.2 Potential-field studies

### 3.2.1 Introduction

The geographic extent of the MHB has been defined on the basis of potential-field data and drillcore information (Ross et al. 1991; Villeneuve et al. 1993). In this study, filtered versions of gridded total magnetic field intensity and Bouguer gravity data are used to enhance the internal features and boundaries of the MHB, and to further investigate its tectonic relationship with the surrounding basement domains. In general, the magnetic signature of the MHB consists of prominent linear northwest- and north-trending anomalies, except for the westernmost portion, which shows a large sub-circular magnetic high (Figure 3). Similar trends are seen for the Bouguer gravity anomalies, especially on the short-wavelength bandpass filtered Bouguer gravity map illustrated in Figure 8. The purpose of the wavelength (bandpass) filtering is to isolate the short- and long-wavelength components of the potential-field data in order to enhance trends at different depths within the crust and mantle.

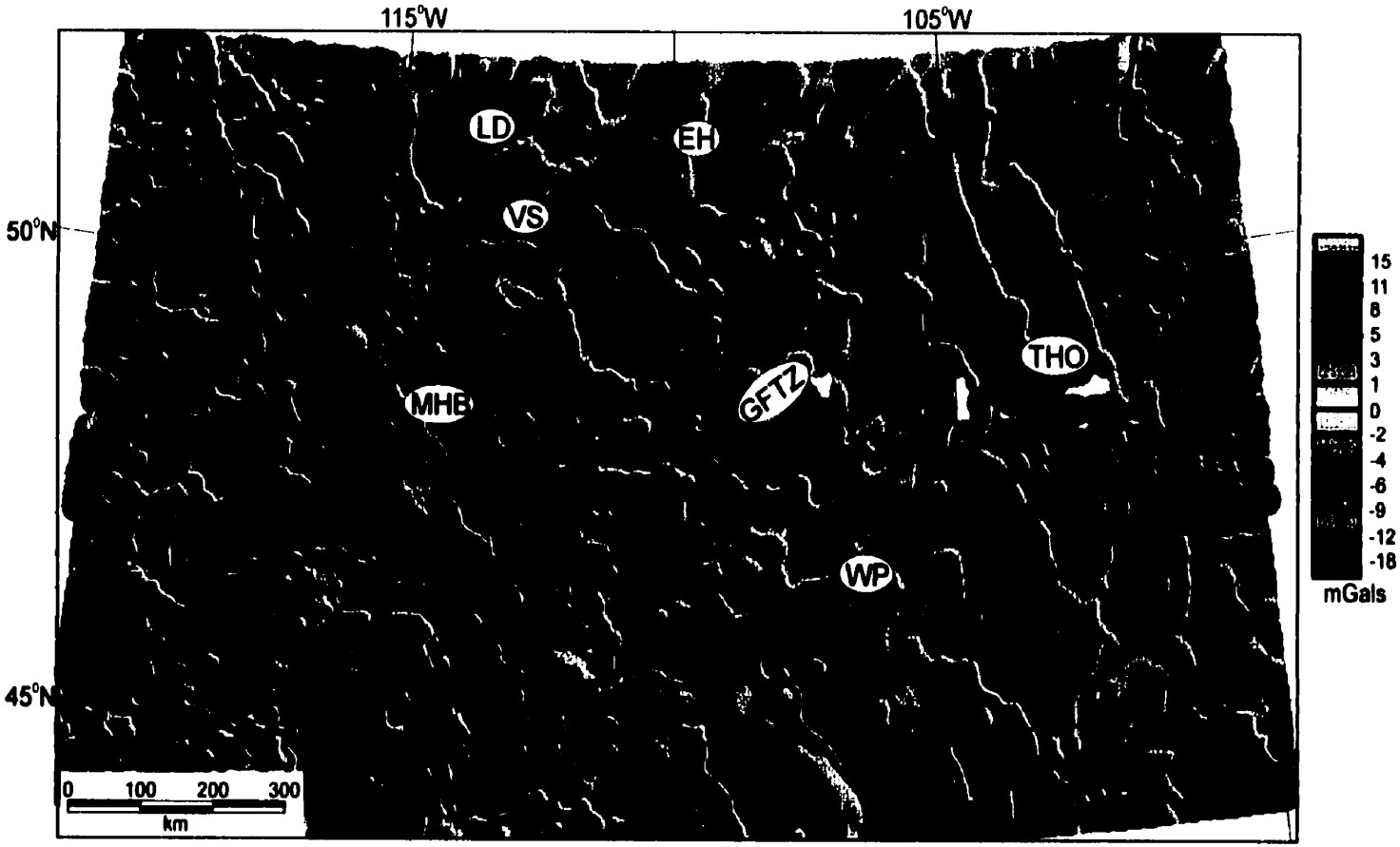


Figure 8. Short-wavelength filtered Bouguer gravity anomaly map (400-200/20-10 km) showing linear northwest- and north-trending fabrics of the MHB. Arrows indicate continuity of MHB gravity fabrics across the Great Falls Tectonic Zone.

### 3.2.2 Wavelength filtering procedures

Wavelength or bandpass filtering of gridded magnetic and gravity data uses specific sets of wavelengths to enhance and emphasize anomalies of interest. In this study, anomalies arising from sources within the upper crust, lower crust and upper mantle are of interest. Generally, long wavelengths are attributed to deep sources in the crust and the mantle, whereas short wavelengths are attributed to shallow sources in the upper crust and near the basement surface. It is important to note that long wavelengths may also arise from broad shallow sources, and hence, low-pass (long-wavelength) filters do not eliminate all near-surface anomalies.

As a general rule-of-thumb for gravity anomalies, the maximum depth of a point source is equal to the half-width of the anomaly at half height (Dobrin and Savitt 1988). The half-width of the gravity anomaly is then approximated to equal a quarter of a wavelength, i.e., maximum depth to anomalous source = ¼ wavelength. For example, a maximum depth of 50 km corresponds to a wavelength of approximately 200 km. Thus, a high-pass (short-wavelength) filter of 200 km effectively limits gravity anomalies to within the upper 50 km of the lithosphere. A general rule-of-thumb for magnetic anomalies is based on Peters' slope method for calculating a maximum depth to the top of an anomalous vertical body (Dobrin 1976). The maximum depth is estimated to be 1.6 times the separation of the two points of tangency (Dobrin 1976), which in turn, approximates a quarter of a wavelength. Thus, a depth of 15 km corresponds roughly to a wavelength of 100 km. Magnetic sources approximately are restricted to within the upper 25 km of the lithosphere, as crustal rocks lose their magnetization below the Curie point. For most magnetized materials, the Curie point is about $500^0$ C, which corresponds to depths between 20 to 25 km for average Shield areas when an average geothermal gradient between $20^0$ to $25^0$ C/km is used (Press and Siever 1986). Table 6 summarizes the various wavelength filters used for the interpretation of the gravity and magnetic gridded data with corresponding tapers and estimated depths.

The gridded data were radially filtered in the two-dimensional Fourier wavenumber (spatial frequency) domain using low-pass and high-pass circular filters. Filters define a set of wavenumber values between zero and one that is multiplied by the Fourier transform of the gridded data. Since the filters are applied in the wavenumber domain, and the original gridded data are in the space domain, two-dimensional Fourier transforms provide the physical basis for conversion from the space to wavenumber

| Magnetic data (2-km grid) | | | |
|---|---|---|---|
| Figure # | Bandpass filter Wavelength (km) | Estimated depth (km) | Taper factor |
| 10 | 93.3-70/20-15 | 10-3 | 1.33 |
| 11 | 300-150/20-10 | 25-3 | 2 |
| 12 | 333.3-200/50-30 | 30-8 | 1.67 |
| 13 | 312.5-250/100-80 | 40-15 | 1.25 |
| **Bouguer gravity data (2-km grid)** | | | |
| 8 | 400-200/20-10 | >3 | 2 |
| 14 | Low-pass >10-5 | 50-5 | 2 |
| 15 | 750-600/200-160 | 150-50 | 1.25 |
| 16 | 2000-1000/200-100 | 250-50 | 2 |

Table 6. Parameters used in the bandpass filtering of the gridded magnetic and gravity data. For the magnetic data, the estimated depth is calculated by dividing the wavelengths by 6.4 (depth = ¼ of the wavelength/1.6). For the gravity data, the estimated depth is calculated by dividing the wavelengths by 4 (depth = ¼ of the wavelength). See text for complete explanation.

domain and vice-versa (Dobrin and Savitt 1988). Fourier transform techniques are used to express a space domain function as a continuous function of spatial frequency (Cooley and Tukey 1965).

The bandpass filters designed in this study used various combinations of simple low-pass (long-wavelength) and high-pass (short-wavelength) filters that are defined by four wavenumbers. A symmetrical cosine roll-off function defines the taper at both ends (Figure 9 and Table 6). Two intermediate wavenumbers at a value of L(k) = 1 define the start of the roll-offs, and two end wavenumbers at a value of L(k) = 0 indicate the cut-off points of the filters (Figure 9). Wavenumbers between the two intermediate wavenumbers (values at L(k) = 1) represent the unaltered bandpass, in which all wavelengths are passed (Figure 9). Taper widths (separation between start of roll-off and cut-off wavenumbers) were defined on the basis of a factor between 1.25 and 2.0, and are symmetrical for the same bandpass (Table 6). These width values were found reasonable to prevent edge and filter ringing effects in the filtered maps. As an example, a low-pass filter using a 20-km wavelength (wavenumber = 0.05 cycles/km) as the start of the roll-off, and a 10-km wavelength (wavenumber = 0.1 cycles/km) as the end of the roll-off has a taper width factor of 2.0. Figure 9 illustrates a block diagram of a 2000-1000 km to 200-100 km wavelength bandpass filter with its corresponding two-

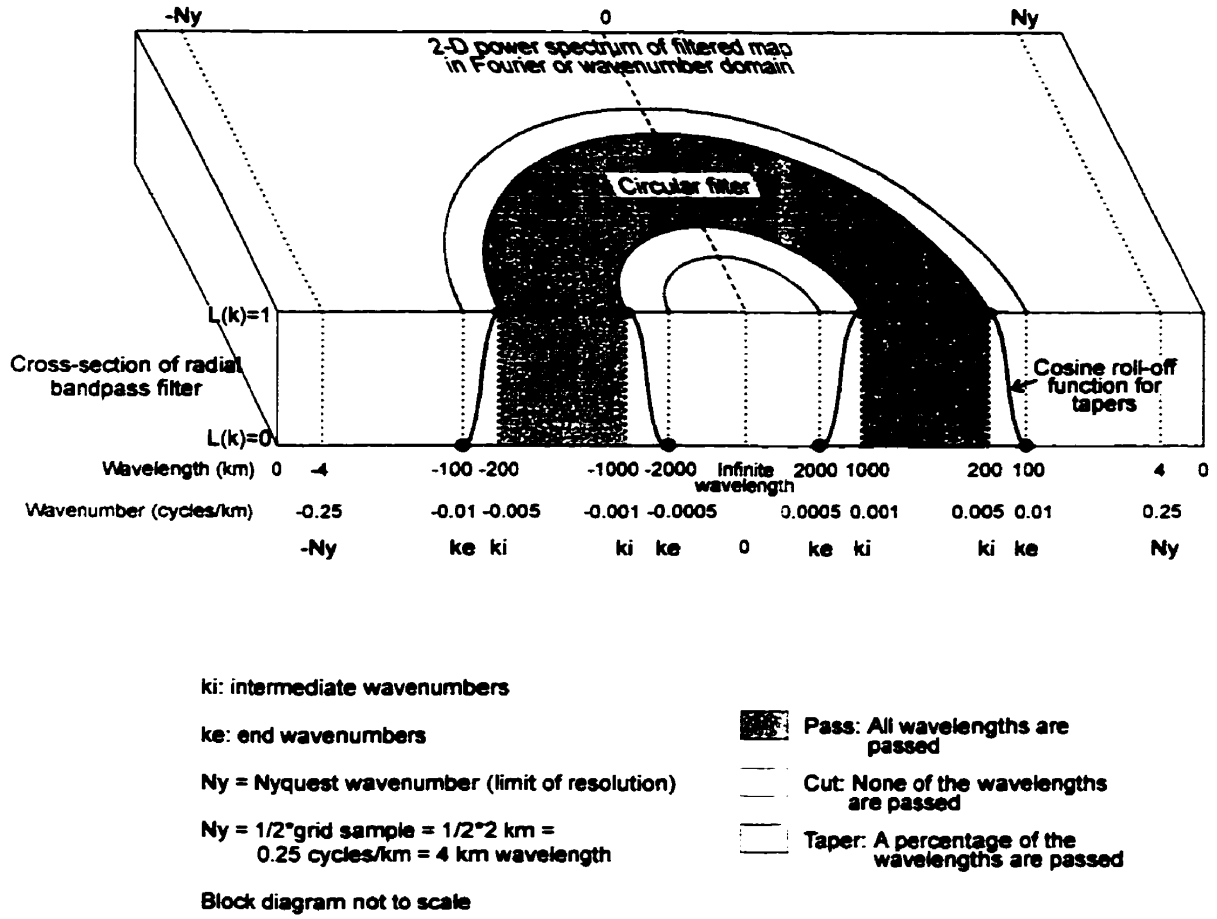


Figure 9. Block diagram of a 2000-1000/200-100 km radial bandpass filter showing pass, cut, and taper regions with associated wavenumbers and corresponding two-dimensional power spectrum. Note that in this perspective, the circular bandpass filter appears as an ellipse.

dimensional power spectrum, in which all events between 1000 km and 200 km wavelengths are passed in all directions.

### 3.2.3 Filtered total-field intensity magnetic maps

The color-shaded total-field magnetic map is illuminated from the southwest using an azimuth of $239^0$ and an inclination of $27^0$, and contains all the wavelengths present in the original gridded data (Figure 3). The internal magnetic fabric of the MHB is enhanced because the incident light vector is nearly perpendicular to the fabric (Figure 3). The linear fabrics of the MHB clearly terminate to the north at the east-trending anomalies associated with the Vulcan structure. To the south, the MHB linear magnetic anomalies appear to continue across the Great Falls Tectonic Zone (arrows in Figure 3) and are lost in a zone containing the southern portion of the Great Falls Tectonic Zone and the northern portion of the Wyoming Province. The eastern limit of the MHB is not well defined, but appears to correspond with a region where the linear MHB fabrics terminate at predominantly north-trending anomalies associated with the merging of the Eyehill High, Vulcan structure and Trans-Hudson orogen anomalies (Figure 3). The northeast-trending anomalies associated with the Great Falls Tectonic Zone appear to terminate at high angle against the anomalies associated with the Trans-Hudson orogen. The western portion of the MHB is characterized by a large magnetic anomaly high and the western limit of the MHB magnetic signature can be followed west of the Cordilleran deformational front (Figure 3).

Two short-wavelength bandpass filters (93.3-70/20-15 km and 300-150/20-10 km) were used to investigate upper crustal anomalies (Figures 10 and 11). The short-wavelength components principally show that, although there is some disruption along the Great Falls Tectonic Zone, the linear magnetic fabric of the MHB appears to correlate with similar fabrics southeast of the Great Falls Tectonic Zone. In Figures 10 and 11, linear north- and northwest-trending anomalies are visible that extend south of the present MHB boundary (arrows). To the south, linear northwest-trending anomalies are visible within the Wyoming Province. The linear short-wavelength MHB anomalies appear more well-defined in that they delineate a magnetic discontinuity in which north-trending anomalies appear to terminate against northwest-trending anomalies (Figures 10 and 11). This termination is also visible on the color-shaded magnetic map (Figure 3).

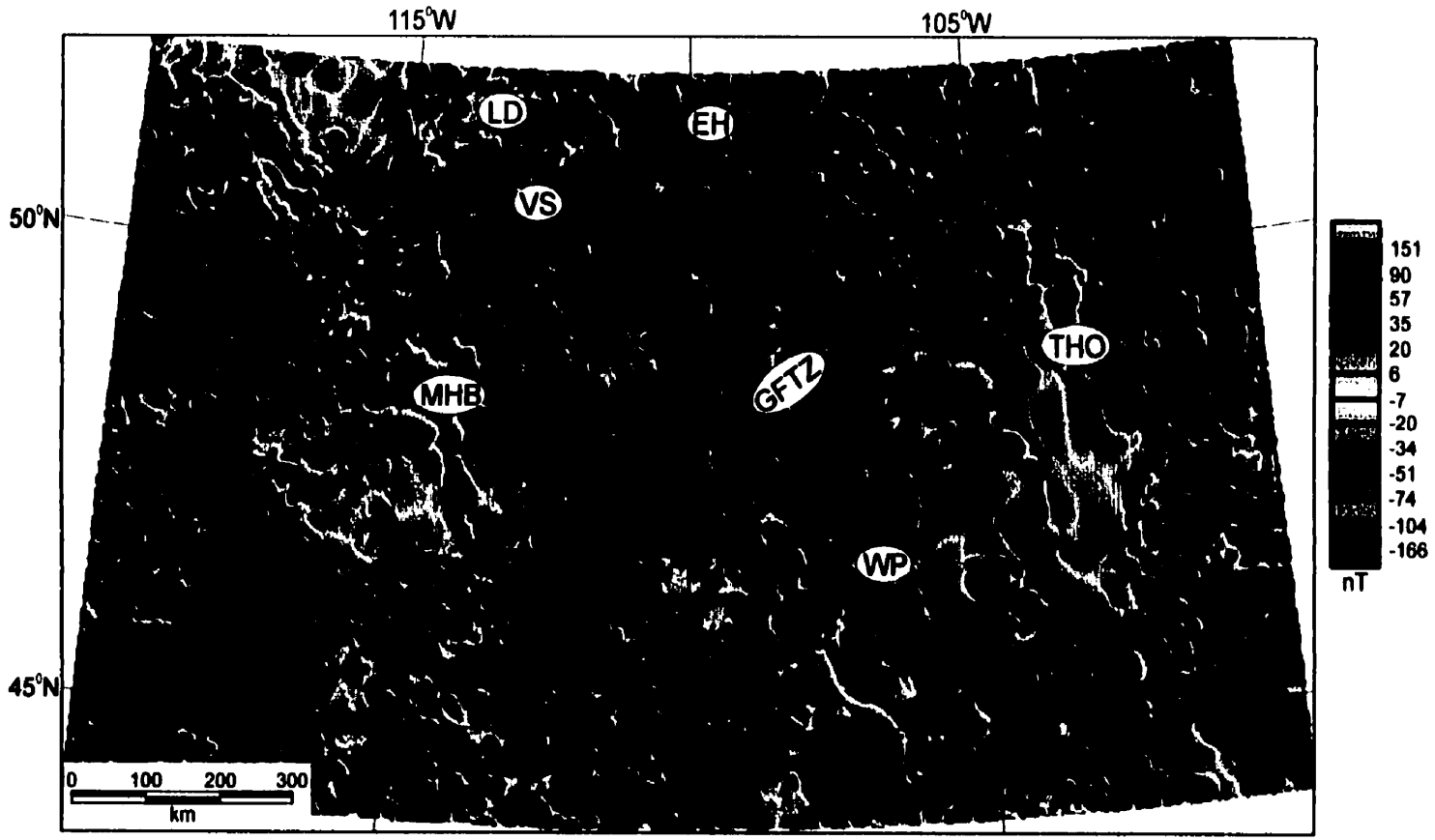


Figure 10. Short-wavelength filtered magnetic anomaly map (93.3-70/20-15 km) showing linear northwest- and north-trending fabrics of the MHB. Arrows indicate continuity of MHB magnetic fabrics across the Great Falls Tectonic Zone. The termination of the north-trending anomalies in the MHB against the northwest-trending anomalies is illustrated by a dotted line.

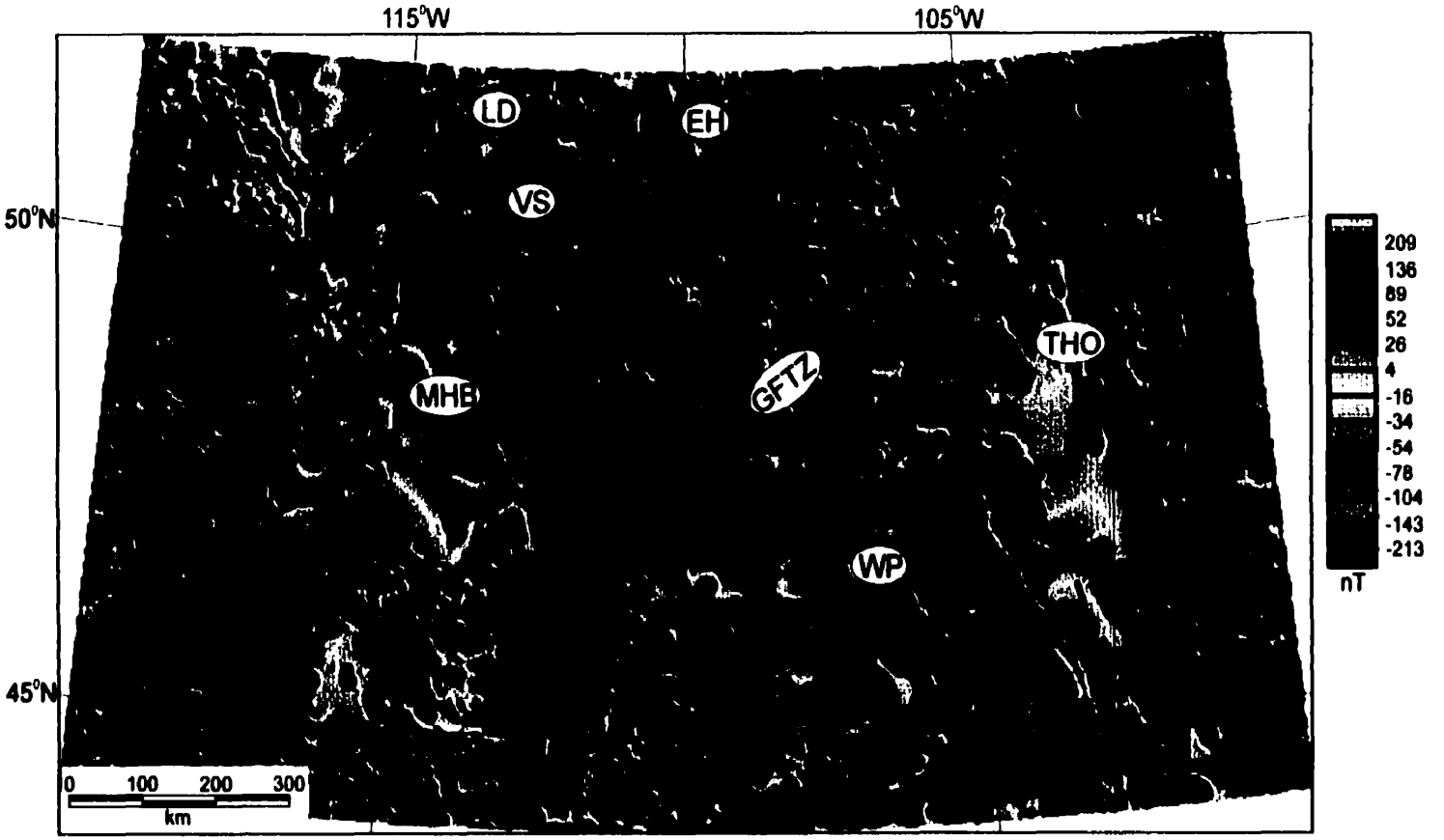


Figure 11. Short-wavelength filtered magnetic anomaly map (300-150/20-10 km) showing linear northwest- and north-trending fabrics of the MHB. Arrows indicate continuity of MHB magnetic fabrics across the Great Falls Tectonic Zone. The termination of the north-trending anomalies in the MHB against the northwest-trending anomalies is illustrated by a dotted line.

In addition, two long-wavelength bandpass filters (333.3-200/50-30 km and 312.5-250-100-80 km) were applied to the magnetic data to investigate crustal anomalies (Figures 12 and 13). The long-wavelength anomalies of the MHB are characterized by a northwest-trending fabric and are terminated to the north by the east-tending anomalies of the Vulcan structure (Figures 12 and 13). The prominent north-trending anomalies of the MHB seen in the unfiltered and short-wavelength filtered maps are completely removed for these wavenumbers (Figures 12 and 13). To the south and southeast of the MHB, linear northeast-trending anomalies coincide with the Great Falls Tectonic Zone, whereas the Wyoming Province is characterized by sub-circular northwest-trending anomalies (Figure 12). In Figure 13, the northeast-trending fabric associated with the Great Falls Tectonic Zone is nearly filtered out for these wavenumbers, whereas the Vulcan structure is still a prominent feature to the north.

### 3.2.4 Filtered Bouguer gravity maps

A low-pass filter with wavelengths larger than 10 km (10-5 km cutoff) was applied to the Bouguer gravity data in order to reduce high-frequency (short-wavelength) noise, which may arise from station errors and inaccurate terrain corrections (Figure 14). The low-pass Bouguer gravity anomaly map principally shows the significant gravity low associated with the Cordillera to the west and the linear fabrics of the MHB that terminate to the north at the east-trending anomalies associated with the Vulcan structure. To the south, the Great Falls Tectonic Zone appears to contain subtle northeast-trending anomalies and the northern portion of the Wyoming Province is characterized by a significant Bouguer gravity high (Figure 14).

A short-wavelength bandpass filter (400-200/20-10 km) was applied to the gravity data to reduce the effect of the long-wavelength anomalies associated with the Cordilleran gravity low (Figure 8). The MHB short-wavelength anomalies are characterized by linear north- and northwest-trending anomalies, similar to the magnetic signature (Figures 3 and 8). In addition, two long-wavelength bandpass filters (750-600/200-160 km and 2000-1000/200-100 km) were applied to the gravity data to investigate the regional anomalies (Figures 15 and 16). The Bouguer gravity low associated with the Cordillera is prominent in the western half of the maps, whereas a significant gravity high is associated with the MHB and extends to the southern portion of the Wyoming Province (Figures 15 and 16).

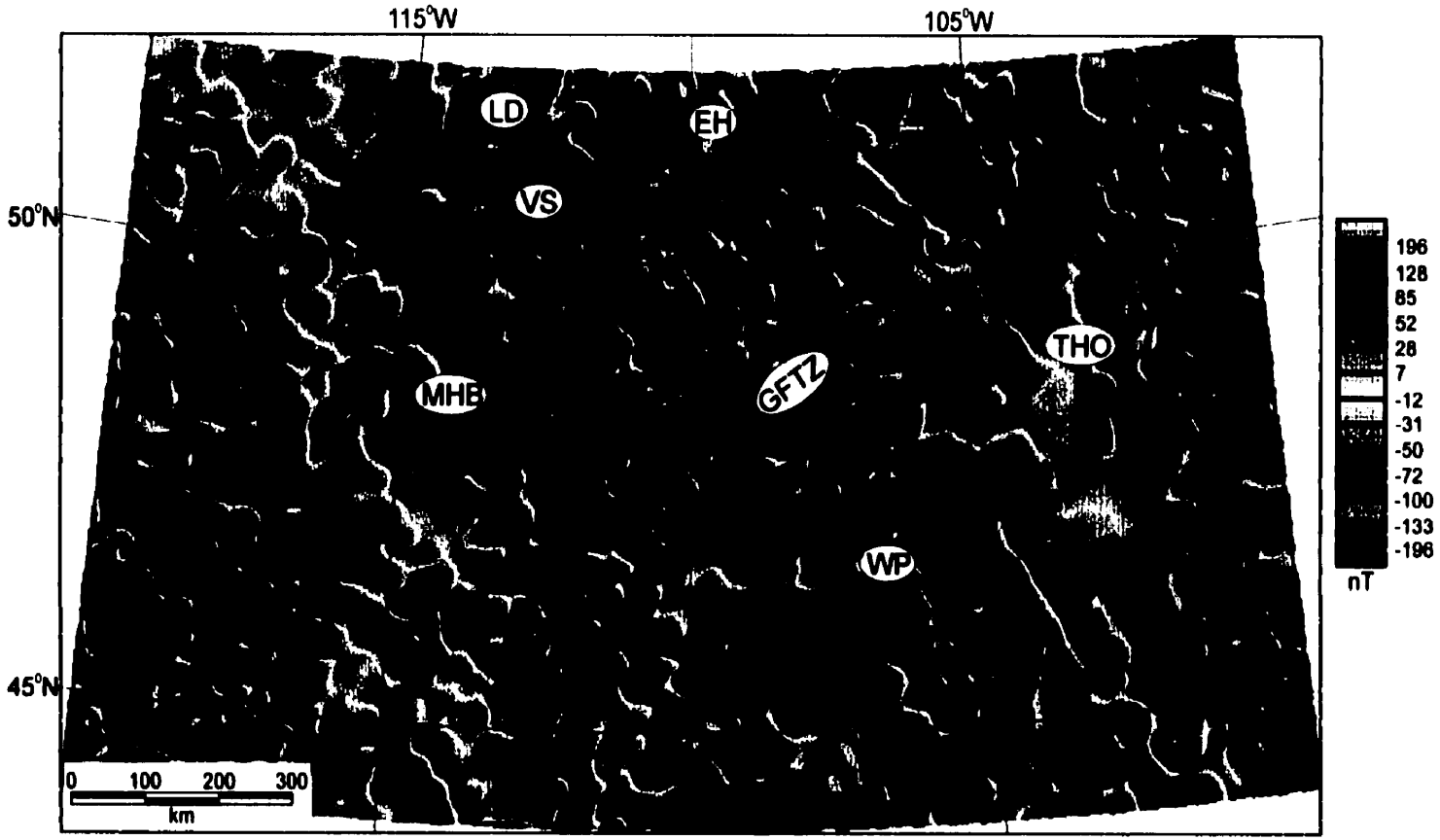


Figure 12. Long-wavelength filtered magnetic anomaly map (333.3-200/50-30 km). The north-trending anomalies of the MHB are completely removed at these wavenumbers.

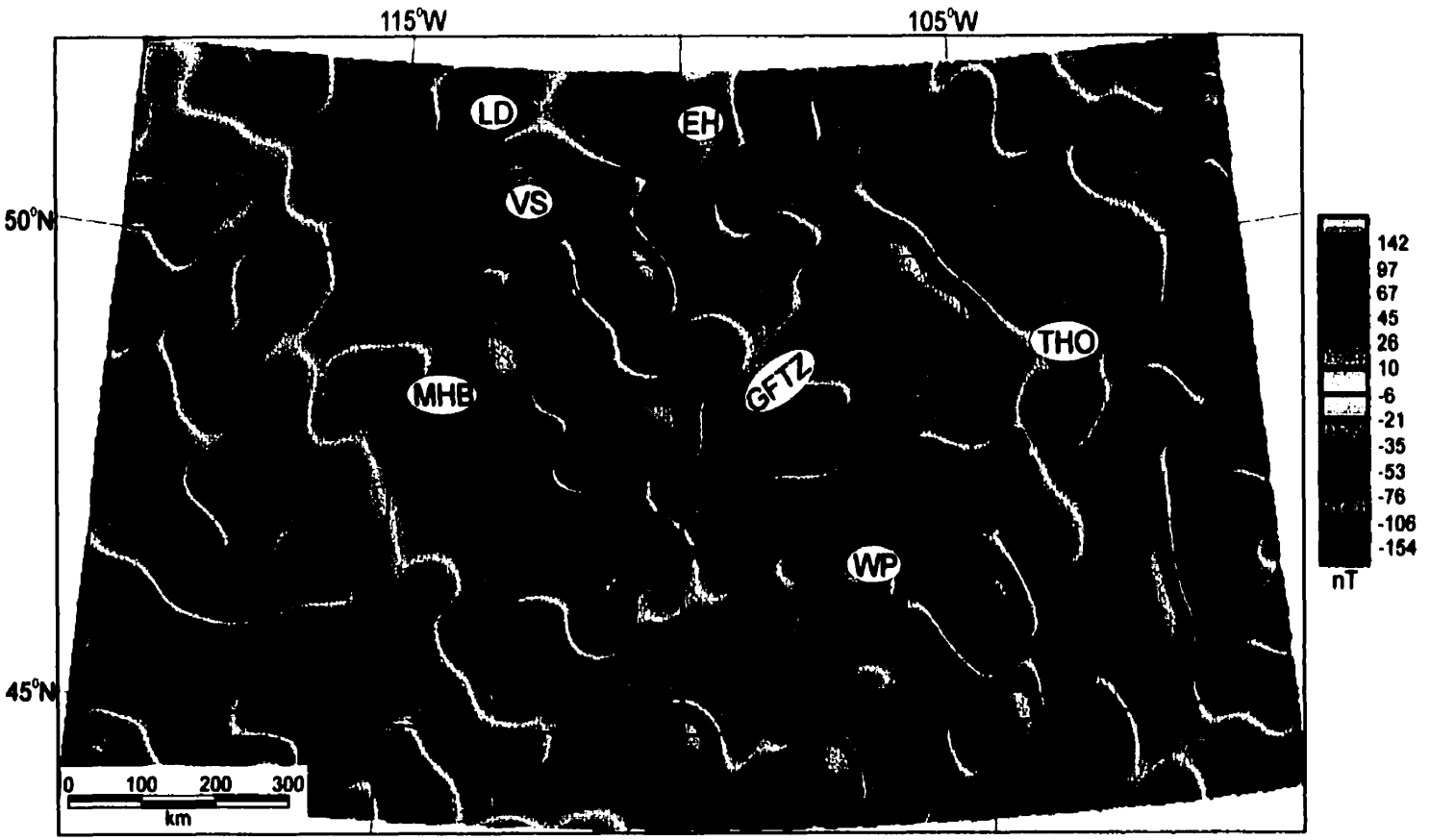


Figure 13. Long-wavelength filtered magnetic anomaly map (312.5-250/100-80 km). The north-trending anomalies of the MHB are completely removed at these wavenumbers.

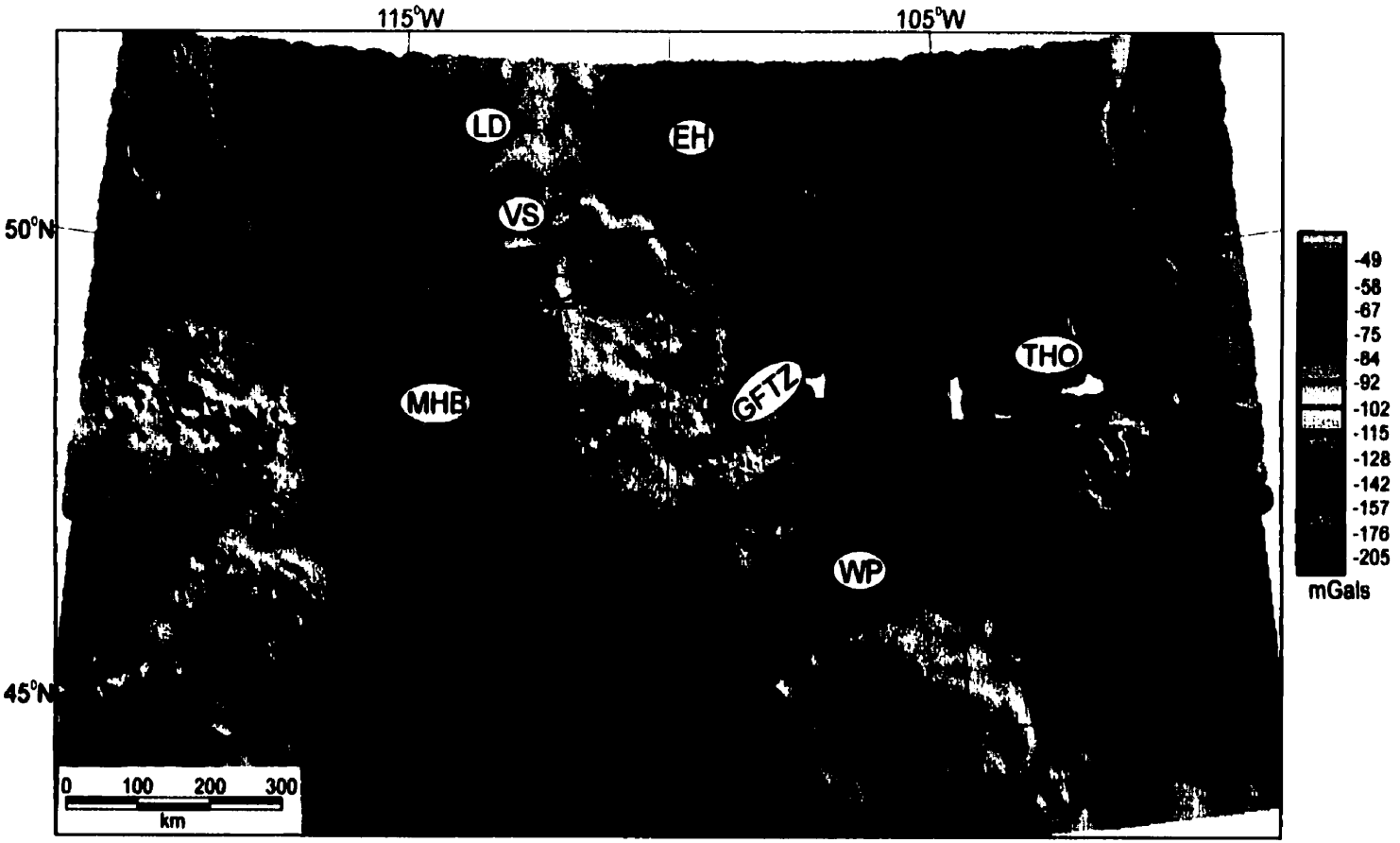


Figure 14. Low-pass filtered Bouguer gravity anomaly map (larger than 10 km) showing linear northwest- and north-trending fabrics of the MHB. The gravity profile (SW-NE) is illustrated by the grey line and is also shown in Figure 2. Arrows indicate continuity of MHB gravity fabrics across the Great Falls Tectonic Zone.

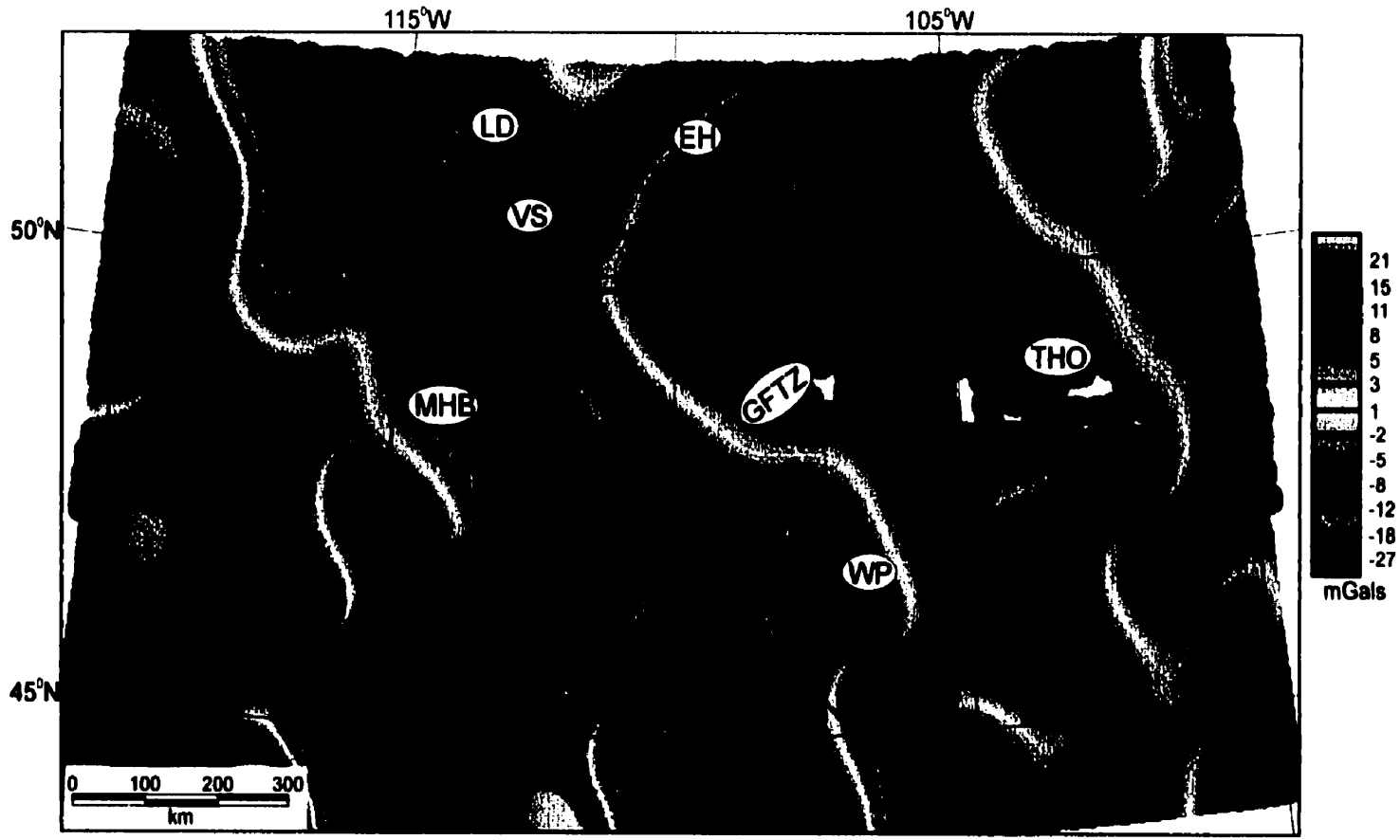


Figure 15. Long-wavelength filtered Bouguer gravity anomaly map (750-600/200-160 km). A significant gravity high is associated with the MHB and Wyoming Province.

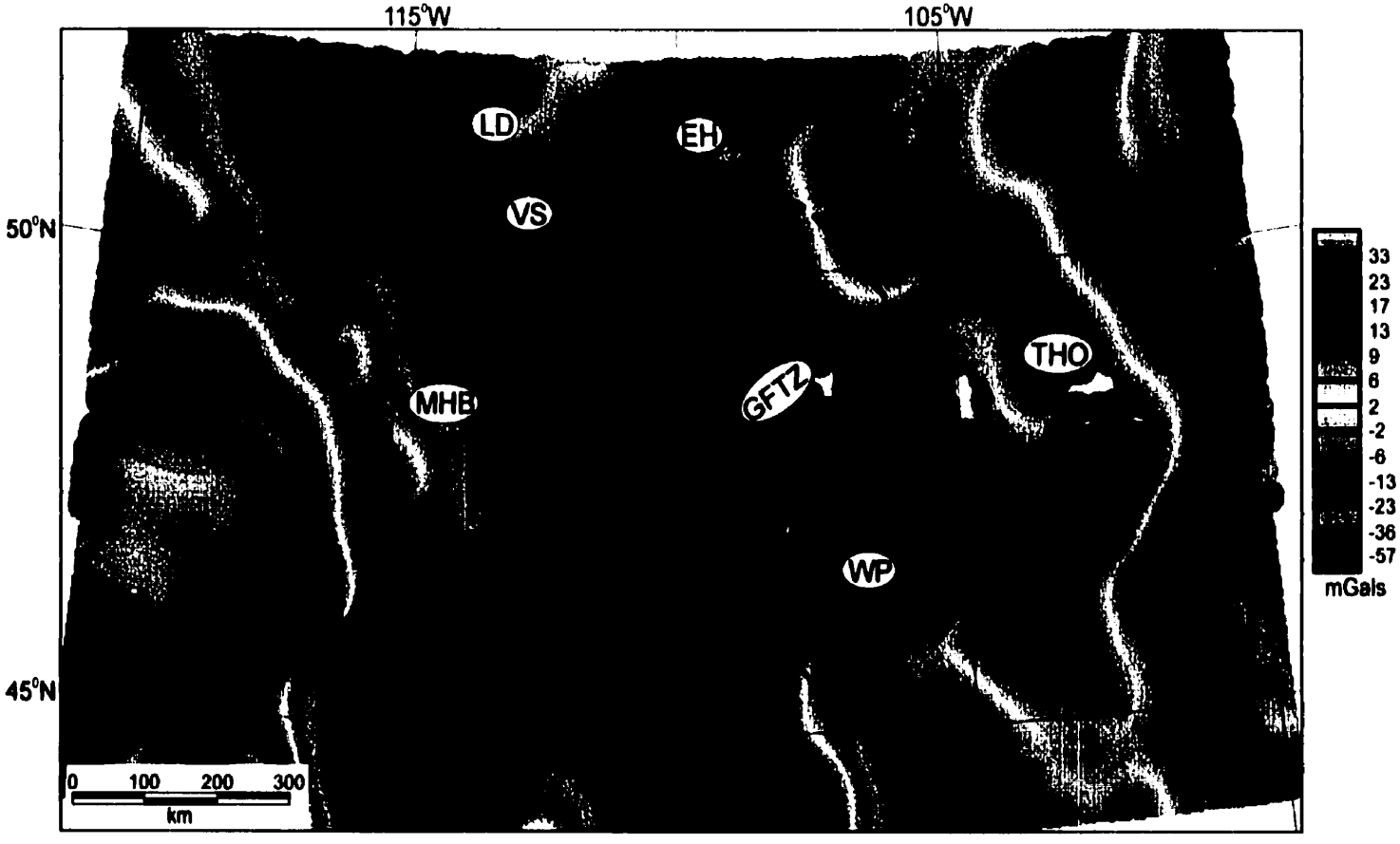


Figure 16. Long-wavelength filtered Bouguer gravity anomaly map (2000-1000/200-100 km). A significant gravity high is associated with the MHB and Wyoming Province.

### 3.2.5 Potential-field interpretations

The patterns of the potential-field anomalies that are characteristic of the MHB terminate northward at the Vulcan structure on all the filtered maps, except on the long wavelength gravity maps (Figures 15 and 16). Hence, the northern potential-field boundary of the MHB is clearly defined by the Vulcan structure as it truncates the MHB linear fabrics. However, the southern boundary of the MHB is not as well-defined on potential-field data, and it is not clear if the Great Falls Tectonic Zone is a significant potential-field discontinuity at crustal and/or mantle depths (Figures 12, 13, 15 and 16).

The short-wavelength (150-20 km) magnetic anomalies (Figure 11) show a northeast-trending anomaly corresponding to the surface location of the Great Falls Tectonic Zone, whereas the long-wavelength (250-100 km) magnetic anomalies continue across the Great Falls Tectonic Zone (Figure 13). Thus, the Great Falls Tectonic Zone potential-field signature appears to be associated with magnetic anomalies of wavelengths shorter than 150 km, which corresponds approximately to the upper 23 km of the crust. However, both the MHB and Wyoming Province are characterized by linear northwest-trending magnetic and gravity anomalies suggesting that they may be tectonically related (Figures 8, 10, 11, 12 and 13). The short-wavelength components (Figures 8, 10 and 11) and the long-wavelength Bouguer anomalies (Figures 15 and 16) of the MHB cross the Great Falls Tectonic Zone suggesting that the Great Falls Tectonic Zone likely does not represent a significant tectonic boundary at lower crustal depths. Long-wavelength gravity highs as seen in Figures 15 and 16 may be representative of an isostatically uncompensated crust, resulting either from a thinner crust than predicted by topography, or anomalously high density material at depth. The long-wavelength gravity high associated with the MHB and the Wyoming Province is interpreted to arise from a high density lower crust, as these basement domains have a faster velocity and thicker crust than average Shield areas (Henstock et al. 1998; Figure 16).

The western potential-field boundary of the MHB is defined where the westernmost northwest-trending anomalies occur (Figures 8, 10 and 11). However, the MHB may continue farther west beneath the Cordillera, but the progressively deeper burial of the crystalline basement together with overprinting by shallower Cordilleran anomalies (e.g., plutons and faults) lead to a reduction in amplitude of the potential-field anomalies associated with the MHB.

As for the internal potential-field signature of the MHB, the termination of the north-trending magnetic anomalies against the northwest-trending anomalies may represent a structural truncation (Figures 3, 10 and 12). The observation that the long-wavelength magnetic signature associated with the MHB is characterized only by linear northwest-trending anomalies suggest that these anomalies may extend deeper in the crust than the short-wavelength linear north-trending anomalies (Figures 10 to 13).

## 3.3 Internal crustal structure

### 3.3.1 Introduction

For the MHB crustal study, a regional composite seismic reflection section containing time-migrated and coherency filtered stacks for SALT lines 29, 30, 31 is plotted with no vertical exaggeration for an average crustal velocity of 6.6 km/s (Figure 17). The seismic profile is characterized by six basic reflection patterns (zones 1 to 6; Figure 17) that are associated with regional Precambrian structures of the MHB, and with the deposition and subsequent deformation of the WCSB.

### 3.3.2 SALT Seismic reflection observations

Subhorizontal strata of the WCSB thicken westward from about 1.4 s twt (~3.2 km assuming an average velocity of 4.5 km/s for the entire sedimentary sequence) in the eastern portion of line 30 and southern portion of line 29, to about 2.6 s twt (~5.9 km) at the west end of line 30, displaying a regional $2^0$ dip to the west (zone 1; Figure 17). Multiple reverberations originating from sedimentary layers occur over an interval of 0.5 to 1.0 s twt below the base of the WCSB and mask reflectivity from the upper portion of the crystalline basement (Figure 17). The sedimentary sequence contains prominent faulting, interpreted to be Late Cretaceous and older, in the eastern half of line 30 and in the western portion of line 31 (Lemieux 1999).

Zone 2 represents a zone of weakly reflective, discontinuous but principally west-dipping reflections that thickens westward to include most of the crust near the west end of the profile (Figure 17). In the western half of line 30, zone 2 appears to change in reflection character from steeply dipping reflections in the western portion of line 31 to shallowly-dipping reflections in the west end of line 30 (Figure 17). Between 3.0 and 7.0 s twt on lines 29 and 30, zone 2 is punctuated by high-amplitude subhorizontal

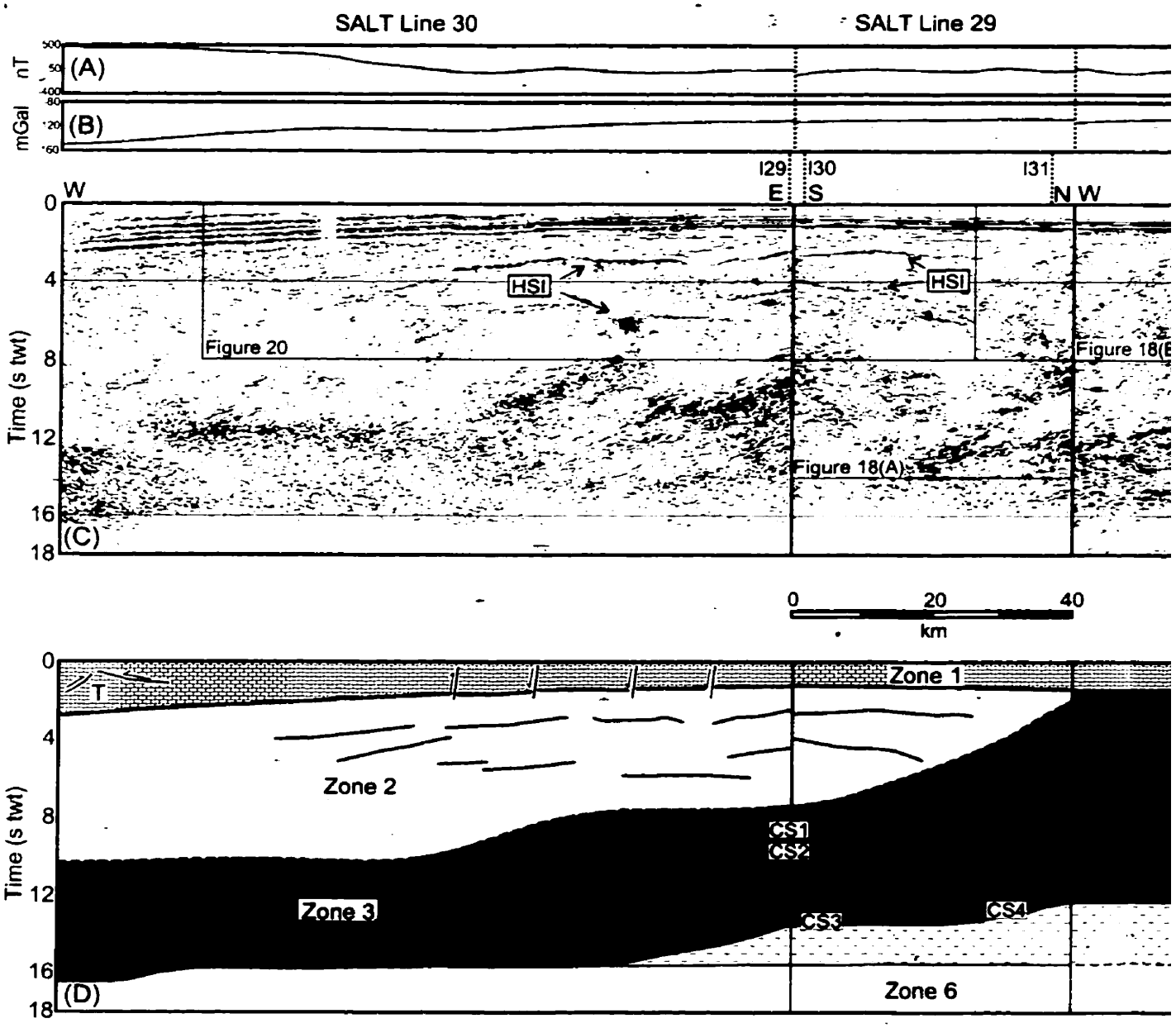


Figure 17. (A) Total-field intensity magnetic profile. (B) Bouguer gravity profile. (C) 290-km regional co reflection profile extends over a large portion of the MHB crust without crossing any significa illustrate the locations of Figures 18(A), 18(B) and 20. Sill reflections are indicated by HSI. I Interpretation of the seismic reflection profile illustrating the six reflection zones recognized WCSB of 4.5 km/s and an average crustal velocity of 6.6 km/s. Crustal surfaces (CS1 to CS (X) are shown.

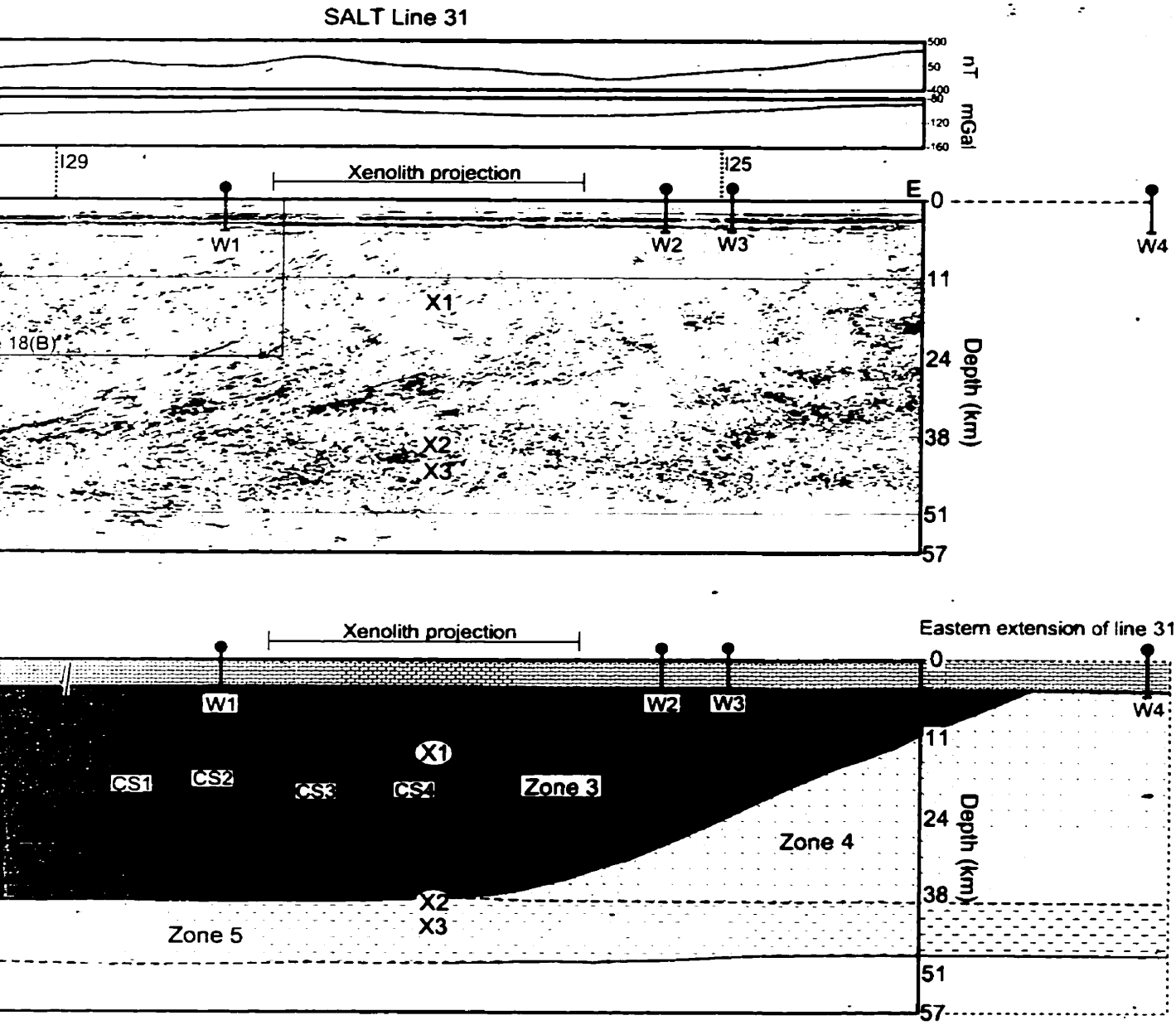


l composite seismic reflection profile of SALT lines 30, 29 and 31 across the MHB. The seismic
nificant tectonic boundary and displays the reflection expression of basement structures. Inset boxes
SI. I25, I29, I30 and I31 represent intersections with SALT lines of the seismic reflection profile. (D)
zed within the MHB crust. Time to depth conversion used an average velocity for the strata of the
o CS4) used to construct the time-structure maps, projected wells (W), and projected crustal xenoliths

reflections (HSI on Figure 17). Zone 3 is dominated by west- and southwest-dipping reflections that appear to be truncated by zone 5 events along line 29 and the western half of line 31 (Figure 17). Near the east end of the profile, subhorizontal and poorly coherent reflections of zone 4 are present throughout most of the crust such that the transition from zone 3 to zone 4 appears as a geometric cutoff along a dipping surface (Figure 17). Zone 3 extends along the entire profile, ranging from about 2 s twt (~4.5 km) in the middle portion of line 31, down to about 15 s twt (~47 km) on line 30, and to ~12 s twt (~38 km) in the western half of line 31. On line 29, zone 3 is present between 2 s to 12 s twt (~4.5 km to 38 km) in the north, and between ~10 to 14 s twt (~31 km to 44 km) in the south. The west-dipping reflections of zone 3 have an estimated apparent dip of $25^0$ in the upper crust and of $18^0$ in the lower crust, based on seismic reflection dips indicating that the dipping reflectivity is listric. Although the dipping reflectivity flattens into the lower crust, a lower detachment is not visible as the dipping reflectivity appears to be truncated by zone 5 (Figure 17). The dipping reflectivity of zone 3 is also characterized by antiformal structures that occur in the upper to middle crust of line 29 and in the upper crust on the western portion of line 31 (Figure 18). These antiformal structures may represent hanging wall anticlines developing along thrusts.

Zone 5 is dominated by highly reflective horizontal to subhorizontal reflections below zones 3 and 4, and above the non-reflective zone 6 (Figure 17). Zone 5 occurs in the easternmost portion of line 30 and along lines 29 and 31, where horizontal reflections are highly reflective and continuous from ~12 to 16 s twt (~38 to ~51 km) in the western half of line 31 and on line 29, and less reflective in the eastern half of line 31 from ~12 to 15 s twt (~38 to 47 km; Figure 17). On line 29, zone 5 is observed between ~14 to 15s twt (~44 to ~47 km) in the south, and between ~12 to 15 s twt (~38 to ~47 km) in the north. Zone 6 is characterized by little to no reflectivity beneath zones 3 and 5, except in the western half of line 31, where it is reflective (Figure 17).

### 3.3.3 COCORP seismic reflection observations

COCORP deep seismic reflection profiling (Montana lines 3 and 4) of the southern portion of the MHB shows reflection patterns similar to the SALT seismic reflection profile (Figures 2, 17, 18 and 19). The 94-km migrated and coherency filtered COCORP seismic reflection profile is characterized by: (1) a diffuse reflection Moho at 14 to 15 s twt (~44 km to 47 km depth assuming a crustal velocity of 6.6 km/s); (2)

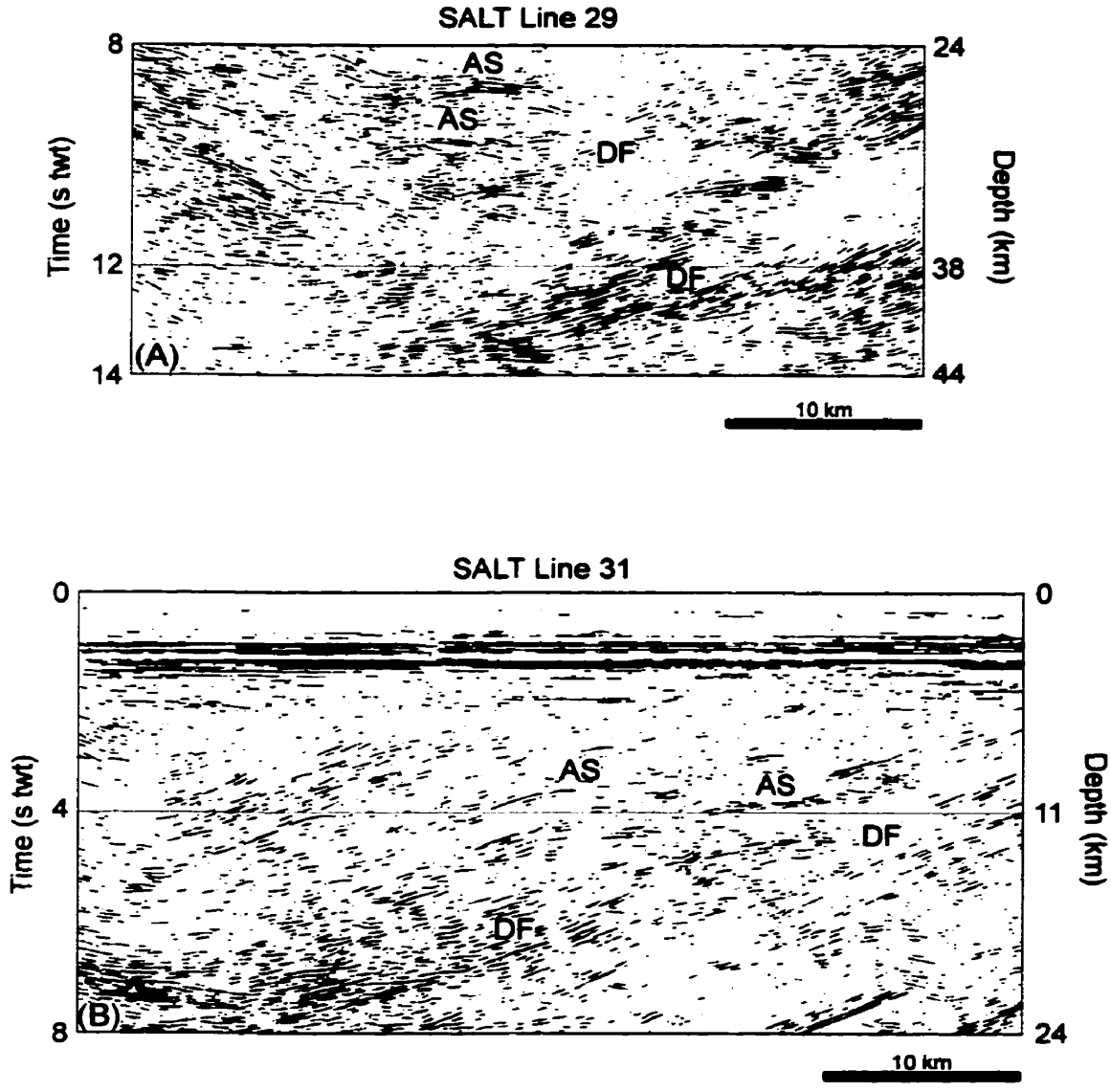


Figure 18. Enlargement of seismic reflection profile: (A) SALT line 29 and (B) SALT line 31, plotted with no vertical exaggeration. The MHB crustal reflectivity is characterized by steeply-dipping fabrics (DF) and antiformal structures (AS) that may represent hanging wall anticlines developing along thrusts during crustal shortening.

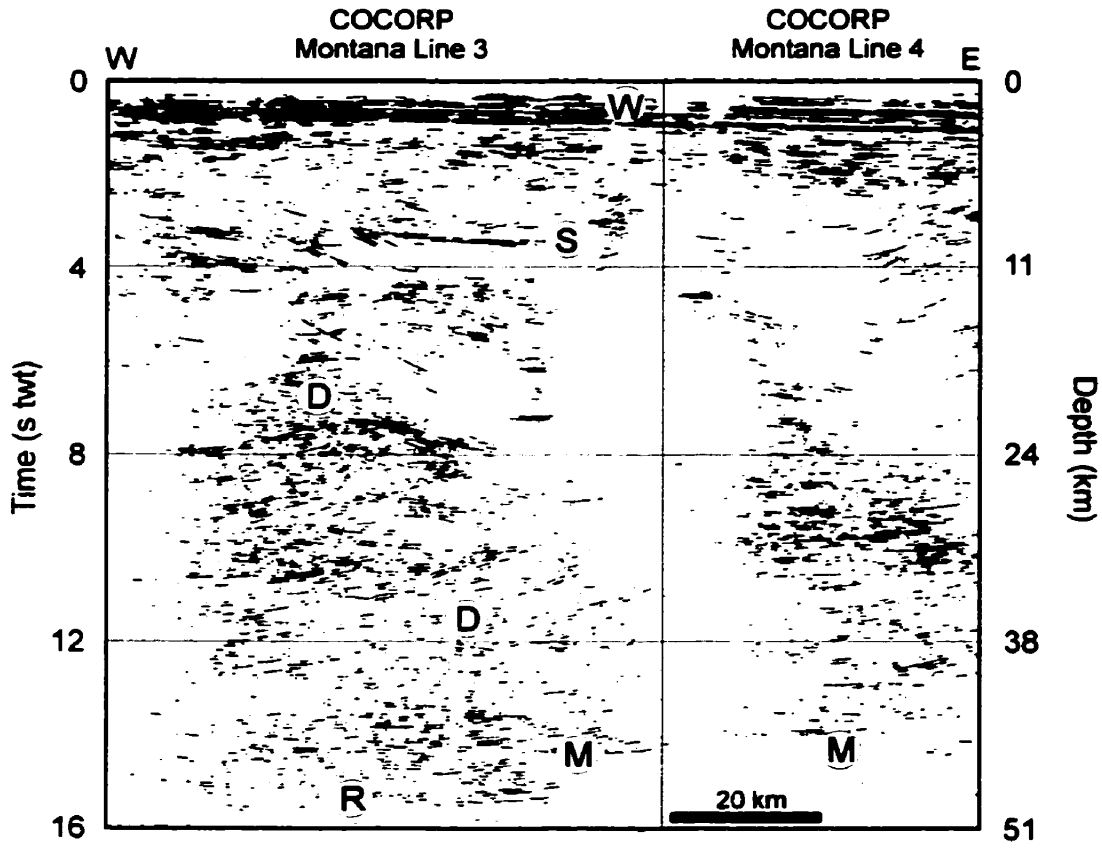


Figure 19. 94-km COCORP deep seismic reflection profile including the west-east Montana lines 3 and 4, plotted to 16 s twt at a 2:1 vertical exaggeration assuming an average crustal velocity of 6.6 km/s. Label descriptions include: WCSB (W); sill reflection (S); dipping crustal reflectivity (D); reflection Moho (M); and reflective lower crust/upper mantle (R).

reflective lower crust/upper mantle on Montana line 3; (3) dipping crustal reflectivity; and (4) a high amplitude subhorizontal reflection in the upper crust of Montana line 3 that may be derived from a sill reflection (Figure 19).

### 3.3.4 Seismic reflection interpretations

The dipping reflectivity of zones 2 and 3 is interpreted as structurally-induced layering on the basis of geometric relationships of seismic reflection fabrics presented in this study and other studies of the Alberta basement (see Ross et al. 1995; Eaton et al. 1999). Hence, three possible tectonic scenarios arise for the origin of the prominent dipping reflectivity of the MHB crust: a compressional origin, an extensional origin, or both. The MHB crust most likely was deformed under a compressional regime for these reasons: (1) presence of prominent dipping crustal reflectivity; (2) truncation of reflections along dipping cutoff surfaces; and (3) antiformal structures developing along the dipping reflectivity (Figures 17 and 18). The west- and southwest-dipping fabrics of zones 2 and 3 are interpreted as east- and northeast-verging crustal imbrication indicating that compression most likely was oriented westsouthwest-eastnortheast. Zone 3 is penetrated by three drillcores (W1, W2 and W3; Figure 2), which yielded Archean ages between 2.6 to 2.7 Ga (Figures 2 and 17; Table 5). In addition, a low pressure thermal event recorded in upper crustal Archean tonalite gneissic xenoliths (X1) may constrain the age of continental crust imbrication to be ca. 2.60 Ga (see Section 2.2; Figure 17).The shallowly-dipping reflection character and low reflectivity in the western portion of zone 2 appear to correspond to a prominent sub-circular magnetic high (Figures 3 and 17). This suggests that the crust to the west of line 30 is probably different in crustal geometry and lithology than the MHB crust.

The high-amplitude upper crustal subhorizontal reflections of zone 2 have been interpreted as sheet-like intrusions, known as the Head-Smashed-In sills, based on analyses of seismic signature and attributes (Mandler and Clowes 1998). They occur over an area of 6000 $km^2$ and appear to be confined to the northwestern portion of the MHB, suggesting that they are Early Proterozoic or older (>1.8 Ga; Mandler and Clowes 1998). Establishing a well-defined age constraint on sill emplacement is difficult as dipping crustal reflectivity is weak in that portion of the crust (Figure 20). However, the sill reflections appear to be displaced along the west-dipping fabric of zone 2, with up to 3 km of offset for the sill reflections at around 5 and 6 s twt and an upward diminishing

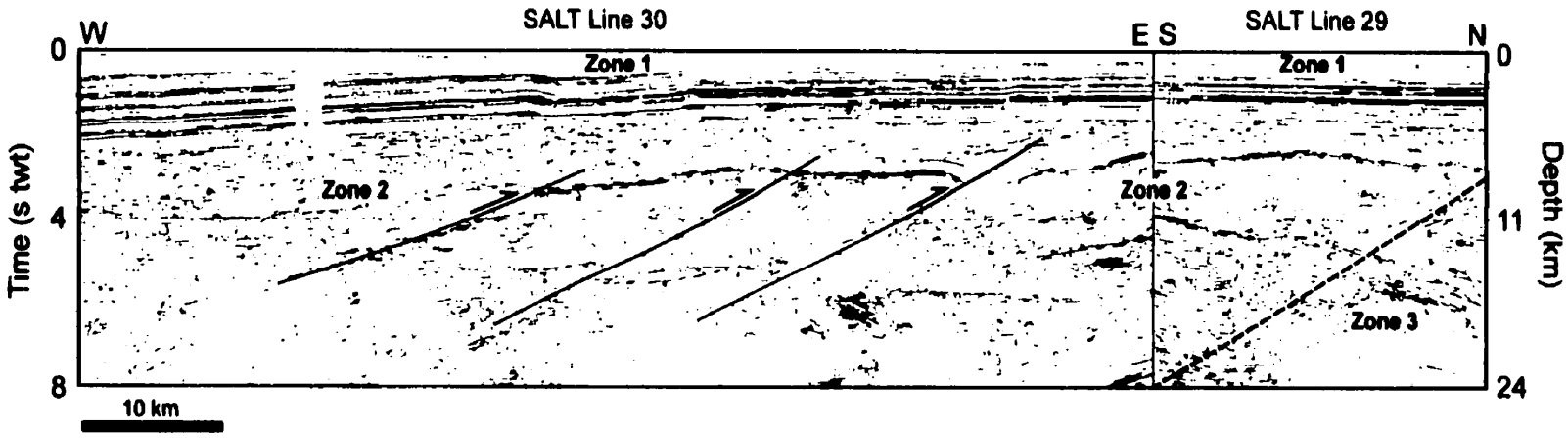


Figure 20. Enlargement of upper to middle crust of seismic reflection lines 30 and 29 showing high-amplitude sill reflections of zone 2. The sill reflections appear to be offset up to 3 km along the west-dipping fabrics at 5 and 6 s twt and show an upward diminishing thrust displacement. The dashed line represents the boundary between zones 2 and 3.

thrust displacement for the shallower sill reflections at around 3 and 4 s twt (Figures 17 and 20). If indeed the sills are displaced along the east-verging imbrication of zone 2, then the age of sill intrusion can be estimated to be in the Archean (older than 2.6 Ga), unless zone 2 was reactivated in the Proterozoic. Conversely, the apparent displacement of the sills may have arised from the nature of the intrusion in that they may have intruded in a step-like fashion (Pollard et al. 1975).

Truncation of the dipping reflections of zone 3 at the zone 5 boundary in the lower crust is interpreted as a structural truncation. In turn, truncation of the subhorizontal reflections of zone 4 at the zone 3 boundary is interpreted to occur along a dipping cutoff surface in the eastern end of the seismic profile (Figure 17). This geometry delineates a geometric ramp that extends from near 13 s twt (~41 km depth) in the middle of line 31 to 4 s twt (~11 km depth) in the eastern end of line 31 (Figure 17). Zone 4 subcrops approximately 15 km east of line 31, where Archean crust is interpreted to underlie the WCSB (from south-southeastern projection of W4: 12-19-014-04W4 into the eastern continuation of line 31; Figures 2, 3 and 17). The transition between zones 4 and 5 in the eastern lower crust of the seismic profile is uncertain because they are geometrically conformable (Figure 17). However, cross-cutting relationships of the MHB basement reflections suggest that zone 5 would be associated with the youngest tectonic event, cutting reflections within Archean zone 3. Zone 5 is interpreted to represent a layered transition zone, as a layered lower crust is often attributed to zones in which injection of mafic melts is believed to be a significant factor in reflectivity generation (Allmendinger et al. 1987).

### 3.3.5 Reflection Moho

The reflection Moho generally occurs at about 15 s twt or ~47 km (2 s twt at 4.5 km/s plus 13 s twt at 6.6 km/s) along the entire seismic reflection profile, which is similar to the 46 km Moho depth estimated from adjacent SAREX (Southern Alberta Refraction Experiment) refraction data (Figures 2 and 17; Burianyk et al. 1997), and is up to 8 km deeper than in surrounding regions north of the MHB. The refraction Moho beneath the eastern portion of the MHB is 5 to 10 km deeper than the refraction Moho in most Archean regions, and is comparable to Moho depths in orogenic belts (Christensen and Mooney 1995; Rudnick and Fountain 1995; Henstock et al. 1998). Moreover, average crustal velocities of the MHB, Great Falls Tectonic Zone, and Wyoming Province (6.6

km/s) are faster than the 6.4 to 6.5 km/s average crustal velocities for Shield areas (Henstock et al. 1998). North of the Vulcan structure, the reflection Moho is well-defined and occurs at 13 s to 14 s twt (38 to 41 km depth), which is comparable to average crustal thicknesses for Shield areas of 42 km (Christensen and Mooney 1995; Eaton et al. 1999). COCORP seismic reflection lines 3 and 4 reveal that the reflection Moho in the southern portion of the MHB occurs at about 15 s twt, which is comparable to the reflection Moho observed on the SALT seismic reflection profile (Figures 17 and 19).

The seismic character of the reflection Moho beneath the MHB appears to be diffuse in that the transition region from reflective crust to non-reflective upper mantle can occur within an interval of about 1 s twt or within an interval of 3 to 4 km in depth (with an average crustal velocity of 6.6 km/s; Figure 17). The limit of vertical resolution (approximately ¼ of the dominant wavelength; Sheriff 1991) near the crust-mantle boundary approximately equals 250 m, when an average velocity of 6.6 km/s and frequencies of about 5 Hz are used. Hence, the reflection Moho beneath the MHB is not as well-defined as reflection Moho north of the MHB (Eaton et al. 1999), but it is deeper than normal for Shield areas.

An anomalous region of high reflectivity in the lowermost crust/upper mantle is recognized along the seismic reflection profile in the western half of line 31 (Figure 17). High reflectivity occurs to about 17 to 18 s twt corresponding to a region of highly imbricated crust within the upper to middle crust (zone 3) and a thickly layered lower crust (zone 5; Figure 17). Based on reflection geometries, reflection Moho in that region may originally have been Archean, and present Moho depth would have been established in the Proterozoic.

### 3.3.6 Time-structure maps

Time-structure maps were constructed from the seismic reflection data to study the three-dimensional geometry and architecture of the MHB crust. By correlating the geometry of crustal surfaces defined by time-structure maps to potential-field trends, the 2D seismic profile information can be effectively extended into the third dimension. In this study, four time-structure maps were constructed from the upper to middle crustal reflections of zone 3 (Figure 17). The four dipping surfaces were chosen on the basis of reflection continuity. Determination of prominent dip directions of reflection patterns within the crust is essential in interpreting geometrical relationships, and hence, the

tectonic history of the southern Alberta crust. The upper to middle crustal reflections of zone 3 previously have been interpreted to have a uniform dip to the southwest (Vasudevan et al. 1995); however, the detail provided by the time-structure maps indicate that zone 3 crust actually consists of at least two distinct packages with different dips (Figure 21). Time-structure maps CS1 and CS2 illustrate two surfaces within the upper part of zone 3 that consist of prominent west-dipping reflections, whereas time-structure maps CS3 and CS4 show two prominent surfaces within the lower part of zone 3 that dip southwest and have a listric character (Figure 21).

From the geometric constraints delineated on seismic reflection data, the dipping reflectivity has been interpreted as a series of thrust imbricates arising from crustal-scale compression. The two different dips observed in zone 3 crust are interpreted as east- and northeast-verging imbrication. Time-structure map CS2 displays a west-southwest dip, perhaps representing a transitional region between the two dipping packages. The upper part of zone 3 contains reflections that extend along lines 29, 30 and 31, whereas the lower part of zone 3 contains reflections that extend along lines 29 and 31, and to the easternmost portion of line 30 (Figure 17). Furthermore, the lower dipping surfaces (CS3 and CS4) reach the top of the crystalline basement farther east along line 31 than do the upper dipping surfaces (CS1 and CS2; Figure 17).

## 3.4 Gravity modeling of the Medicine Hat Block crust

### 3.4.1 Introduction

Gravity modeling of the MHB crust was undertaken mainly to test the geometric constraints interpreted from the seismic reflection data, more specifically the crustal-scale geometric ramp and a lower crustal layered zone interpreted as high density mafic material. The gravity profile (SW-NE) was extracted from the low-pass (larger than 10 km) 2-km Bouguer gravity data illustrated in Figure 14. The profile extends for 235 km across the MHB and trends perpendicular to the prominent northwest-trending potential-field anomalies (Figures 2 and 14). In the gravity model, anomalous bodies are represented by zones of constant density that extend to infinity parallel to the regional strike. In addition, the modeled bodies on the southwest and northeast ends of the profile extend to infinity perpendicular to strike to avoid edge effect problems that occur at the edge of the model.

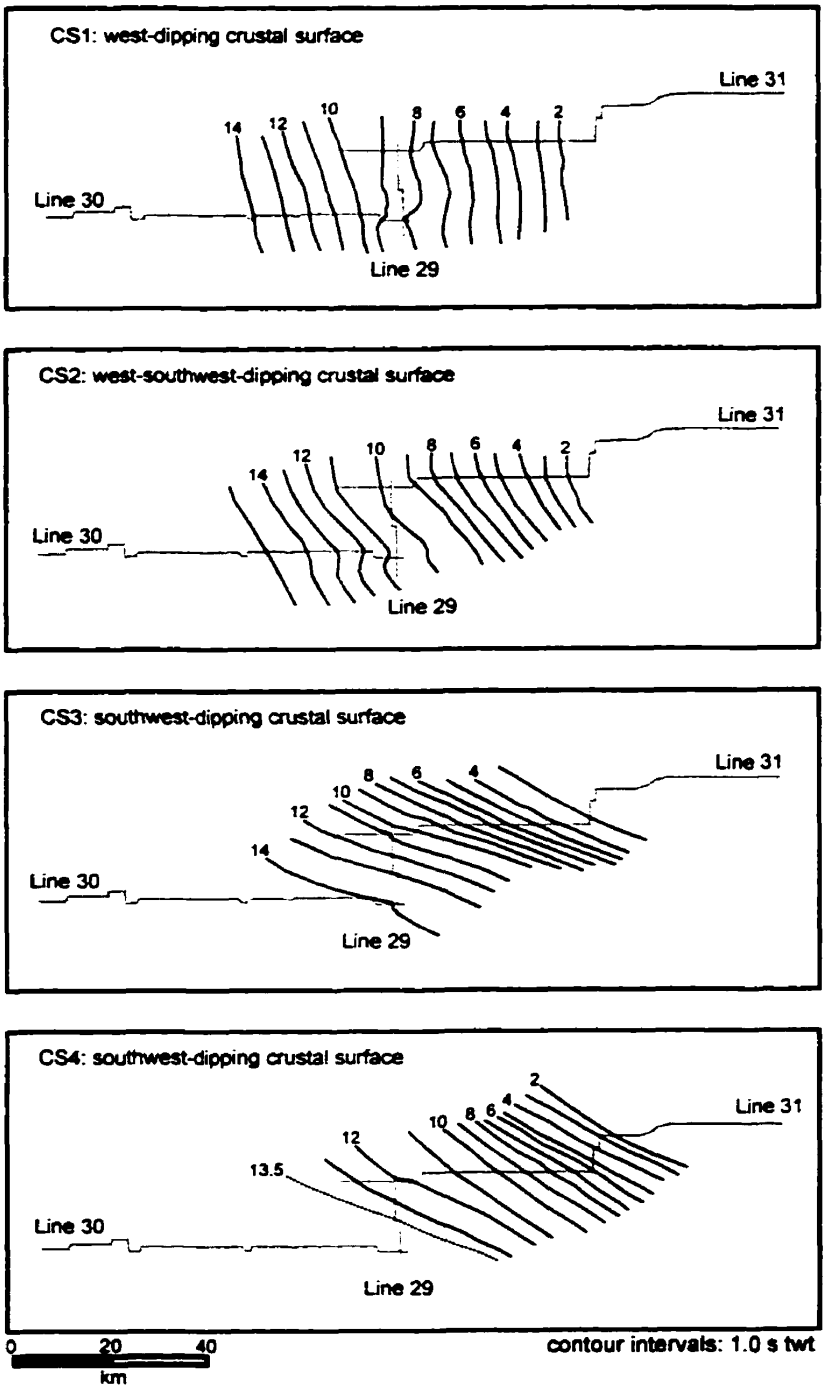


Figure 21. Time-structure maps illustrating four upper to middle crustal surfaces in zone 3. Crustal surfaces 1 (CS1 - shallowest and westernmost) and 2 (CS2) predominantly dip to the west, whereas crustal surfaces 3 (CS3) and 4 (CS4 - deepest and easternmost) predominantly dip to the southwest.

### 3.4.2 Seismic refraction results and densities

The densities used to constrain the eastern portion of the gravity model of the MHB crust are derived from the adjacent north-south SAREX refraction results (Figure 22; Buryanik et al. 1997). A table of physical properties of rocks listing densities as a function of pressure, elastic p-wave velocities, and corresponding lithologies allowed for the estimation of densities according to the SAREX seismic velocity model (Table 7; Hellwege 1982). The north-south SAREX seismic velocity model, illustrated in Figure 22, shows the location of shotpoint 3 (SP3), which lies 8 km east of the eastern end of seismic reflection line 31 (Figure 2).

| P-wave velocity (km/s) | Density ($g/cm^3$) | Pressure (kbar) | Corresponding lithologies |
|---|---|---|---|
| ~4.0 | 2.10 - 2.70 | 0 – 1 | Basinal strata |
| 5.9 - 6.2 | 2.63 - 2.66 | 0.5 – 2 | Granite |
| 6.2 - 6.5 | 2.71 - 2.74 | 2 – 8 | Granite to quartz diorite, tonalite |
| 6.5 - 6.8 | 2.80 - 2.90 | 2 – 8 | Quartz diorite |
| 6.8 - 7.1 | 2.93 - 2.98 | 6 – 10 | Diorite to norite |
| 7.1 - 7.3 | 3.00 - 3.27 | 8 – 10 | Granulite, gabbro, metagabbro |
| ~8.1 | 3.29 - 3.31 | 8 – 10 | Peridotite |

Table 7. Crustal velocities from SAREX results with corresponding densities, pressures and lithologies (Hellwege 1982).

### 3.4.3 Crustal density model and interpretations

The MHB crustal density model principally was built by using the geometric constraints interpreted from the seismic reflection data (Figure 17) and densities derived from the adjacent SAREX refraction survey (Figure 22). Densities for the strata of the WCSB (2.51 $g/cm^3$), the upper mantle (3.33 $g/cm^3$) and the easternmost portion of the profile (2.68 $g/cm^3$, 2.73 $g/cm^3$, 2.91 $g/cm^3$, 2.96 $g/cm^3$ and 3.15 $g/cm^3$) were set prior to iteration. The resultant crustal density model presented in this study displays an almost perfect fit between the observed (low-pass Bouguer gravity data) and calculated (modeled) curves as both long- and short-wavelength gravity anomalies were modeled (Figure 23). The long wavelength anomalies (approximately 100 to 250 km) principally are constrained by a geometric ramp in the east, the presence of a high density lower crustal layer in the eastern half (3.15 $g/cm^3$); and (3) an upper mantle density of 3.33

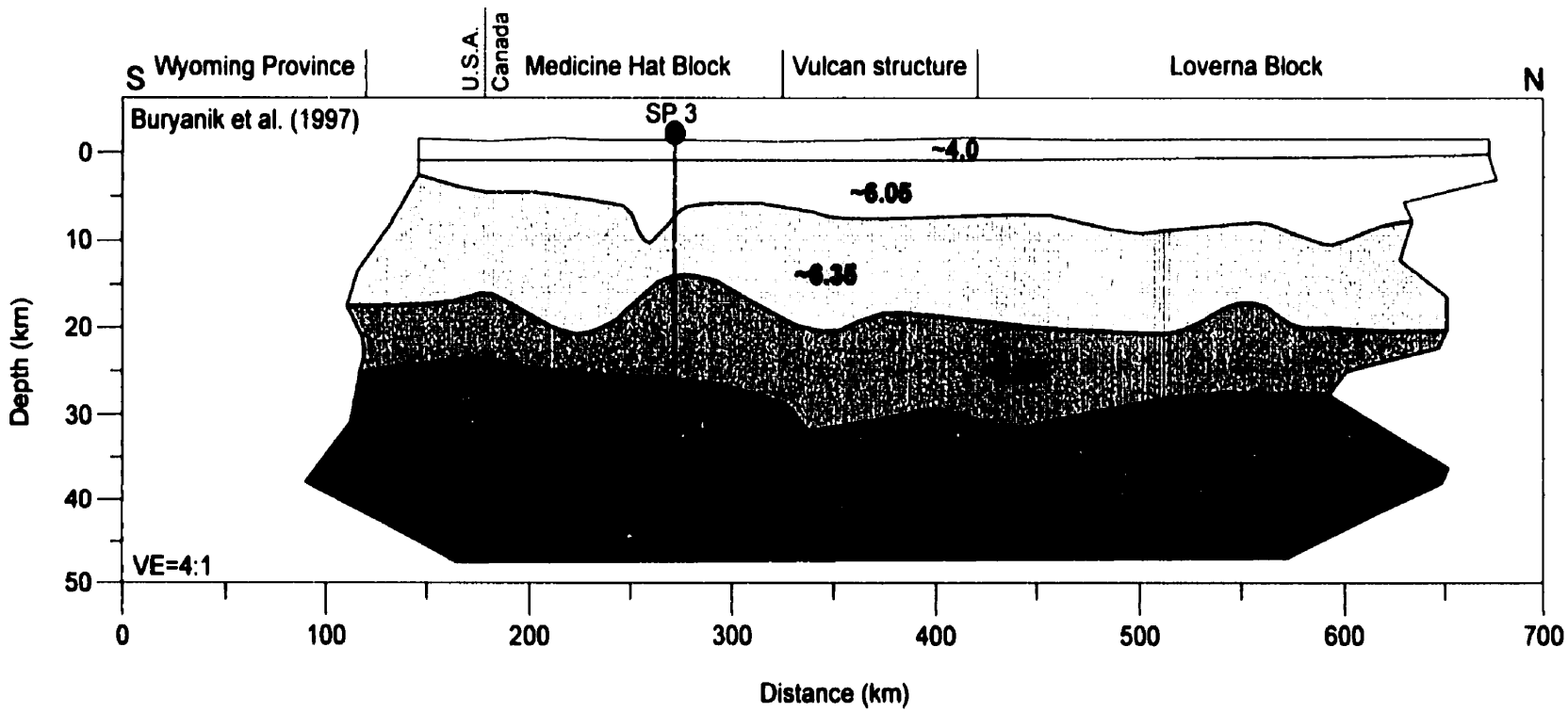


Figure 22. North-south seismic velocity model of the southern Alberta basement from SAREX seismic refraction experiment (Buryanik et al. 1997). Location of the SAREX seismic refraction line is indicated in Figure 2. Velocities are in km/s and represent averages for the different colored crustal regions. SP3 indicates the location of shotpoint 3 on the seismic refraction survey, which lies 8 km east of the eastern end of seismic reflection line 31.

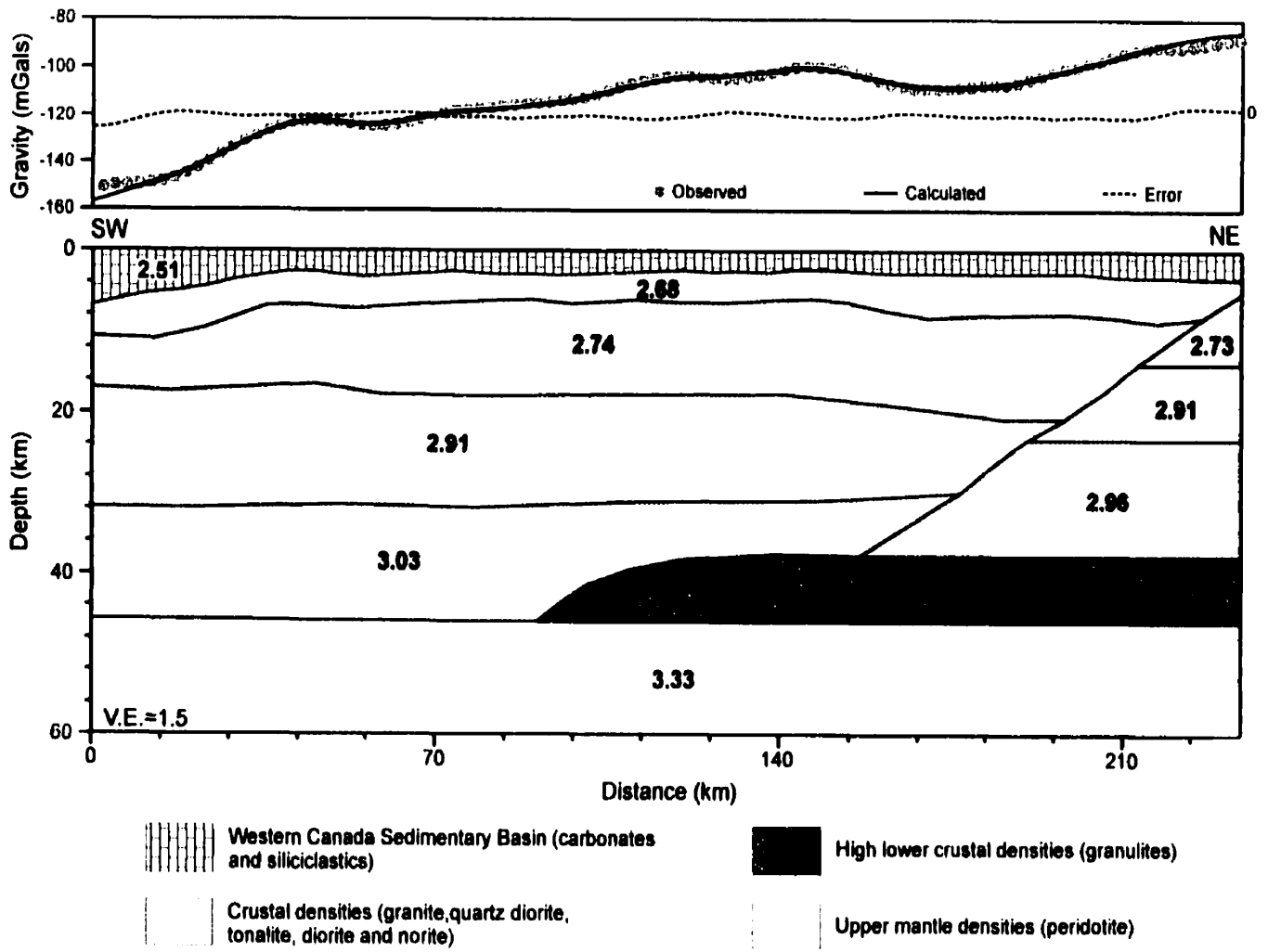


Figure 23. Southwest-northeast crustal density model of the MHB (see Figures 2 and 14 for location) with corresponding lithologies (see Table 7). Densities are in g/cm$^3$.

g/cm$^3$ (Figure 23). The short wavelength anomaly of roughly 35 km in the western portion of the gravity profile effectively is constrained by an approximate 3 to 4 km thickening of the basinal strata near the triangle zone (strata are approximately 7 to 8 km thick in that region). Other short wavelength anomalies in the order of 20 km or less are attributed to basement topography of 400 m or less, and to topography in the upper crustal layer (2.74 g/cm$^3$) of 3 km or less (Figure 23).

In summary, gravity modeling of the MHB crust supports the geometric constraints interpreted from the seismic reflection data and has shown that the Bouguer gravity data require: (1) approximately 8 km of high density lower crustal material (3.15 g/cm$^3$) that extends from 38 km to 46 km depth in the eastern half of the profile; (2) the presence of a geometric ramp in the upper to middle crust in the east; (3) seven crustal density layers (from 2.68 g/cm$^3$ to 3.03 g/cm$^3$); and (5) an upper mantle density of 3.33 g/cm$^3$ (Figure 23).

A high density lower crustal layer of 3.15 g/cm$^3$ (velocities between 7.1 km/s to 7.3 km/s) is compatible with mafic granulite compositions, such as the lower crustal xenoliths found in Eocene minette dykes associated with the Sweetgrass Hills intrusives of southern Alberta and northern Montana (Figure 2; Davis et al. 1995). On a regional scale, the long-wavelength gravity high in the eastern half of the gravity profile (Figure 23) can be followed across the Great Falls Tectonic Zone and into the Wyoming Province on the long-wavelength filtered gravity map (Figure 16). Furthermore, this gravity high corresponds to the extent of the intermediate velocity layer in the lower crust of the MHB and the Wyoming Province, interpreted from the Deep Probe seismic refraction experiment (Henstock et al. 1998). Hence, the long-wavelength gravity high is interpreted to arise from this high density (intermediate velocity) lower crustal layer, and not from the crustal-scale ramp.

# CHAPTER 4. STRUCTURAL ANALYSIS OF THE WESTERN CANADA SEDIMENTARY BASIN IN SOUTHERN ALBERTA

## 4.1 Introduction

In the Western Canada Sedimentary Basin (WCSB), the macroscopic eastern limit of Cordilleran deformation occurs at the triangle zone in the eastern margin of the Foothills of Alberta and British Columbia, but in reality, deformation, including duplexing, imbrication, and structural inversion occurs as far as 65 km east of the triangle zone within the foreland basin of southern Alberta (e.g., Skuce et al. 1992; Hiebert and Spratt 1996). The term "triangle zone" was first published by Gordy et al. (1977) to describe a structure in southwestern Alberta that is characterized on the east side by east-dipping beds of the Paleocene Porcupine Hills Formation, on the west side by west-dipping thrusted late Cretaceous to early Tertiary strata, and at depths by an autochthonous horizontal sequence. The structural analysis of the WCSB in southern Alberta presented here illustrates subsurface examples of Late Cretaceous extensional faulting in the Phanerozoic strata that occur as far as 140 km east of the triangle zone, and of structural inversion that occurs 52 km east of the triangle zone (Figure 5). This chapter also examines evidence for basement involvement in the formation and inversion of significant extensional faults in southern Alberta.

## 4.2 Stratigraphic correlation wells

Four petroleum industry wells were used to constrain the age of faulting and to determine the regional stratigraphic trends of the WCSB in southern Alberta: Gulf Blood 05-18-007-23W4; Gulf et al. South Blood 15-12-006-24W4; Husky et al. Cranford 16-20-008-18W4; and Home Yellow Lake 01-36-009-13W4 (Figures 2, 5 and 6). These wells were chosen on the basis of their proximity to the seismic reflection lines used in this study and on the extent of available formation picks (IPL [International Petrodata Ltd.] picks for Cretaceous to Cambrian strata), which allowed the entire Phanerozoic sequence to be tied to the seismic reflection data. Only Gulf Blood 05-18-007-23W4 intersects the Precambrian basement. The well logs, including sonic delta-T compressional, density and depth curves were obtained from QcData. Synthetic seismograms were calculated in GMA Plus Modelling using sonic, density and depth curves (except for Home Yellow Lake 01-36-009-13W4; see Table 8), and a zero-phase

| Well name | Location | Projection | Types of logs | KB (m ASL) | Start of log (m below KB/m ASL) |
|---|---|---|---|---|---|
| Gulf Blood | 05-18-007-23W4 | 13.5 km to south | Sonic, Bulk density, Depth | 1016.2 | 316.7 / 699.5 |
| Gulf et al. South Blood | 15-12-006-24W4 | 2.8 km to south | Delta-T compressional, Bulk density, Depth | 1037.7 | 452.0 / 585.7 |
| Husky et al. Cranford | 16-20-008-18W4 | 260 m to north | Delta-T compressional, Bulk density, Depth | 903.8 | 224.0 / 678.8 |
| Home Yellow Lake | 01-36-009-13W4 | 250 m to northwest | Sonic, Depth | 816.6 | 312.9 / 503.7 |

| Well number on figures | Well name | Calculation using t=2d/v | Start of log on seismic (s twt) |
|---|---|---|---|
| S1 | Gulf Blood | 500.5 m @ 2700 m/s | 0.371 |
| S2 | Gulf et al. South Blood | 614.3 m @ 2700 m/s | 0.455 |
| S3 | Husky et al. Cranford | 521.2 m @ 2700 m/s | 0.386 |
| S4 | Home Yellow Lake | 696.3 m @ 2700 m/s | 0.520 |
| Seismic reflection datum = 1200 m<br>Replacement velocity = 2700 m/s | | | |

Table 8. Well log and projection information, along with well tie calculations. The start of log in m ASL is subtracted from the seismic reflection datum of 1200 m. Then, this value is timed by two and divided by the replacement velocity of 2700 m/s to give the start of log in twt associated with the seismic reflection data. Abbreviations used: KB (Kelly Bushing), ASL (above sea level), t (time), d (depth), v (velocity), and twt (two-way-time).

Ricker wavelet of 25 Hz. They were plotted at the same scale as the seismic reflection data and multiples were not included in the synthetic calculation. Formation tops include Deadwood (Cambrian), Exshaw (Devonian), Livingstone and Turner Valley (Mississippian), Rierdon (Jurassic), Base of Fish Scales (lowermost Upper Cretaceous), and Milk River and Belly River Group strata (Upper Cretaceous). Figure 24 (A, B and C) shows the four synthetic seismograms projected into the SALT seismic reflection data with the formation picks. The four synthetic seismograms were tied to the seismic reflection data using depth and velocity information from the well logs and the seismic reflection data (see Table 8 for explanation and for projection information).

## 4.3 Seismic reflection observations

### 4.3.1 Introduction

For the regional stratigraphic and structural study of the WCSB in southern Alberta, two different scales of seismic reflection plots are used. Figures 25, 26 and 27 show the migrated SALT lines 30, 29, and 31 displayed to 3 s twt with a vertical exaggeration of 3:1. Figure 28 illustrates a concatenated migrated seismic section including SALT lines 30, 29, and 31. The concatenated seismic profile is plotted at a vertical exaggeration of approximately 20 times in order to accentuate the regional stratigraphic features of the WCSB in southern Alberta, and to emphasize more subtle features within the sedimentary sequence, such as faults and onlap features. The seismic profile contains every eighth trace (7/8 of the traces were decimated such that the plotted trace spacing is 100 m) and was plotted from 0 to 2.6 s twt. However, the lines originally were plotted with no vertical exaggeration and no trace decimation (trace spacing 12.5 m) in order to tie the synthetic seismograms to the seismic reflection data.

One of the main aims of this chapter is to study the geometry of the faults observed on the SALT dataset, and thus, the issue of vertical resolution is very important. Vertical resolution of seismic reflection data is limited to approximately ¼ of the dominant wavelength (Sheriff 1991). Frequency plots reveal that dominant frequencies present with the basinal portion of the SALT dataset range from 30 to 40 Hz. Vertical resolution for the SALT dataset translates to approximately 30 m, when using a dominant frequency of 35 Hz and an average velocity for the sedimentary sequence of 4500 m/s. Thus, faults displaying a vertical throw of 30 m or less are probably not

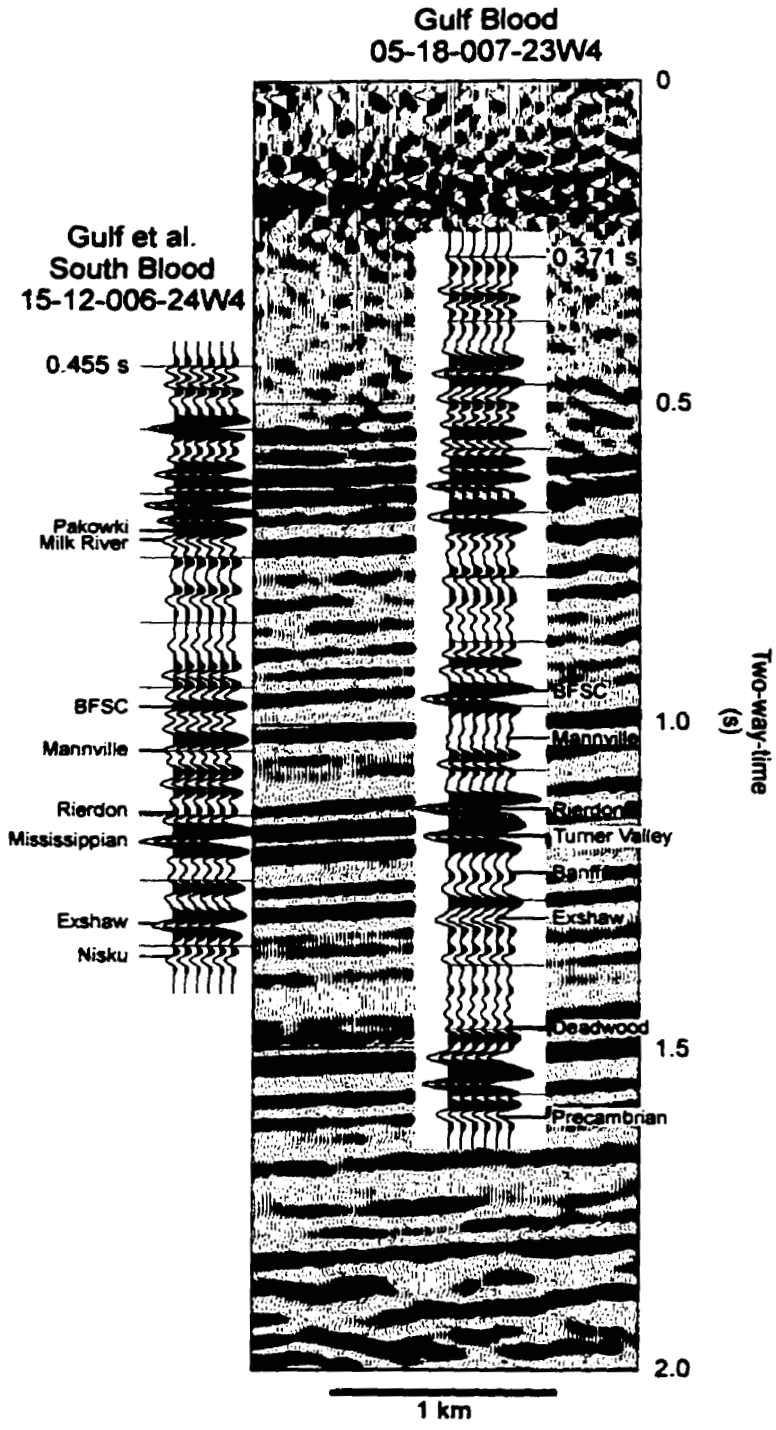


Figure 24(A). Synthetic seismograms calculated for Gulf Blood 05-18-007-23W4 and Gulf et al. South Blood 15-12-006-24W4 displayed at normal polarity. BFSC refers to Base of Fish Scales. Note that formation ties of Gulf Blood are not accurate for the Cretaceous strata as this well was projected 13.5 km to the south. However, Gulf Blood gives an accurate tie for the Paleozoic and near-basement reflectors.

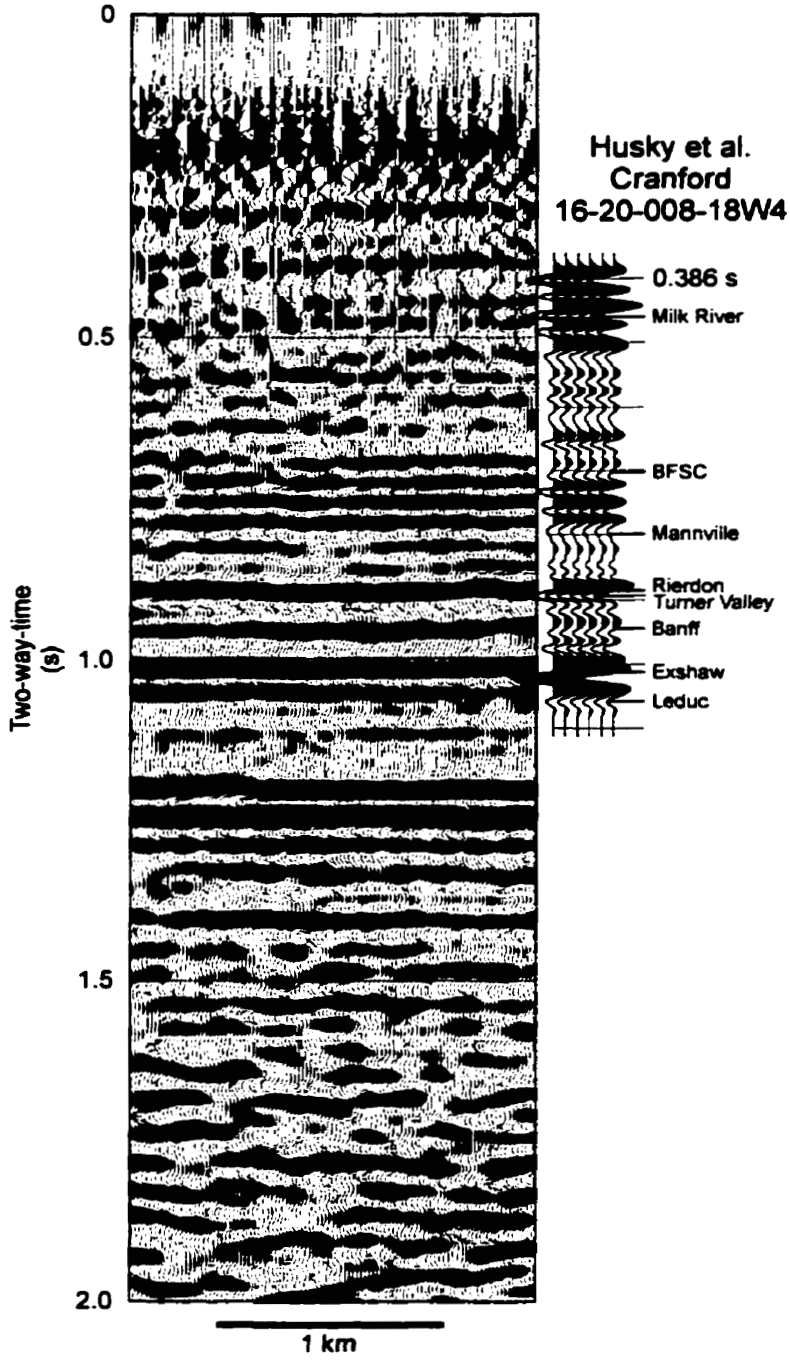


Figure 24(B). Synthetic seismogram calculated for Husky et al. Cranford 16-20-008-18W4 displayed at normal polarity. BFSC refers to Base of Fish Scales.

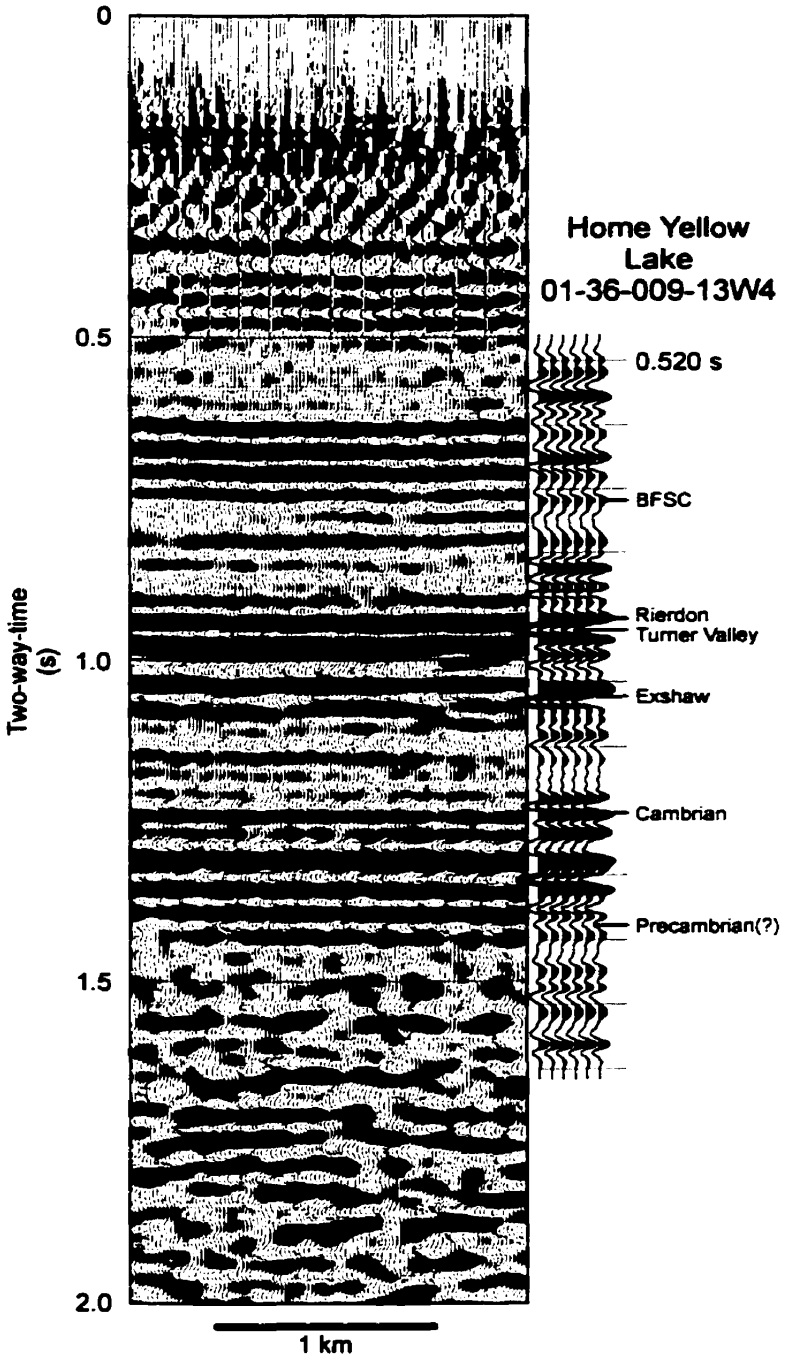


Figure 24(C). Synthetic seismogram calculated for Home Yellow Lake 01-36-009-13W4 displayed at normal polarity. BFSC refers to Base of Fish Scales. No IPL pick for the Precambrian crystalline basement was available for this well, but the synthetic seismogram does extend into the Precambrian basement (approximate pick is indicated).

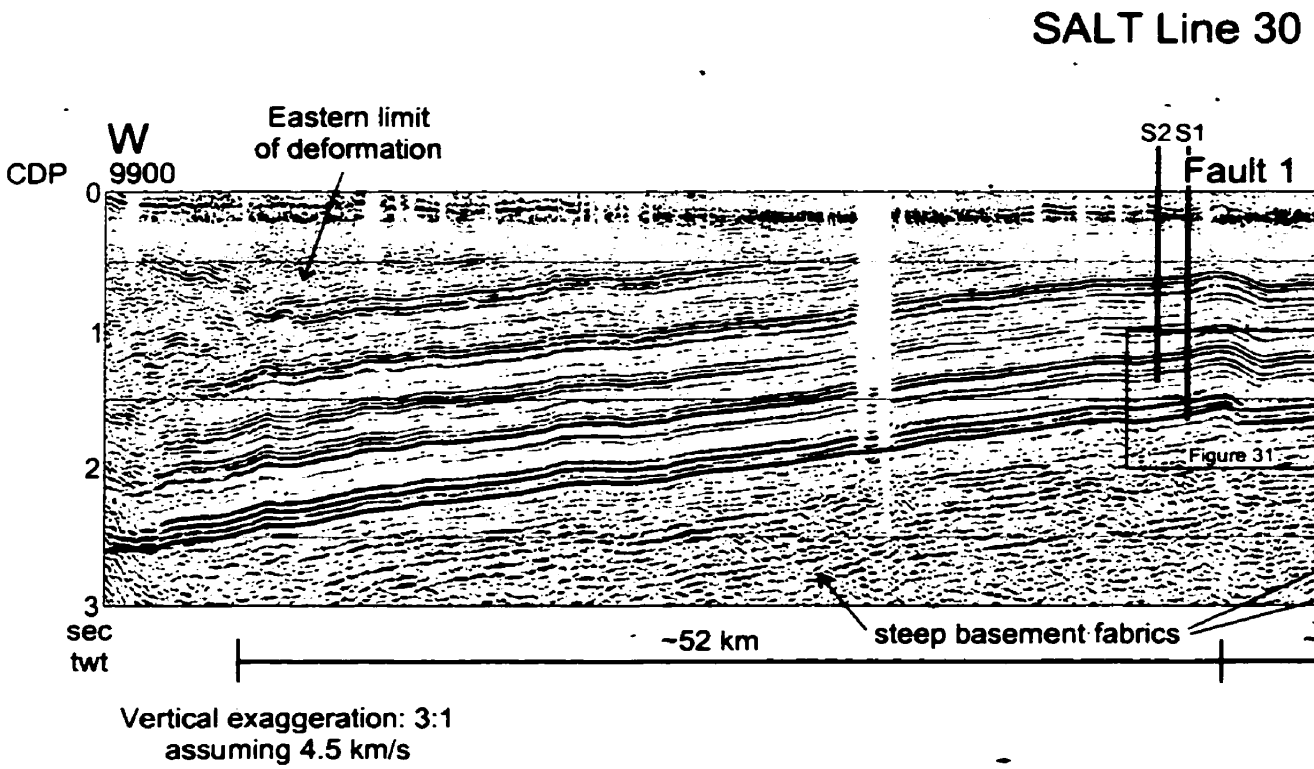


Figure 25. SALT line 30 extending west-east for 110 km. The grey marker represents the ne
15-12-006-24W4 (S2) and Gulf Blood 05-18-007-23W4 (S1) is shown. Four signi
the eastern half of line 30. Fault 1 occurs ~52 km east of the triangle zone (easter
west-dipping compressional fault. The remaining three faults are interpreted as e
significantly to the west to reach a depth of ~6 km at the western end of the profil
basement fabrics and sub-parallel high-amplitude reflections occur in the upper p

30

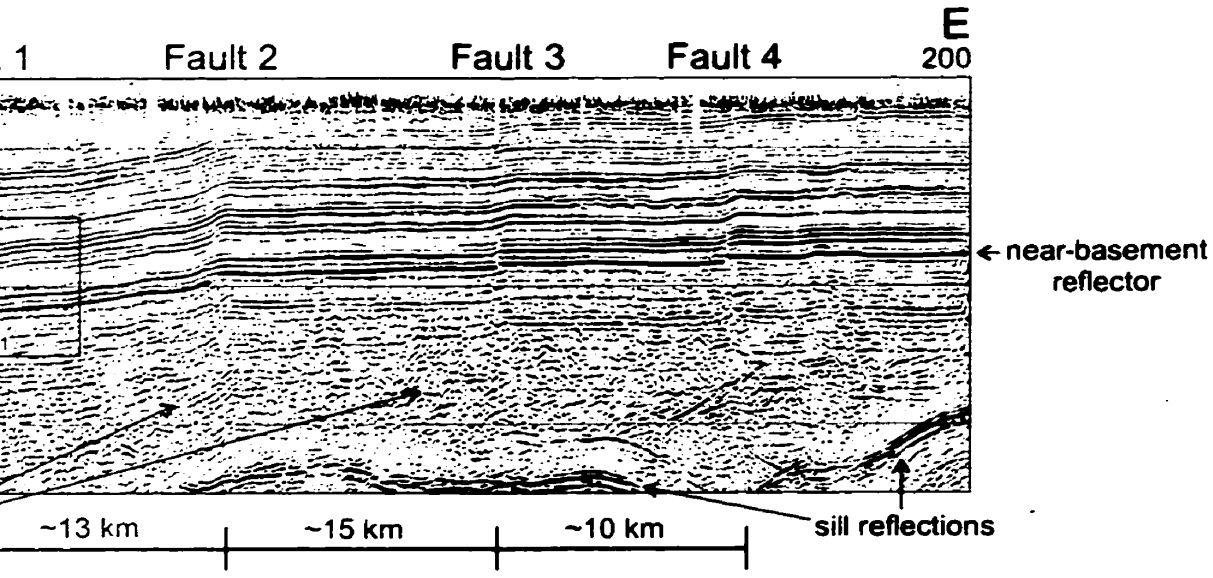


e near-basement reflector. The location of wells Gulf et.al. South Blood
ignificant faults, separated at intervals from 10 to 15 km are visible in
stern limit of Cordilleran deformation) and is interpreted to represent a
s extensional faults downthrown to the west. The basin deepens
rofile using an average velocity of 4.5 km/s for 2.6 s twt. Steep
er portion of the basement. Inset box shows location of Figure 31.

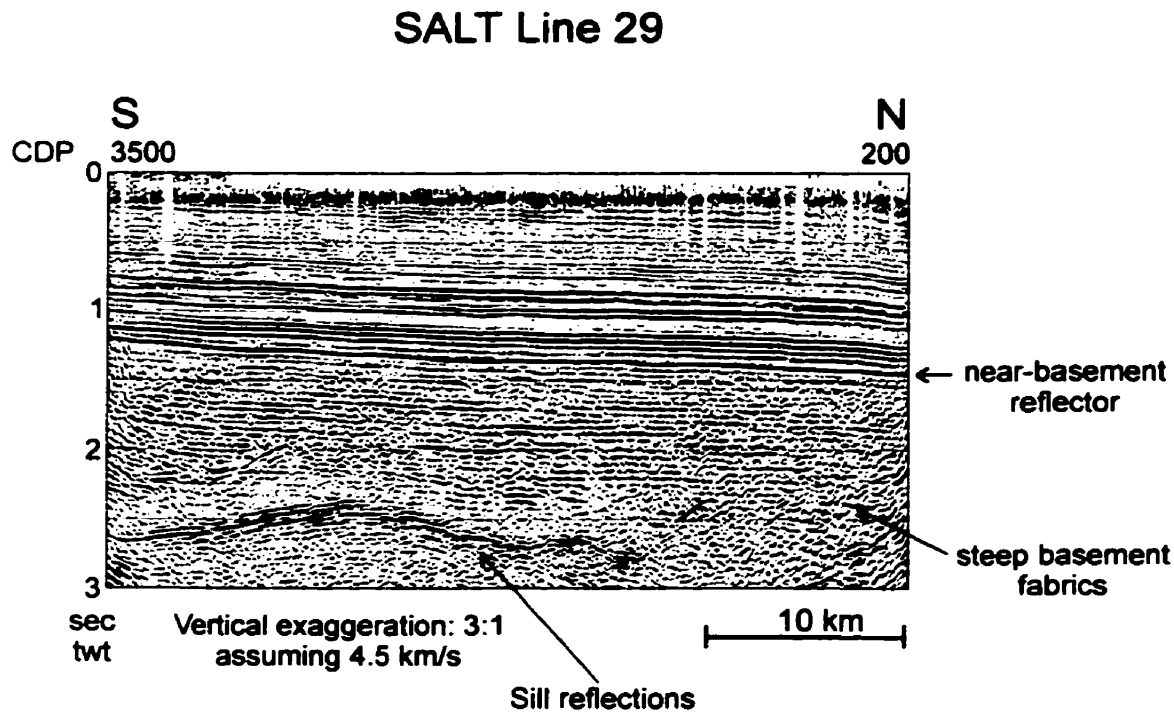


Figure 26. SALT line 29 extending north-south for 40 km. The grey marker is the near-basement reflector. The basin deepens significantly to the north and no faults are visible on this line. Steep basement fabrics and sub-parallel high-amplitude reflections (sills) occur in the upper portion of the basement.

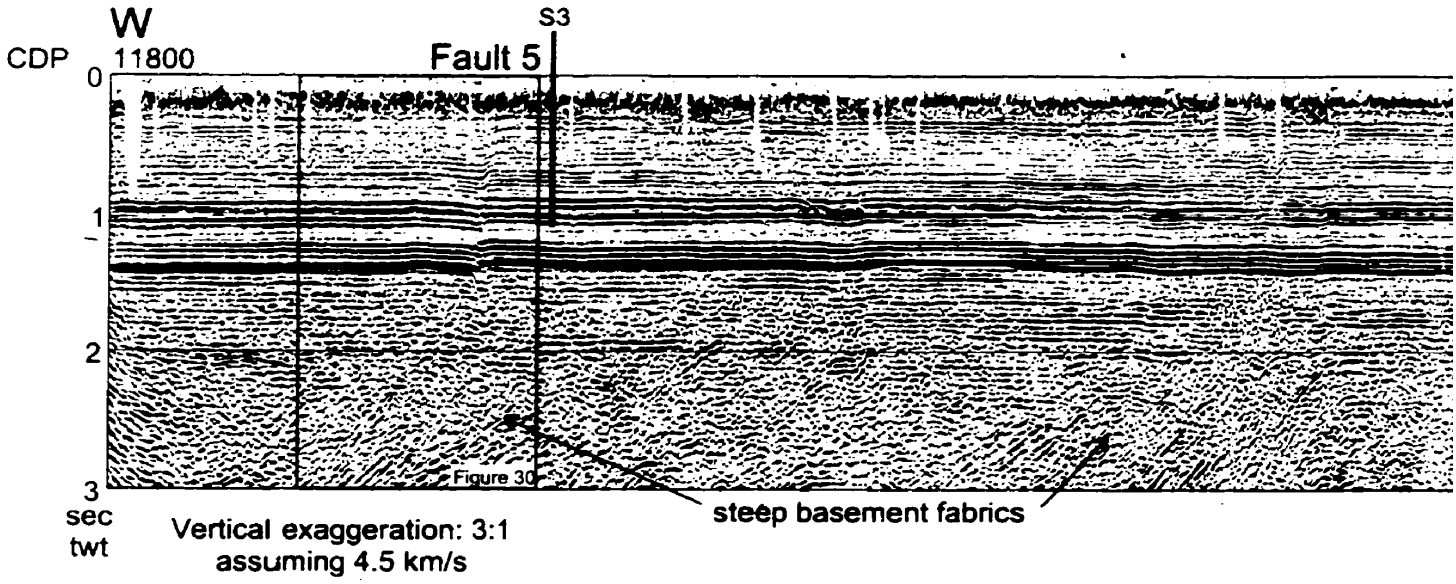


Figure 27. SALT line 31 extending west-east for 140 km. The grey marker represents the near-base
01-36-009-13W4 (S4) are shown. Extensional Fault 5 is visible in the western portion of th
Fault 5 is located ~140 km east of the triangle zone and 40 km north of line 30. The basin
basement fabrics are prominent in the western half of the profile. Inset box shows location

LT Line 31

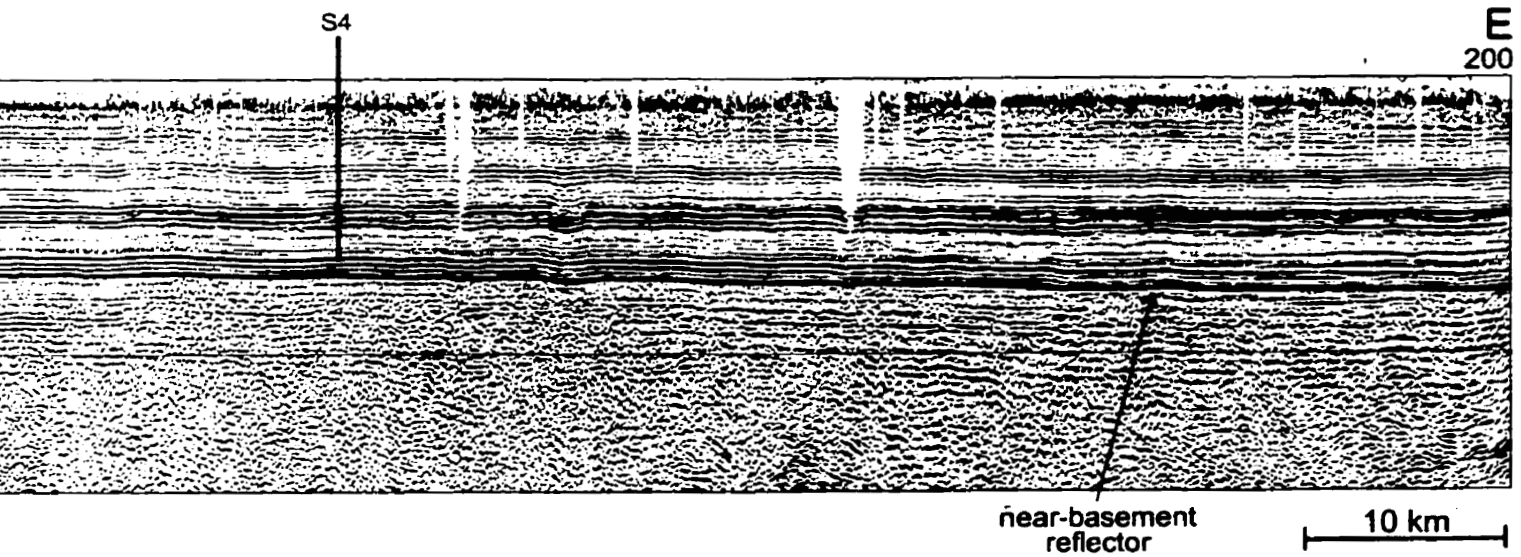


-basement reflector. The location of wells Husky et al. Cranford 16-20-008-18W4 (S3) and Home Yellow Lake
n of the line and aligns directly with a steeply-dipping basement fabric that can be followed to the middle crust.
basin deepens slightly to the east where it coincides with the westernmost portion of the Williston Basin. Steep
cation of Figure 30.

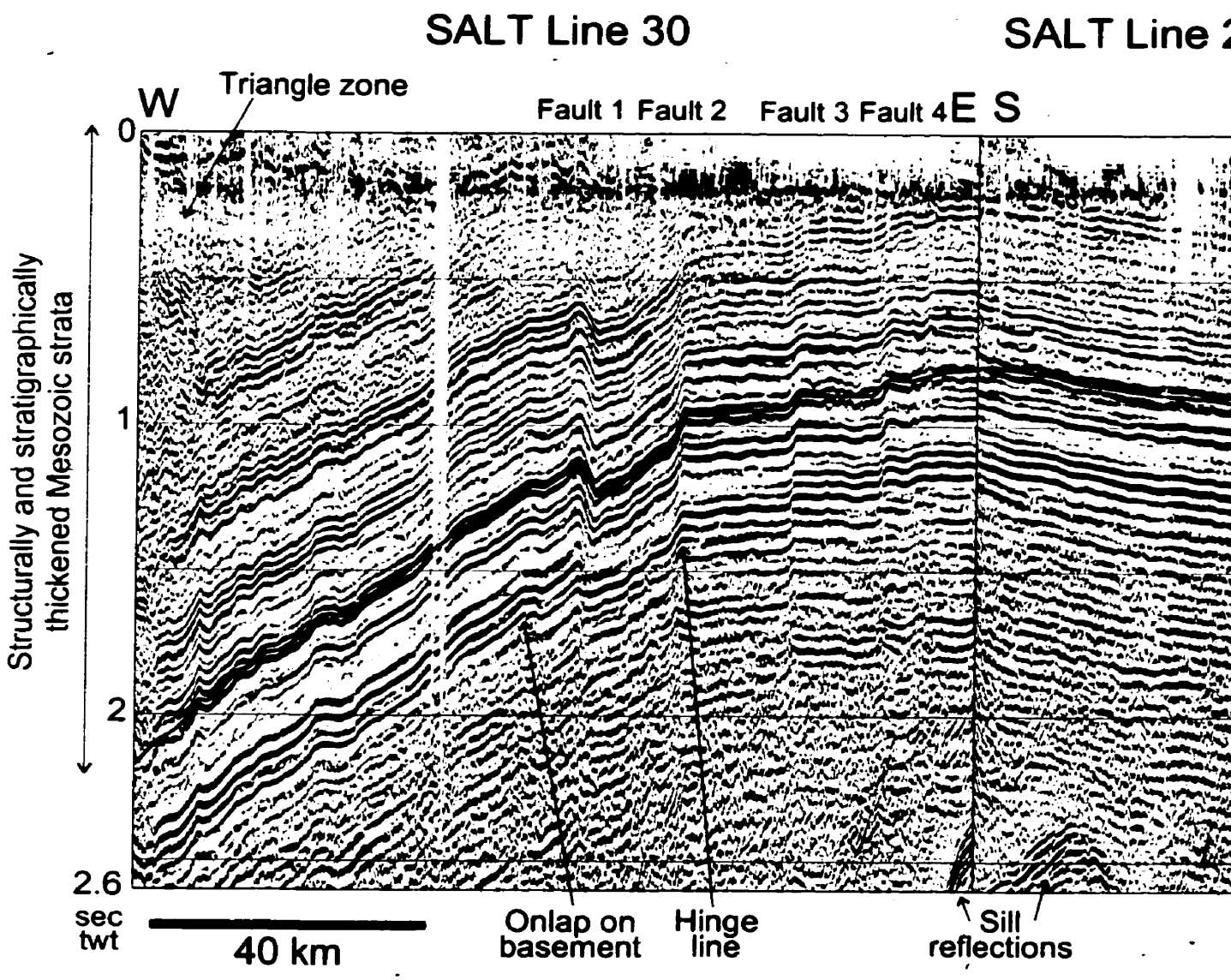


Figure 28: 290-km concatenated seismic reflection profile including SALT lines 30, 29 and 31, plotte
grey marker indicates the top of Mississippian separating the Mesozoic and Paleozoic str
to ~5 km thick), triangle zone, fault distribution, a hinge zone marked by Fault 2, arching c
eastern portion of the profile. Note that the basement surface has a northwest dip in the n

ine 29

SALT Line 31

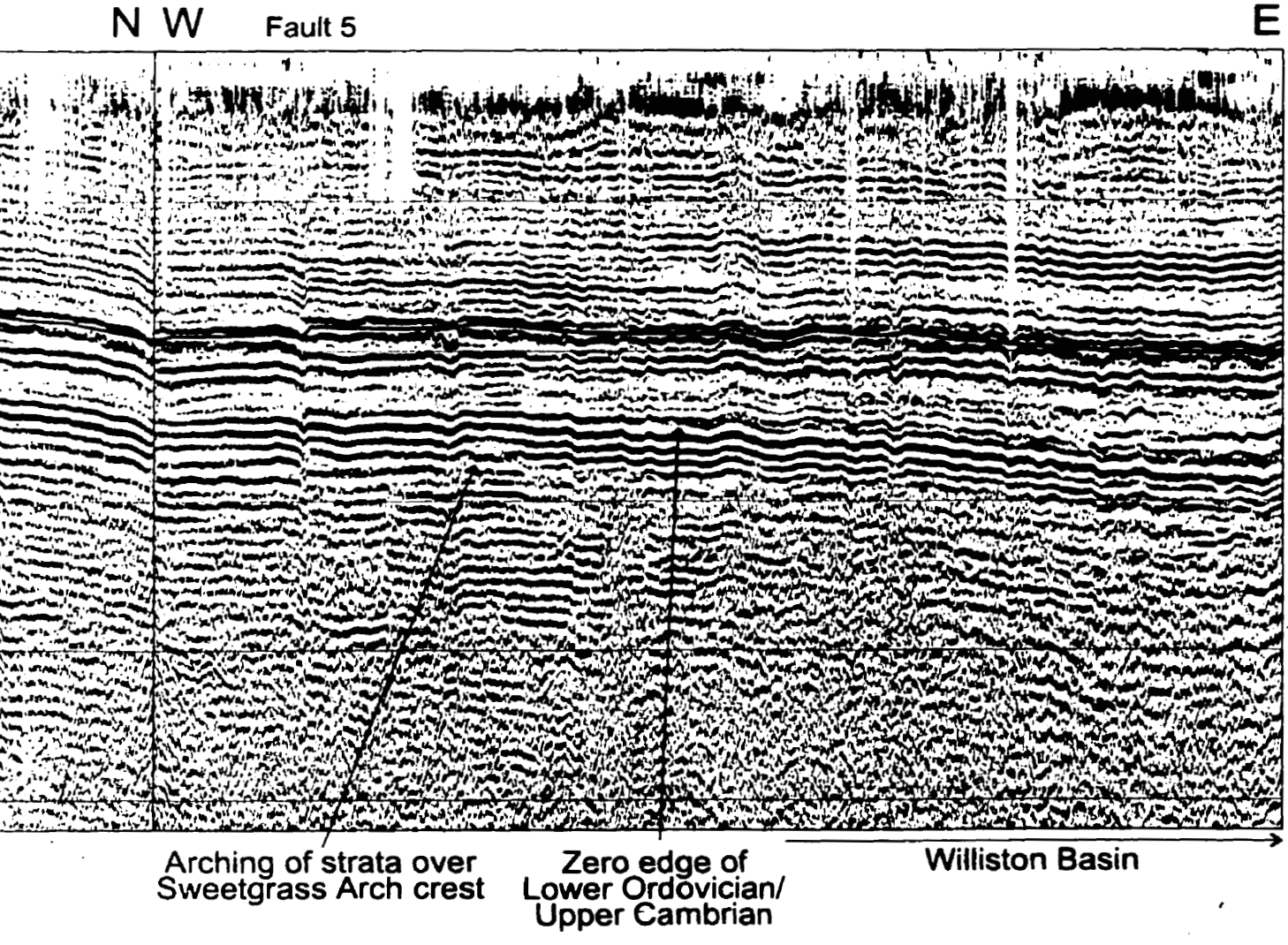


1, plotted with a vertical exaggeration of approximately 20:1 assuming an average velocity of 4.5 km/s. The ozoic strata. The concatenated profile illustrates the considerable western thickening of Mesozoic strata (up arching of Phanerozoic strata over the Sweetgrass Arch, and the western limit of the Williston Basin in the in the middle of the profile.

resolvable seismically. In addition, the SALT dataset contains prominent multiple reverberations in the upper portion of the basement that are generated from the strata of the WCSB and obscure the geometric relationship between basement fabrics and faults within the sedimentary sequence.

### 4.3.2 Regional stratigraphic trends

The Phanerozoic sedimentary section is recognizable by the continuous horizontal to sub-horizontal layering of the WCSB strata, ranging from 0.0 to 1.25 s twt (~3.0 km) in the middle of the seismic profile to 0.0 to 2.6 s twt (~6.0 km) in the westernmost portion of the seismic profile (Figures 25 and 28). Furthermore, the Phanerozoic isochron thins considerably to the south from 1.5 to 1.2 s twt (overall thinning of ~675 m) on line 29, indicating that the basement surface has an actual dip to the northwest in that region (Figure 26), in agreement with a basement structure contour map of the area (Burwash et al. 1994; Figure 29). Along line 31, a subdued arching of the strata over the middle of the line illustrates the geometry of the Sweetgrass Arch (Figures 27 and 28). There, the Lower Ordovician/Upper Cambrian zero edge is visible, indicating the western margin of the Williston Basin (Figure 28). Onlap features on the near-basement reflector occur sporadically throughout the seismic reflection data and are attributed to local basement relief during early Cambrian time (Figure 28). Regionally, the thickness of Paleozoic strata does not appear to change east-west along the seismic reflection profile (Figure 28). In contrast, the Mesozoic strata are structurally and stratigraphically thickened westward reaching a thickness of approximately 5 km at the westernmost end of the seismic reflection profile (Figure 28).

### 4.3.3 Basement fabrics

Steeply-dipping basement fabrics that project to the top of the basement occur throughout the seismic reflection data where multiple reverberations are not particularly prominent. These steep basement fabrics relate to the dipping reflectivity of zones 2 and 3 within the upper to middle crust of the Medicine Hat Block (see Section 3.3). They are recognizable especially in: (1) the middle of line 30, where sporadic basement fabrics appear to align with the faults in the sedimentary sequence (e.g., Faults 2 and 3 in Figures 25 and 28); (2) the western half of line 31, where steeply dipping basement fabric appears to align directly with a fault (Figures 27 and 30); and (3) along line 29

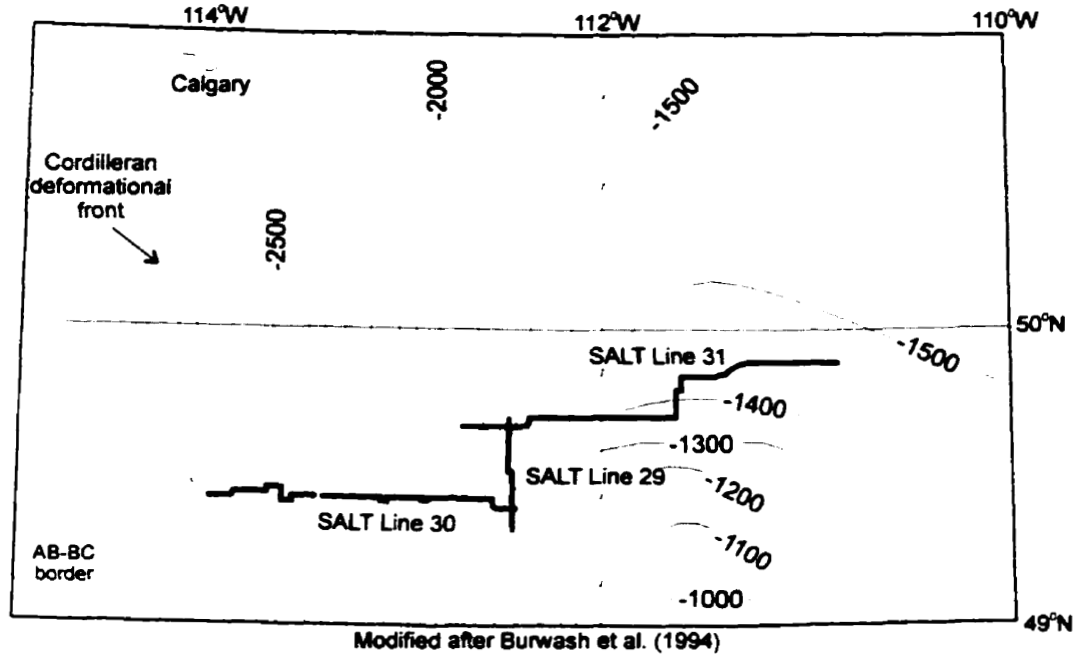


Figure 29. Structure contour map of the Precambrian basement surface (Burwash et al. 1994). Basement surface is dipping to the northwest near the intersection of SALT lines 29 and 31 representing the western flank of the Sweetgrass Arch. Contour intervals are in meters.

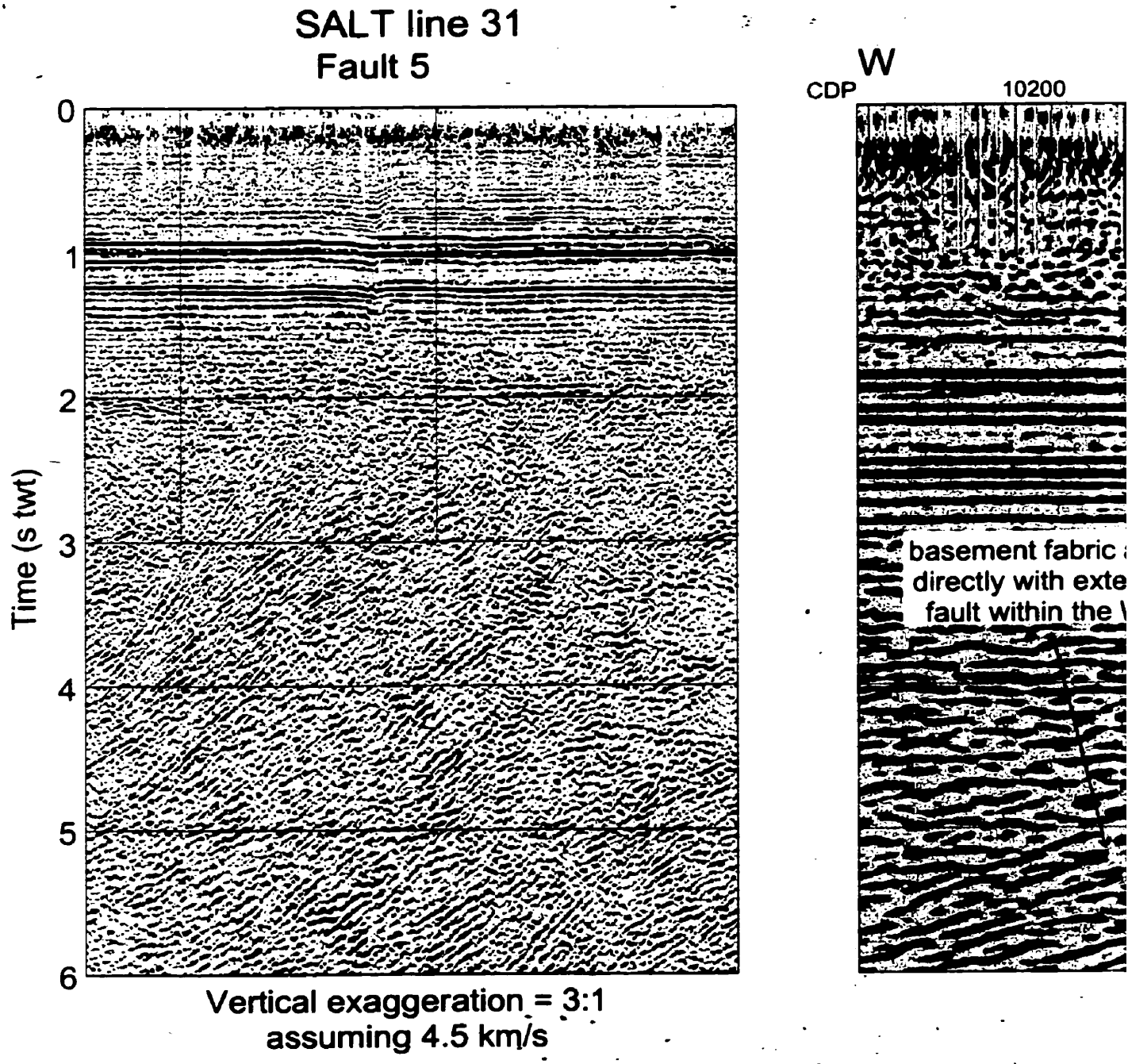


Figure 30. Geometric correlation of basement fabrics with faulting within the sedimentary sequenc
extensional Fault 5 suggesting that basement structure may have controlled the positio
observed in this figure relate to the dipping crustal reflectivity of Archean zone 3 (see S

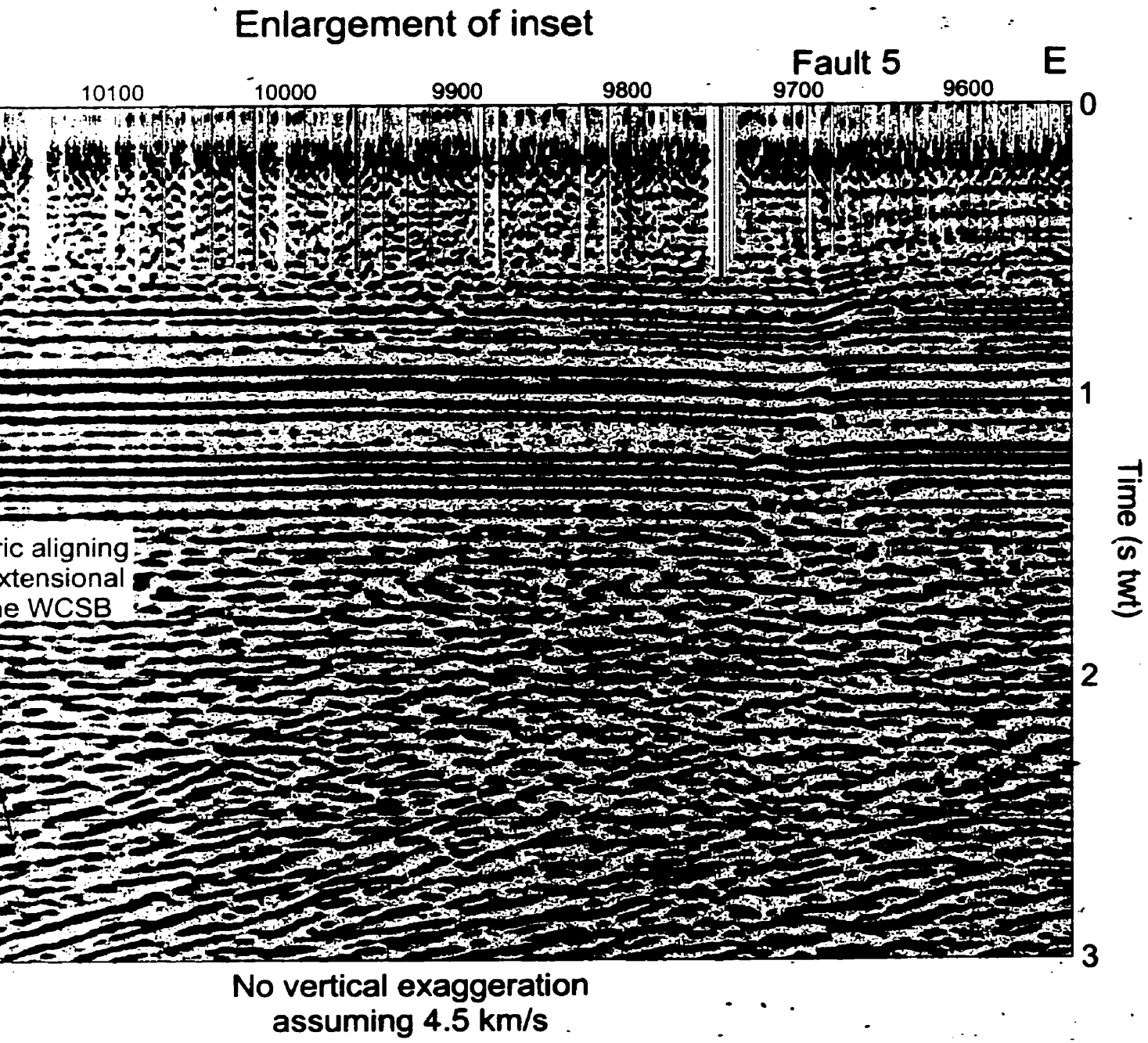


ence in the western portion of line 31. A west-dipping basement fabric appears to align directly with sitioning of this Late Cretaceous extensional fault. The steeply west-dipping basement fabrics e Section 3.3) as the dipping basement fabrics extend to the middle crust.

(Figures 26 and 28). In addition, the Precambrian sill reflections are visible in the eastern half of line 30 and along line 29, between 2.0 and 3.0 s twt (Figures 25 and 26). The strike of the basement fabrics seen on seismic reflection data (zones 2 and 3; Figure 17) is constrained as northwest-southeast and north-northwest-south-southeast on the basis of potential-field fabric trends (Lemieux et al. 2000).

## 4.4 Structural interpretation

### 4.4.1 Seismic reflection expression of fault geometries

Five significant faults are observed on the SALT dataset (Figures 25, 27 and 28). The westernmost fault occurs at about 52 km east of the triangle zone, whereas the easternmost fault occurs at about 140 km east of the triangle zone. The reflection geometry of the westernmost fault (Fault 1) appears to indicate extensional motion with downdropping to the east. However, the strata on the western side of the fault (hanging wall), immediately adjacent to the fault, are elevated above regional stratal isochrons, suggesting a west-dipping compressional fault (Figures 31 and 32; Williams et al. 1989). Moreover, Fault 1 is associated with a hanging wall anticline, and a syncline on the eastern, footwall side of the fault (Figure 32). In contrast, the remaining faults (Faults 2, 3, 4 and 5) display extensional offset downdropping to the west (Figures 25, 27, 28, and 33 to 36). Faults 3 and 4 show onlap features within Lower Cretaceous, Jurassic, and Mississippian reflectors, which are interpreted to represent growth strata (Figures 34 and 35). The five faults appear to be separated at approximately uniform west-east intervals, from 11 to 15 km (Figures 25 and 28). The presence of what appears to be a hinge line, delineated by Fault 2 on line 30, indicates the location of an abrupt change in dip of the basement, and marks the westward thickening of the Jura-Cretaceous strata (Figure 28).

Two different fault geometries emerge from the detailed study of the faults observed on SALT lines 30 and 31. On the one hand, Faults 1 through 4 on line 30 display a definite break in reflections for the near-basement through Devonian strata. They also influence the younger, overlying strata as folding of Mississippian to uppermost Cretaceous strata (at least into Milk River and Belly River Groups) is recognized (Figures 32 to 35, and 37). On the other hand, Fault 5 on line 31 displays a definite break in reflections from the near-basement into lowermost Upper Cretaceous strata (Base of Fish Scales) with different offsets along the fault (Figures 36 and 37).

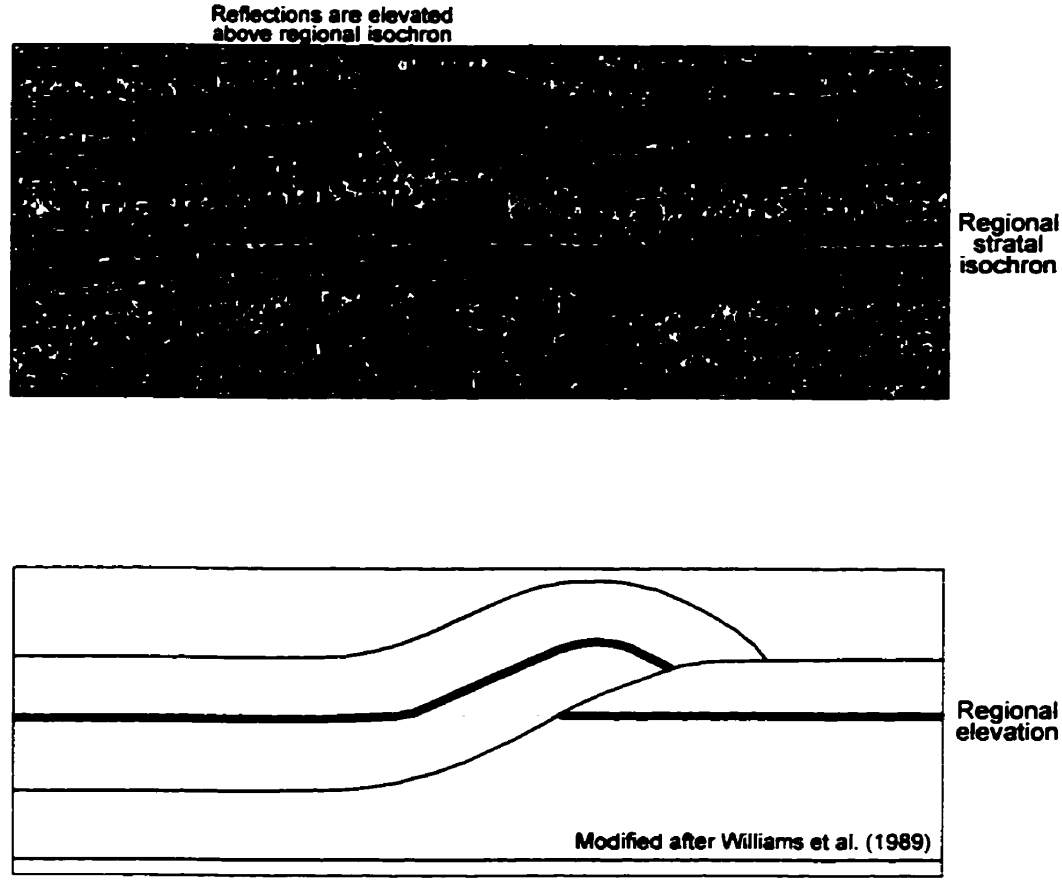


Figure 31. Reflection geometry of west-dipping compressional Fault 1. The reflections immediately adjacent on the western side of the fault (hanging wall) are elevated above a regional stratal isochron suggesting a west-dipping compressional fault (Williams et al. 1989).

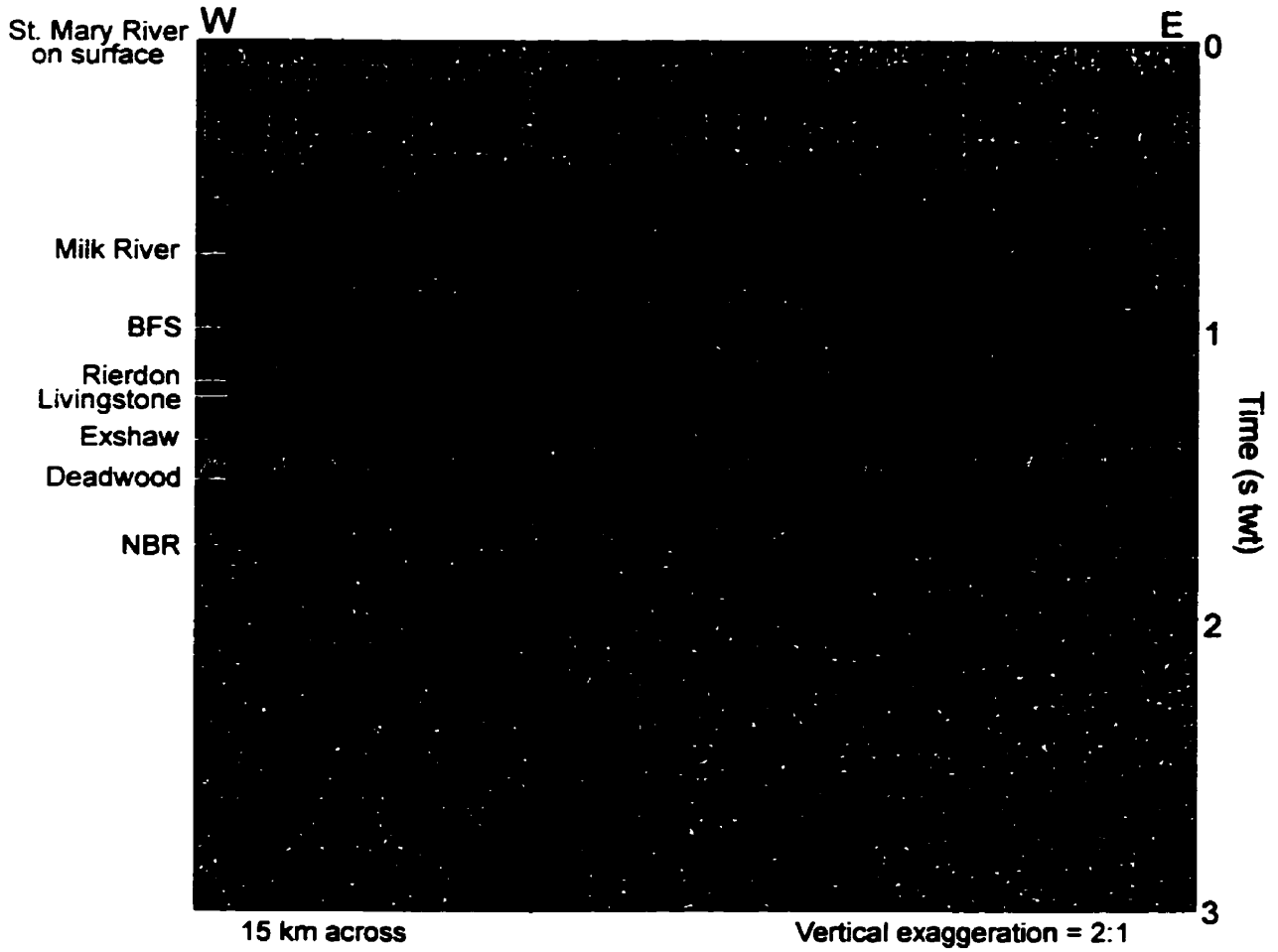


Figure 32. Fault 1 on SALT line 30 located ~52 km east of the triangle zone. This fault shows a break in near-basement (NBR), Cambrian (Deadwood) and Devonian (Exshaw) reflectors with folding of overlying Mississippian (Livingstone), Jurassic (Rierdon), Lower Cretaceous (Base of Fish Scales - BFS) and Upper Cretaceous (at least into Belly River Group) reflectors. The geometry of Fault 1 is distinct from the other faults on the SALT dataset in that the hanging wall (western side) appears to be elevated above regional suggesting that this fault is a west-dipping compressional fault. Note the presence of a hanging wall anticline on the west side of the fault.

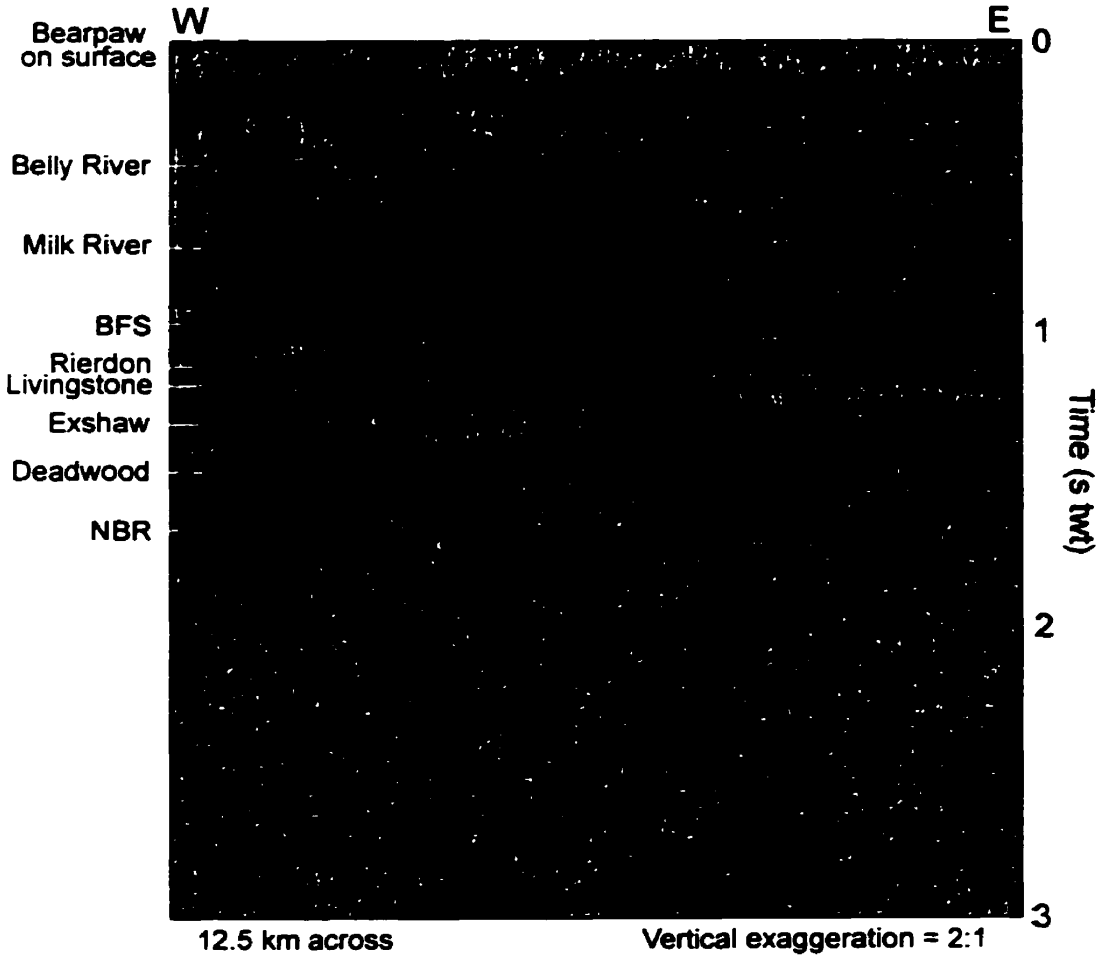


Figure 33. Fault 2 on SALT line 30 located ~65 km east of the triangle zone. This down-to-the-west extensional fault displays a break in near-basement (NBR), Cambrian (Deadwood) and Devonian (Exshaw) reflectors with folding of overlying Mississippian (Livingstone), Jurassic (Rierdon), Lower Cretaceous (Base of Fish Scales - BFS) and Upper Cretaceous (at least into Belly River Group) reflectors.

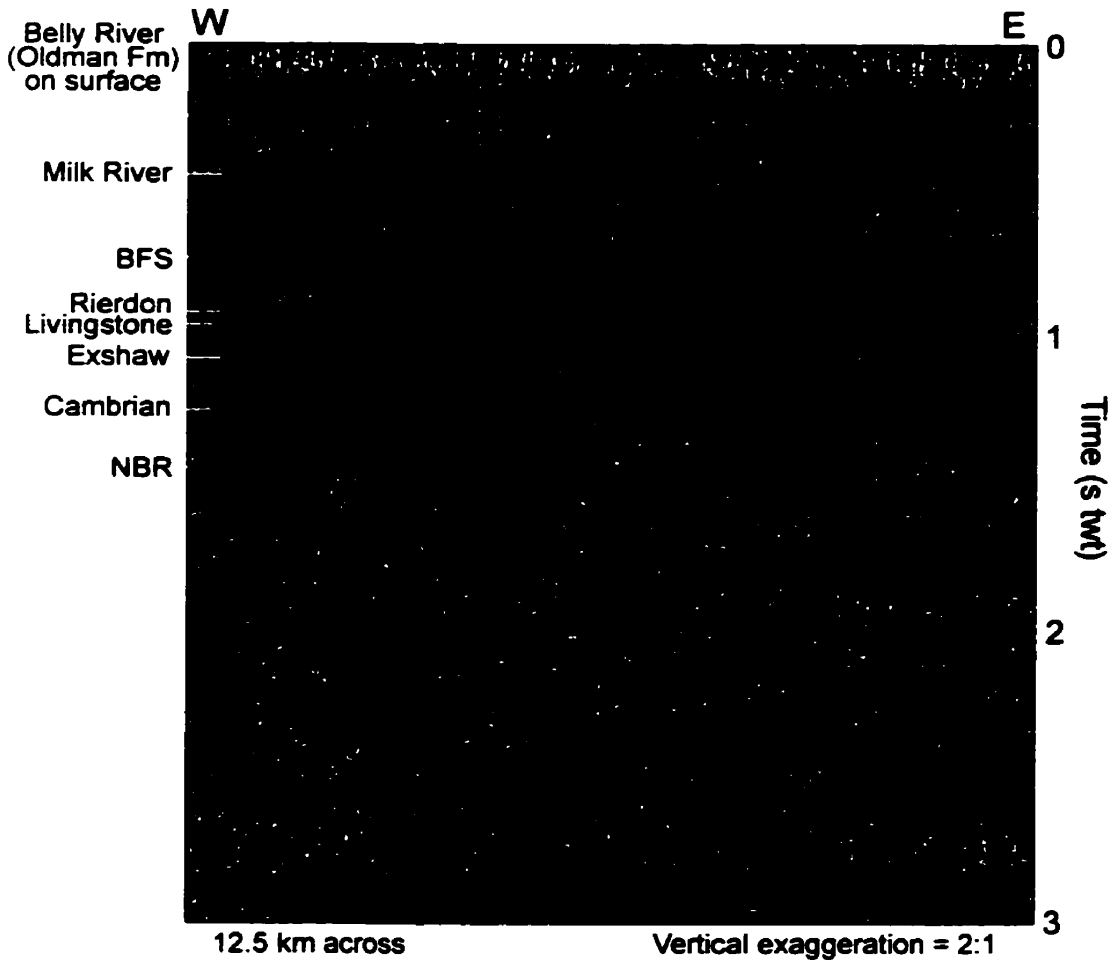


Figure 34. Fault 3 on SALT line 30 located ~80 km east of the triangle zone. This down-to-the-west extensional fault exhibits a break in near-basement (NBR), Cambrian and Middle to Upper Devonian reflectors with folding of overlying Exshaw, Mississippian (Livingstone), Jurassic (Rierdon), Lower Cretaceous (Base of Fish Scales - BFS) and Upper Cretaceous (at least into Milk River Group) reflectors. Note onlap of Lower Cretaceous reflectors onto the extensional fault.

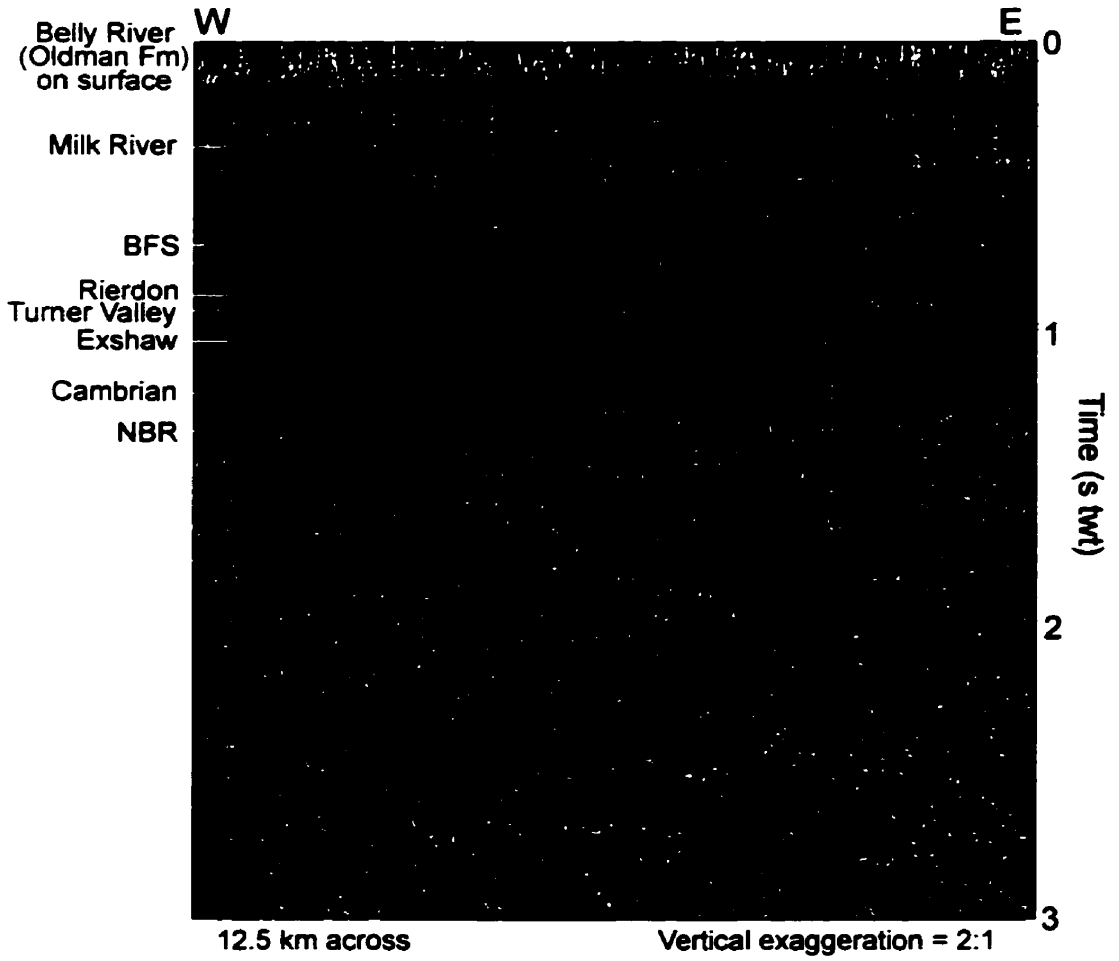


Figure 35. Fault 4 on SALT line 30 located ~90 km east of the triangle zone. This down-to-the-west extensional fault shows a break in near-basement (NBR), Cambrian and Devonian (Exshaw) reflectors with folding of overlying Mississippian (Turner Valley), Jurassic (Rierdon), Lower Cretaceous (Base of Fish Scales - BFS) and Upper Cretaceous (at least into Milk River Group) reflectors. Note onlap of Mississippian and Lower Cretaceous reflectors onto the extensional fault.

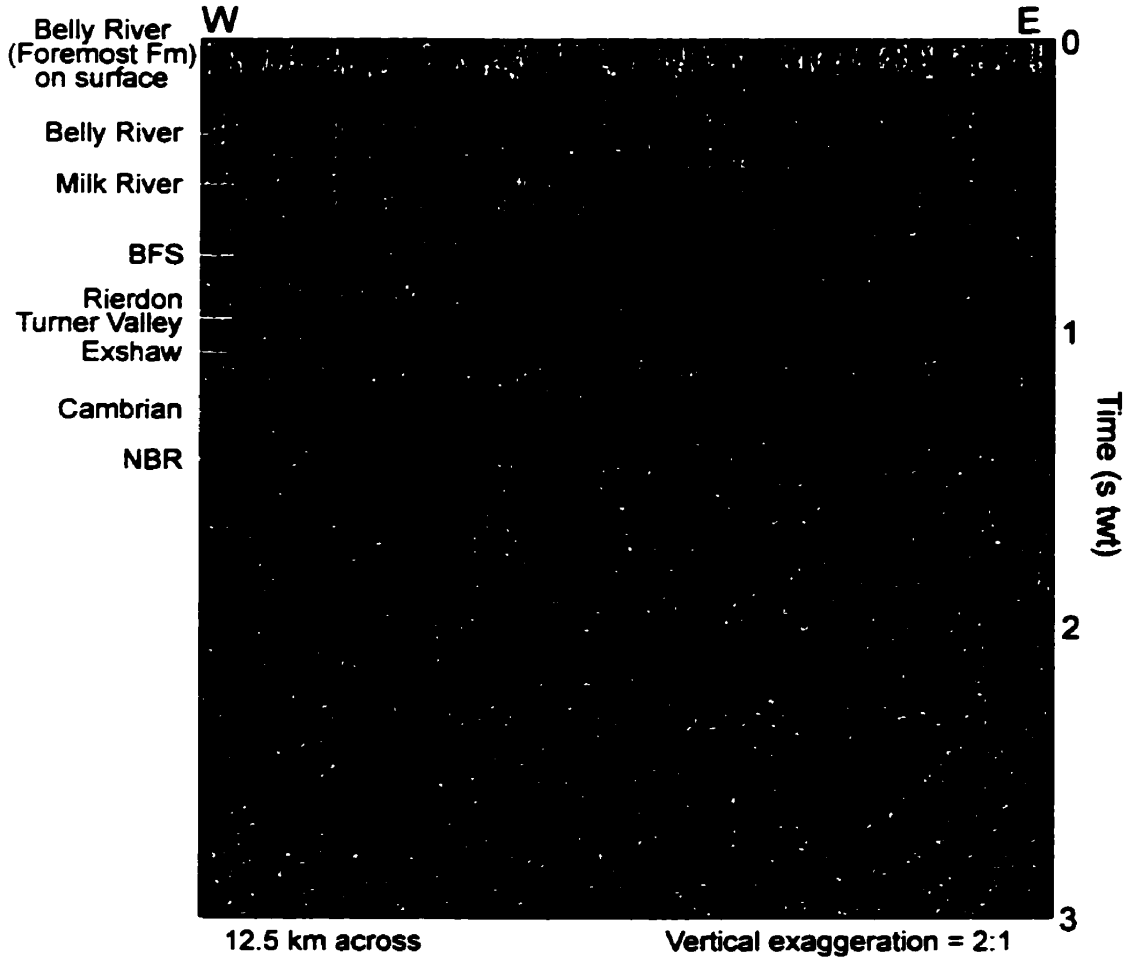


Figure 36. Fault 5 on SALT line 31 located ~140 km east of the triangle zone. This down-to-the-west extensional fault displays a break in near-basement (NBR) to Lower Cretaceous reflectors (Base of Fish Scales - BFS), folding of lower Upper Cretaceous reflectors (Milk River Group) and horizontal undeformed uppermost Upper Cretaceous reflectors (Belly River Group and younger).

Figure 37. (next page) Line diagram interpretation of fault geometries in time showing vertical offsets for Faults 1 to 5. (A) Fault 1 has a throw of ~105 ms (~235 m) for the Cambrian reflectors. (B) Fault 2 has a throw of ~150 ms (~340 m) for the Cambrian and Devonian reflectors. (C) Fault 3 has a throw of ~50 ms (~110 m) for the Cambrian and Devonian reflectors. (D) Fault 4 has a throw of ~70 ms (~155 m) for the Cambrian and Devonian reflectors. (E) Fault 5 has a throw of ~50 ms (~110 m) for the Cambrian and Devonian reflectors, ~70 ms (~155 m) for the Mississippian reflectors, ~50 ms (~110 m) for the Jurassic reflectors, and ~60 ms (~135 m) for the Lower Cretaceous reflectors. An average velocity of 4.5 km/s was used for conversion to depth.

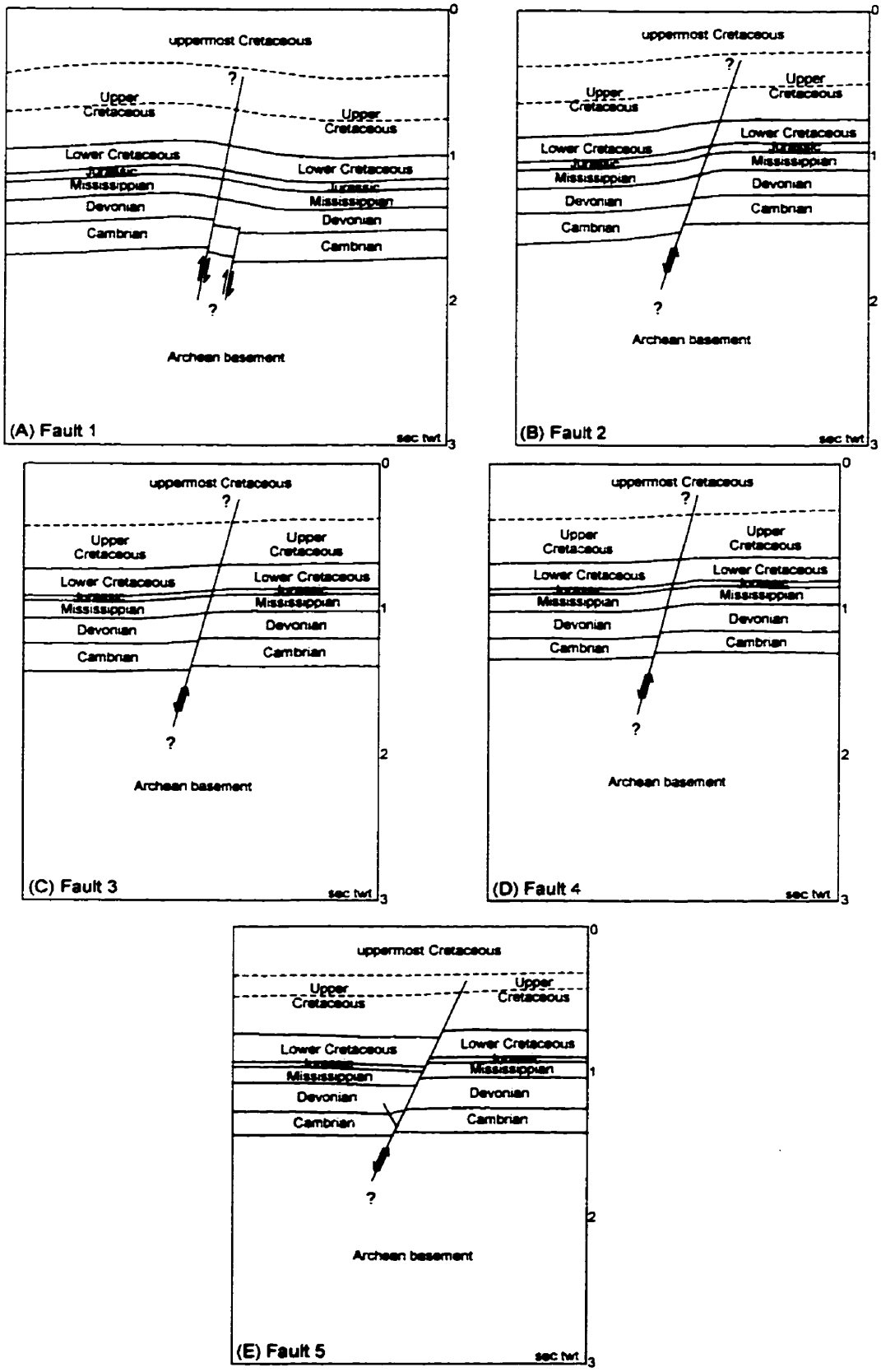
uppermost Cretaceous
Upper Cretaceous
Lower Cretaceous
Jurassic
Mississippian
Devonian
Cambrian
Archean basement
(A) Fault 1
(B) Fault 2
(C) Fault 3
(D) Fault 4
(E) Fault 5
sec twt
0
1
2
3

Furthermore, folding of Upper Cretaceous strata (Milk River Group) occurs and horizontal uppermost Cretaceous strata (Belly River Group and younger) are recognized in the topmost sedimentary section (Figure 36). These two predominant fault geometries have also been observed on numerous other industry seismic reflection lines (proprietary data courtesy of Shell Canada) in the vicinity of SALT line 30, located from approximately 10 to 40 km north of line 30 (Figure 6). The differential vertical throws for the five faults present on the SALT dataset are summarized in Figure 37. Regarding the other extensional faults in the vicinity of SALT line 30, they display vertical throws ranging from ~50 ms to 200 ms (~110 m to 450 m) for Cambrian and Devonian strata. One fault (referred to as S in Figure 6) shows a break in reflections from the near-basement reflector into the Upper Cretaceous strata, ranging from 50 ms to 150 ms (~110 m to 340 m), which is similar to the geometry of Fault 5 on the SALT dataset (Figure 36).

The extensional faults observed on the SALT dataset undoubtedly offset the near-basement reflector, implying that these extensional faults must detach within the basement. Unfortunately, Faults 1 to 4 cannot be traced deeper than the near-basement reflector due to the presence of a zone of multiple reverberations generated from the strata (Figures 25 and 32 to 35). However, Fault 5 shows an alignment with west-dipping basement reflectivity that is carried to approximately 5 s twt or 14 km depth (Figure 30).

### 4.4.2 Extensional faults and forced folding model

The geometry of Fault 5 is particularly instructive in terms of determining fault style and mechanism. Fault 5 shows clear down-to-the-west displacement on the basis of displaced reflections of Cambrian through lowermost Upper Cretaceous (Base of Fish Scales) strata. Upper Cretaceous reflections are continuous across the extensional fault but show folding (into Belly River Group strata; Figure 36). The development of a fold over a downdropped extensional fault block is known as extensional forced folding and has been modelled by Withjack et al. (1990) using single- and multiple-layer clay models. Extensional forced folds represent upward-widening monoclines, where secondary extensional faults develop (Figure 38; Withjack et al. 1990). The seismic reflection character of Faults 2, 3 and 4 also resembles a series of extensional forced folds that developed above master extensional faults. The Withjack et al. (1990) models provide an explanation for the break in reflections (up to 450 m of vertical throw) seen in

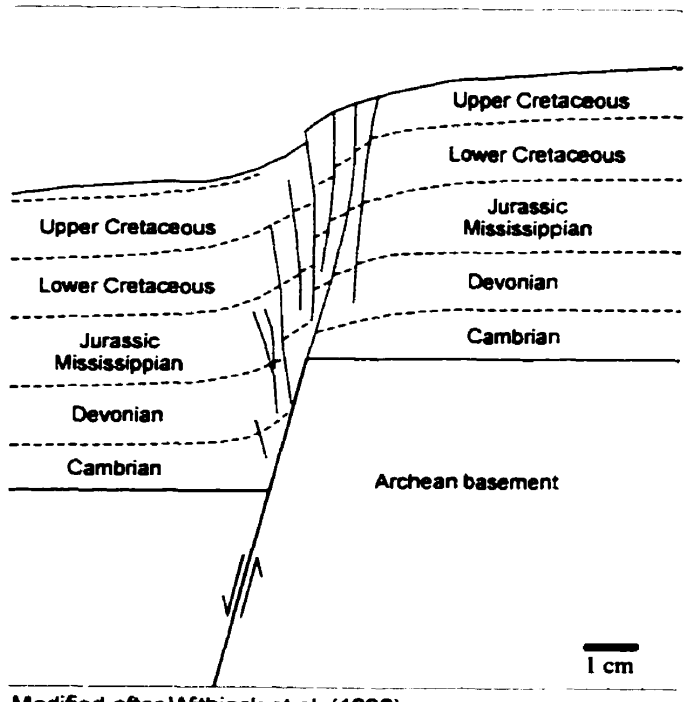


Modified after Withjack et al. (1990)

Figure 38. Schematic diagram of an extensional forced fold showing a master extensional fault with secondary extensional and reverse faults. The diagram illustrates the result of a physical model involving a single-clay layer with a dip of 75° (Withjack et al. 1990). The sketch is adapted to the WCSB stratigraphy of southern Alberta and shows an explanation for the fault geometries observed on the SALT dataset, as well as in the vicinity of the SALT lines. Migration may image the smaller offsets in strata as smooth, continuous reflections and/or vertical resolution may not be able to image these small offsets (see Hope et al. 1999 and Eaton et al. 1999 for other examples in the WCSB).

the lower part of the Paleozoic section, which is overlain by folding of the Mississippian through Cretaceous strata. The near-basement and Lower Paleozoic strata (Cambrian and Devonian) are interpreted to develop master extensional faults, whereas overlying Mississippian through Cretaceous strata are interpreted to deform in a more distributed fashion, accommodating the formation of extensional forced folds (Figure 38). Deformation in the shallow part of the sedimentary section may be more distributed, and therefore, resolved as folds rather than a discrete fault, or discrete faults not seismically resolvable. This could reflect competency contrasts between rigid, carbonate-rich Paleozoic strata versus shale- and sandstone-rich Mesozoic strata.

### 4.4.3 Fault reactivations

Flattening of a seismic reflection profile on a particular horizon eliminates structures that are of the same age or younger than the horizon. This allows for a better understanding of pre-Laramide deformation and paleostructure, as the tectonic overprinting of Laramide faulting and folding may have masked earlier structures. Fault 1 is a Laramide compressional fault, but it may have an older history. Two flattened sections were produced across Fault 1 in order to investigate in more detail its geometry and timing, and provide evidence for fault reactivation throughout the Phanerozoic. A post-Milk River Group (Upper Cretaceous) and Livingstone Formation (top of Mississippian) reflectors were selected as the flattened horizons because they represent the most continuous reflectors throughout the seismic profile, and because these are thought to represent times of tectonic activity in the WCSB (Figures 39 and 40). In addition, isochron thicknesses for the Mesozoic section (post-Milk River Group to top of Jurassic; Figure 39) and the Paleozoic section (top of Mississippian to top of Cambrian; Figure 40) section were measured across Fault 1.

Thickness changes occur across Fault 1 on both flattened seismic profiles. The post-Milk River to top of Cambrian isochron is approximately 130 m thicker on the west side of the fault. The post-Milk River to top of Rierdon isochron is 35 ms or ~75 m (with an average velocity of 4140 m/s) thicker on the west side of Fault 1 (Figure 39). Similarly, the top of Mississippian to top of Cambrian isochron is 20 ms or ~55 m (with an average velocity of 5420 m/s) thicker on the west side of Fault 1 (Figure 40). In addition, the flattened Livingstone horizon profile shows that the top of Cambrian reflector (Deadwood) on the east side of Fault 1 is elevated above regional by

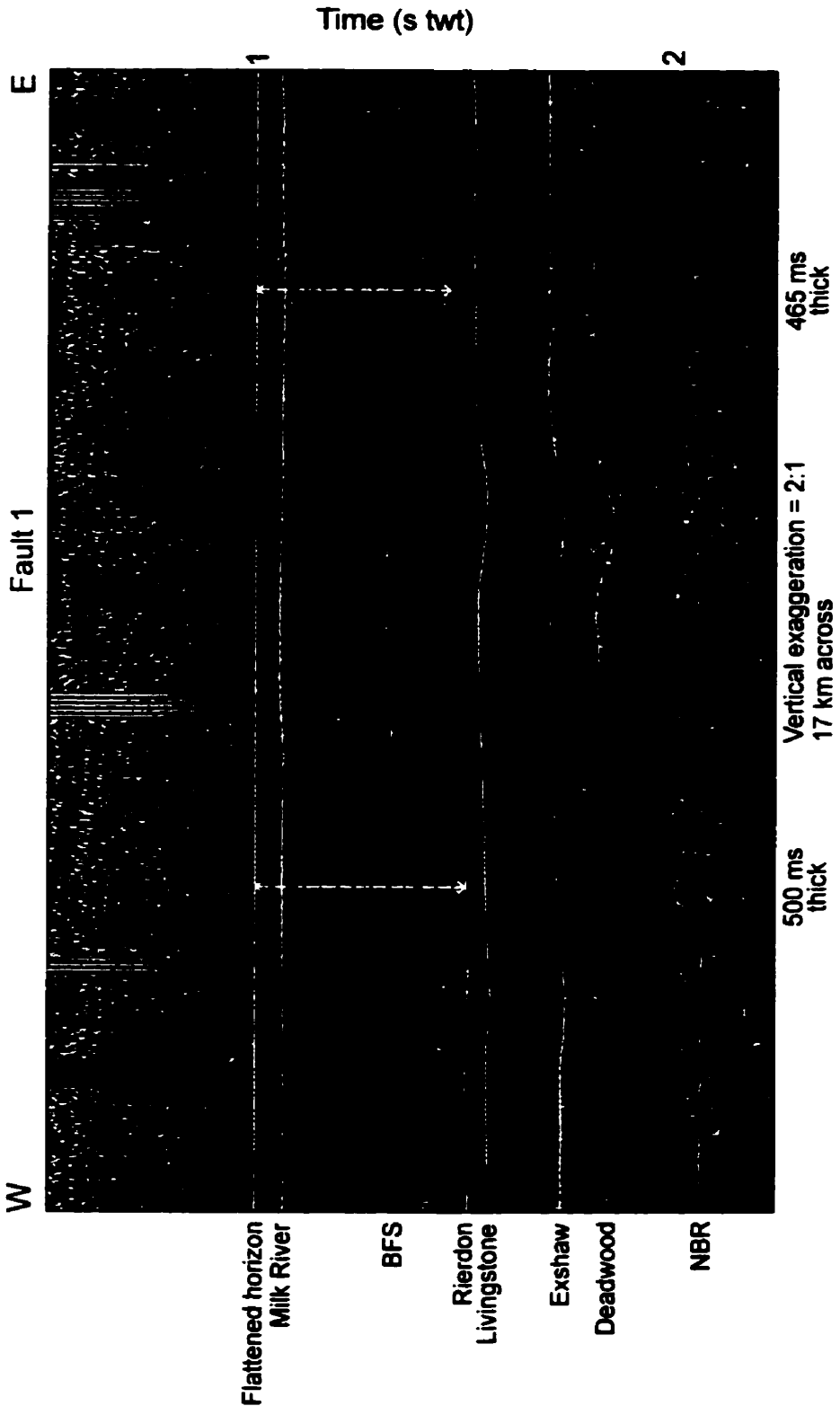


Figure 39. Flattened seismic reflection profile across Fault 1 on line 30. A post-Milk River Group (Upper Cretaceous) reflector represents the flattened horizon. The post-Milk River to top of Jurassic (Rierdon) isochron is ~75 m (35 ms) thicker on the west side of Fault 1.

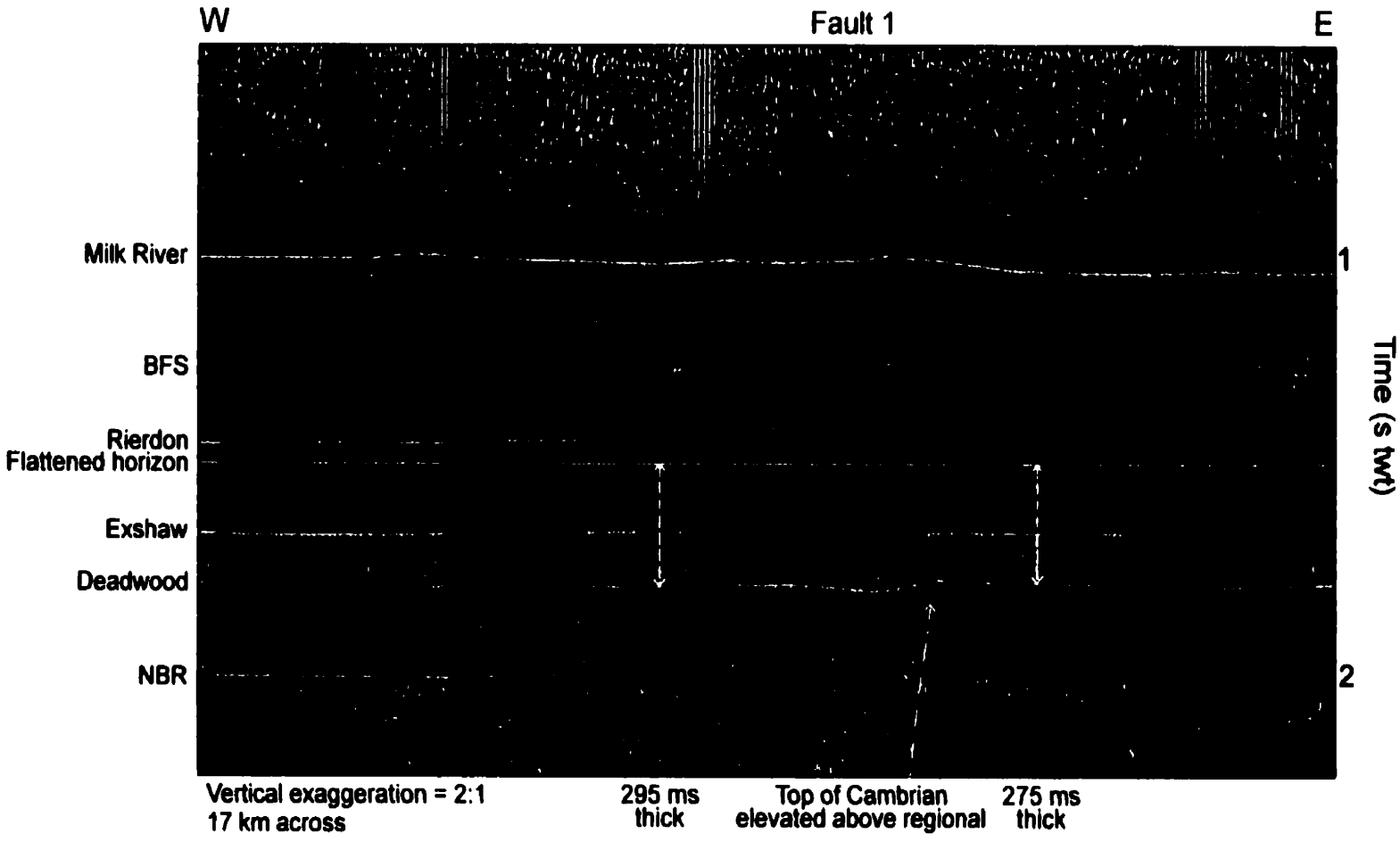


Figure 40. Flattened seismic reflection profile across Fault 1 on line 30. The Livingstone Formation reflector represents the flattened horizon. The top of Mississippian (Livingstone) to top of Cambrian (Deadwood) isochron is ~55 m (20 ms) thicker on the west side of Fault 1. In addition, the Deadwood reflector on the east side of Fault 1 is elevated above regional by ~50 m (18 ms) suggesting that the hanging wall (west) side of Fault 1 was downthrown to the west repeatedly throughout the Phanerozoic, until it was structurally inverted into its present geometry during Laramide thrusting.

approximately 18 ms or ~50 m (with an average velocity of 5420 m/s; Figure 40). This, combined with the evidence for a thicker Cambrian to Upper Cretaceous sequence on the west side of Fault 1, may indicate that the hanging wall side of Fault 1 was downthrown to the west repeatedly throughout the Phanerozoic, until it was structurally inverted into its present geometry (from a west-dipping extensional fault into a west-dipping compressional fault) during Laramide thrusting. Erosion throughout the Phanerozoic of the upthrown eastern (footwall) side may have produced the thickness variation across Fault 1. However, the thicker Cretaceous section (post-Milk River to top of Rierdon isochron) on the west side of Fault 1 solely may reflect the western thickening of the Cordilleran-derived sedimentary wedge.

In summary, isochron thickness changes across Fault 1 throughout the Phanerozoic, onlap features (growth strata) in the Lower Cretaceous, Jurassic, and Mississippian reflectors visible on Faults 3 and 4, and evidence for a down-to-the-west extensional origin for Fault 1, together suggest that multiple fault reactivations occurred throughout Phanerozoic. Thus, the faults present on the SALT dataset represent inherited old features of the WCSB.

#### 4.4.4 Surface expression of faulting

Two distinct surface expressions appear to be associated with subsurface faulting of Fault 1 and the Monarch Fault zone (Figure 6). Fault 1 represents the only fault on SALT lines 30, 29 and 31 that occurs in the vicinity of outcrops in the St. Mary River valley (Figure 6), and hence, offers the only opportunity to investigate the surface expression of faulting within the study area. At the surface, Fault 1 appears to be associated with a hanging wall anticline and a footwall syncline, and has been interpreted as the northern continuation of the Del Bonita structure in southernmost Alberta (Figure 6). The Del Bonita structure is a northwesterly-plunging anticline and syncline pair that crops out in the Milk River valley. This structure is known from surface mapping (Irish 1967), and in the subsurface, from structure contour mapping on top of the Oldman River Formation (Russell and Landes 1940) and on top of the Rundle Group (White 1960). Clearly, the shallow seismic reflection data show that Fault 1 indeed is associated with an anticline in the west and a syncline in the east (Figures 25, 32 and 37). The Del Bonita structural trend passes through the Del Bonita and Spring Coulee fields and appears to delineate a significant structural trend within the WCSB in southern

Alberta (Figure 6). The Monarch Fault zone has been interpreted as being partially positioned by basement extensional faulting that was inverted during Laramide thrusting on the basis of seismic reflection data (Figure 6; Hiebert 1992; Hiebert and Spratt 1996).

#### 4.4.5 Basement influence on basinal structures

The principal evidence for basement influence on the sedimentary section includes: (1) alignment of dipping basement fabrics with faults in the overlying strata (e.g. Fault 5 on line 31; Figure 30); (2) draping or onlap of strata over pre-existing local basement relief (Figure 28); (3) arching of strata over the Sweetgrass Arch (Figure 28); and (4) reactivation of Fault 1. Perhaps the most dramatic evidence of direct basement control is from seismic reflection sections that show alignment of dipping reflectivity in the basement with the position of extensional faults (e.g. from line 31 in Figure 30). Interpretation of the significance of dipping reflectivity in crystalline basement rocks in terms of possible control on younger sedimentation is difficult (Ross and Eaton 1999). In the examples from the SALT lines (this research; Lemieux et al. 2000) and from the Lithoprobe Central Alberta Transect (Ross et al. 1995), dipping reflectivity in the basement is interpreted as structurally-induced layering. The alignment with extensional faults suggests that these structural fabrics have been reactivated.

In this study, the strike of faulting on seismic reflection data (SALT lines and proprietary data from the Fort MacLeod and Lethbridge regions) generally is interpreted to be northwest-southeast, with a north-northwest-south-southeast strike south of line 30, on the basis of fault pattern control and correlation to a mappable anticline and syncline pair (Figure 41). In addition, the strike of normal faulting mapped in the Oldman River is northwest-southeast (Russell and Landes 1940) and the strike of the Monarch Fault zone extends north-northwest-south-southeast (Figure 41; Hiebert and Spratt 1996). All of these provide an estimate on the strike of faulting within the WCSB in southern Alberta, which coincides with the trend of the basement potential-field fabrics, indicating basement control on fault development. The anticline-syncline pair associated with the Del Bonita structural trend is well defined on the aeromagnetic data as a linear north-northwest-south-southeast trending magnetic low (Figure 41). North of line 30, the magnetic anomalies appear to trend northwest-southeast, which corresponds to the strike of faulting with the sedimentary basin (Figure 41). However, additional seismic reflection data in this region are needed in order to carefully constrain the regional extent

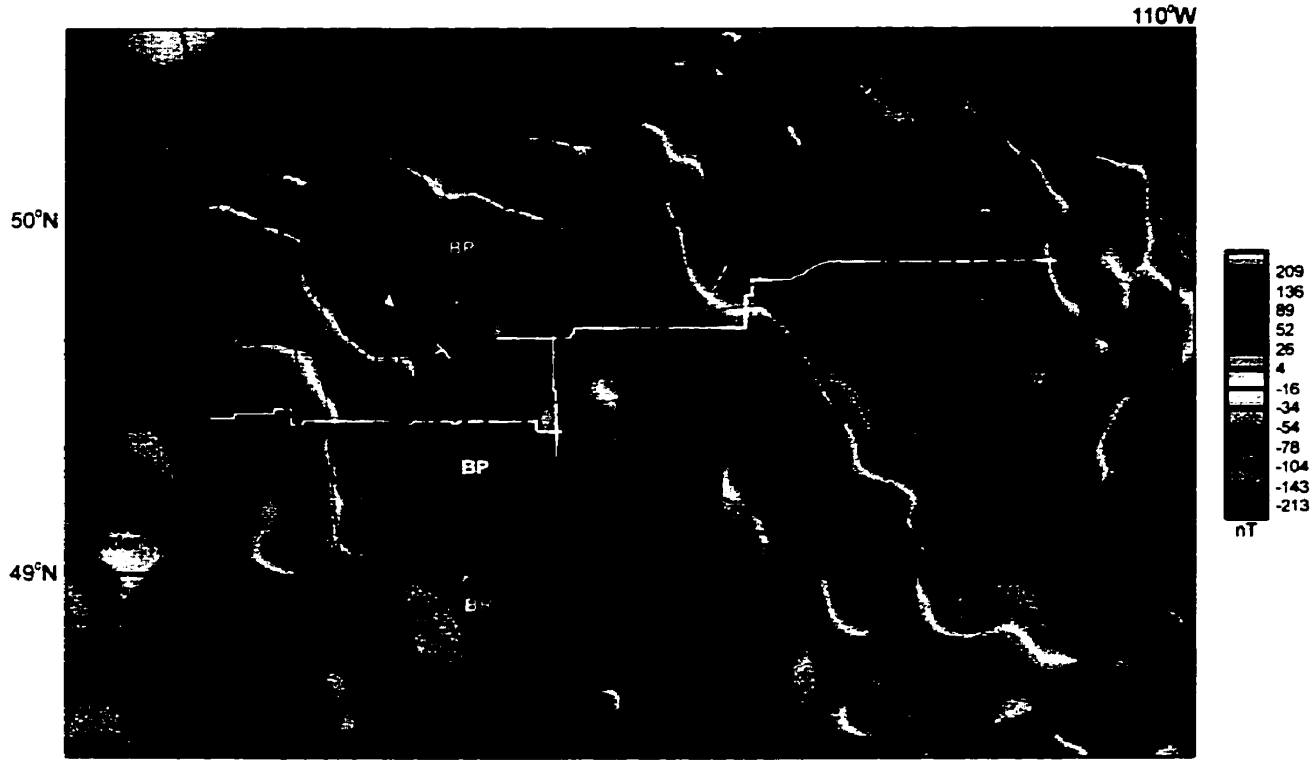


Figure 41. Short-wavelength filtered (300-150/20-10 km) magnetic anomaly map of the MHB with superposed structures and stratigraphy of the WCSB in southern Alberta. Black fault symbols refer to subsurface faults, whereas white fault symbols refer to faults mapped in the Oldman River. Fault T is a down-to-the-west extensional fault observed on seismic reflection data in the south Taber area (H.A. Balkwill, personal communication 1999). Northwest-trending Eocene dykes (Ross et al. 1997) are represented by dashed grey lines. Basement structure contours are in meters (see Figure 29). Stars represent wells penetrating the Precambrian crystalline basement and they were projected into the SALT lines along the dashed lines. North of line 30, faults strike northwest-southeast, whereas south of line 30, faults strike north-northwest-south-southeast. The Del Bonita structural trend, and the Blood Reserve (BR) and Bearpaw (BP) geological contacts appear to follow this north-northwest-south-southeast trend. This similarity in strikes of magnetic anomalies and basinal structures suggests that basement structural fabrics have reactivated and controlled the positioning of faults of the WCSB in southern Alberta.

of these extensional faults. Altogether, the evidence for alignment of basement fabric with Fault 5 and the similarity in strikes of magnetic basement fabrics and basinal structures suggest that basement structural fabrics have reactivated and controlled the positioning of faults throughout the Phanerozoic in southern Alberta.

### 4.5 Timing of extensional faulting

Evidence for onlap features and growth strata that could help to constrain the latest age of the extensional faults is lacking on the SALT dataset, most likely due to the fact that post-Cretaceous erosion has been extensive within the study area. Based on coal rank data, Kalkreuth and McMechan (1988) estimated that approximately 2 km of Mesozoic and Cenozoic strata have been eroded from the Alberta Plains since Oligocene time. According to Magara (1976) and Hacquebard (1977), as much as 1.5 to 2.0 km of strata may have been eroded from the western side of the basin from the latest Paleocene to Middle Eocene. In addition, large near-offsets limit the seismic resolution in the topmost 0.25 s twt (see Figures 32 to 36). However, the evidence for forced folding of Mississippian, Jurassic, and Cretaceous reflectors, a break in reflections from the near-basement reflector up into lowermost Upper Cretaceous strata across Fault 5 and Fault S (Figures 6 and 41), and horizontal undeformed uppermost Upper Cretaceous (Belly River Group and younger) strata across Fault 5 together suggest that the youngest phase of displacement on these faults is Late Cretaceous. Thus, the two types of fault geometries imaged on the SALT dataset lead to the interpretation that an extensional event must have originated during the Late Cretaceous tectonic evolution of the WCSB in southern Alberta. Although Fault 5 appears to be Late Cretaceous, extensional faulting of the WCSB in southern Alberta is not believed to be exclusively Late Cretaceous. The extensional faults actually are younging to the west, as Belly River Group strata appear unaffected by Fault 5, but Belly River Group strata and younger are definitely disturbed by Faults 1 to 4, as they show forced folding (Figures 32 to 37). Thus, the latest extension originated in Late Cretaceous, but an upper age limit cannot be determined from the seismic reflection data.

Seismic reflection profiling east of Fort MacLeod displays a break in reflections up into Devonian strata and forced folding of overlying strata (Figure 6). Wright et al. (1994) state that these extensional faults are associated with fractures within Mississippian and Cretaceous cores. Ross et al. (1997) interpreted the extensional faults

in the Fort MacLeod area as Eocene based on their colinearity with Eocene dykes interpreted from high resolution magnetic anomaly data. The faults identified in this study are distinguished from the Eocene faults in areas where Upper Cretaceous Belly River Group and younger are unaffected (e.g. Fault 5 on Figure 36), and where the strike of faulting within the sedimentary basin is different from the strike of the Eocene dykes (e.g. Fault 1 on Figure 41). In addition, the faults postulated by Ross et al. (1997) should be visible on the SALT data (especially line 29). Their absence suggests that either their displacement is below seismic resolution (ca. 30 m) or that they are not as prevalent as suggested by these authors.

### 4.6 Mechanisms of extensional faulting and structural inversion

The principal mechanism for Late Cretaceous to Paleocene(?) extensional fault formation in the WCSB of southern Alberta is interpreted to be lithospheric loading by Laramide thrust sheets. The Laramide orogeny triggered the latest fault reactivation, as flexural subsidence of the foreland plate was generated by thrust loading along the continental margin of western North America (Beaumont et al. 1993). Since multiple reactivations of these faults occurred throughout the Phanerozoic, the location of the extensional faults is not associated with peripheral bulge migration during Laramide orogenesis. However, some extensional faults may have initiated as Cambrian passive margin extensional faults.

Foreland basins and their peripheral bulges are elements of a dynamic system that evolves as the size and position of the thrust load change, and as the flexural wavelength of the loaded plate changes (Figure 42; Beaumont 1981). Bearing in mind their dynamic system, Fault 1 may have formed originally as a down-to-the-west extensional fault that was subsequently inverted as the tensile stress regime of the foredeep moved into the compressive regime of a foreland system (Figure 42; G. M. Ross and M. A. Cooper, personal communication 1999). This dynamic foreland basin system supports the idea of continuous extension originating in Late Cretaceous and subsequent structural inversion of Fault 1 and the Monarch Fault zone, as the thrust front advanced through the Paleocene. Compressional stress may have been carried along a glide zone situated within the bottom portion of the sedimentary sequence, at the basement-strata interface, or within the upper portion of the basement. Similar examples of inversion of early foreland extensional faults have been reported from the Himalayas

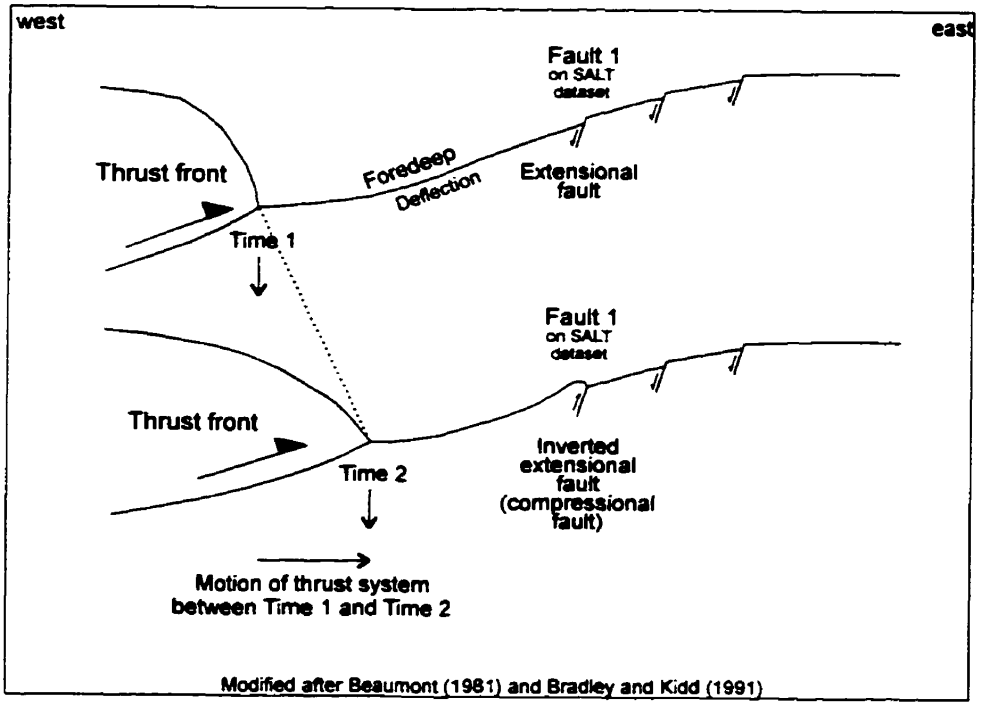


Figure 42. Mechanism for the structural inversion of Fault 1 from extensional to compressional regime. As the thrust front advanced and changed the dynamics of the foreland system, Fault 1 may have inverted from a down-to-the-west extensional fault in the foredeep to a compressional fault dipping to the west.

(Lillie et al. 1987), the Alps (Stockmal and Beaumont 1987; de Graciansky et al. 1989), the North Sea (Chapman and Meneilly 1991), the Appalachians (Lash 1987), and in the Foothills of the Rocky Mountains in the Blackfoot Indian Reserve of northwestern Montana (Figure 43).

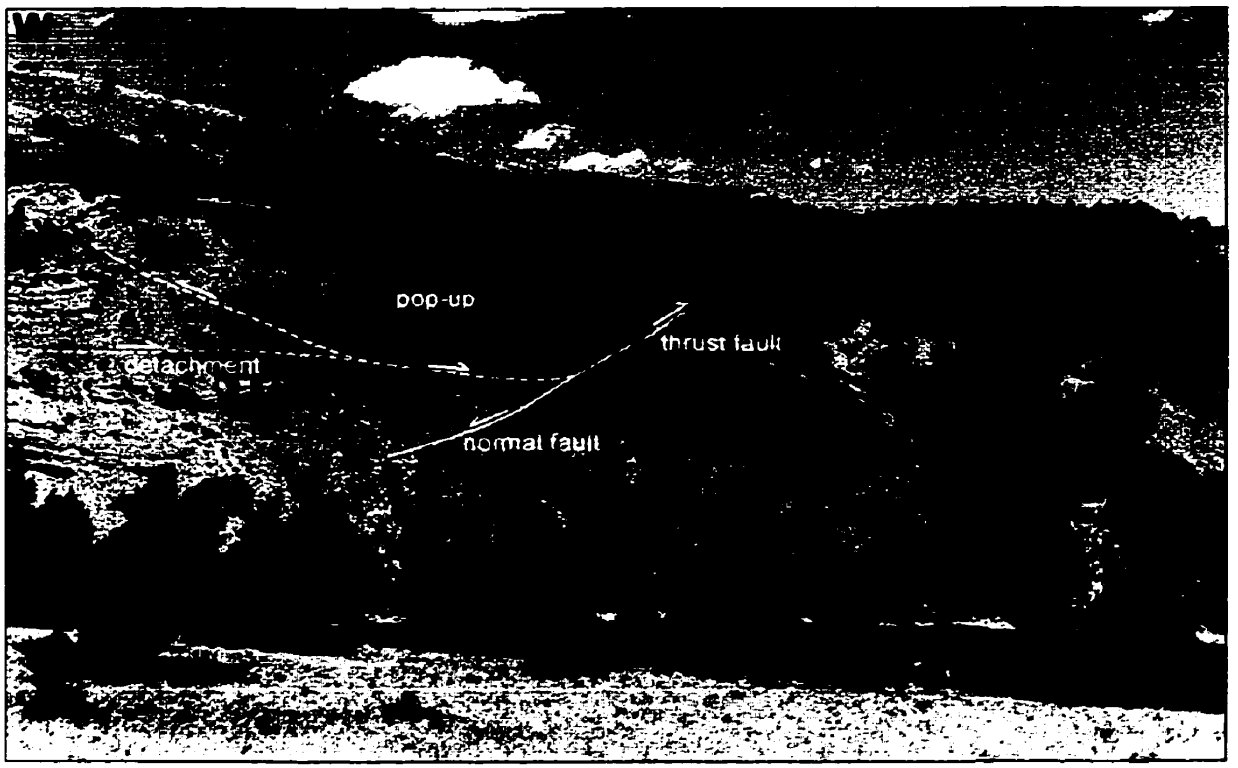


Figure 43. Photograph of a reactivated structure in the Foothills of northwestern Montana (Blackfoot Indian Reserve), showing the partial inversion of an extensional fault into a compressional fault. This outcrop is analogous to the subsurface geometric expression of Fault 1, which is interpreted as the partial inversion of an extensional fault into a compressional fault associated with the Laramide orogeny. The approximate positions of the thrust fault detachment and pop-up structure are indicated by dashed lines. Photograph is a courtesy of M.R. McDonough.

# CHAPTER 5. DISCUSSION

## 5.1 Relationship between seismic reflection fabrics and magnetic trends

Comparison of time-structure maps of four crustal surfaces (Figure 21) and the magnetic signature of the Medicine Hat Block (MHB) allows strikes of reflection basement fabrics in the upper portion of the crust to be correlated to trends in magnetic anomalies. For example, along line 31, magnetic anomalies are oriented north-south and northwest-southeast, corresponding to strikes of crustal surfaces 1 and 2 (west-dipping), and crustal surfaces 3 and 4 (southwest-dipping), respectively (Figures 3, 17, 21 and 44). The nature of the transition between the two dipping packages is interpreted as a structural truncation as the north-trending magnetic anomalies appear to truncate against the northwest-trending magnetic anomalies (Figures 3, 10, 11 and 44). The map pattern of the boundary between them takes a western bend near the intersection of lines 29 and 31, where the boundary between the two magnetic trends becomes unclear (Figures 3 and 44). The southwest-dipping crustal reflections are interpreted to have been thrusted along a northwest-southeast-trending (southwest-facing) frontal ramp, corresponding to the northwest-trending magnetic anomalies in most of the MHB (Figure 44). The west-dipping crustal reflections, correlated to north-trending magnetic anomalies, are sampled by drillcore W5, which gives a crystallization age of 3.3 Ga. This north-trending portion of the MHB may well be a separate older basement domain that was accreted to 2.6 to 2.8 Ga crust in the Late Archean, forming the MHB (Figures 2, 3 and 44).

The dipping basement reflection fabrics can in turn be traced from the upper crust to the lower crust (from ~3 s twt down to ~12 to 15 s twt) on lines 29 and 31, where they appear to flatten, but are truncated along a horizontal cutoff surface at around 12 s twt in the western half of line 31 (Figure 17). The imbricated west- and southwest-dipping fabrics within the MHB are interpreted to be Late Archean, since the magnetic signature, corresponding to strikes of the seismic reflection fabrics, terminates at the Early Proterozoic Vulcan structure to the north. In addition, a low pressure thermal event recorded in upper crustal Archean tonalite gneissic xenoliths may further constrain the age of continental crust imbrication to be ca. 2.60 Ga (see Sections 2.2 and 3.3.4). The magnetic anomaly trends can further be used to project the crustal xenolith data from the Sweetgrass Hills Intrusives onto the SALT lines (Figures 2 and 17).

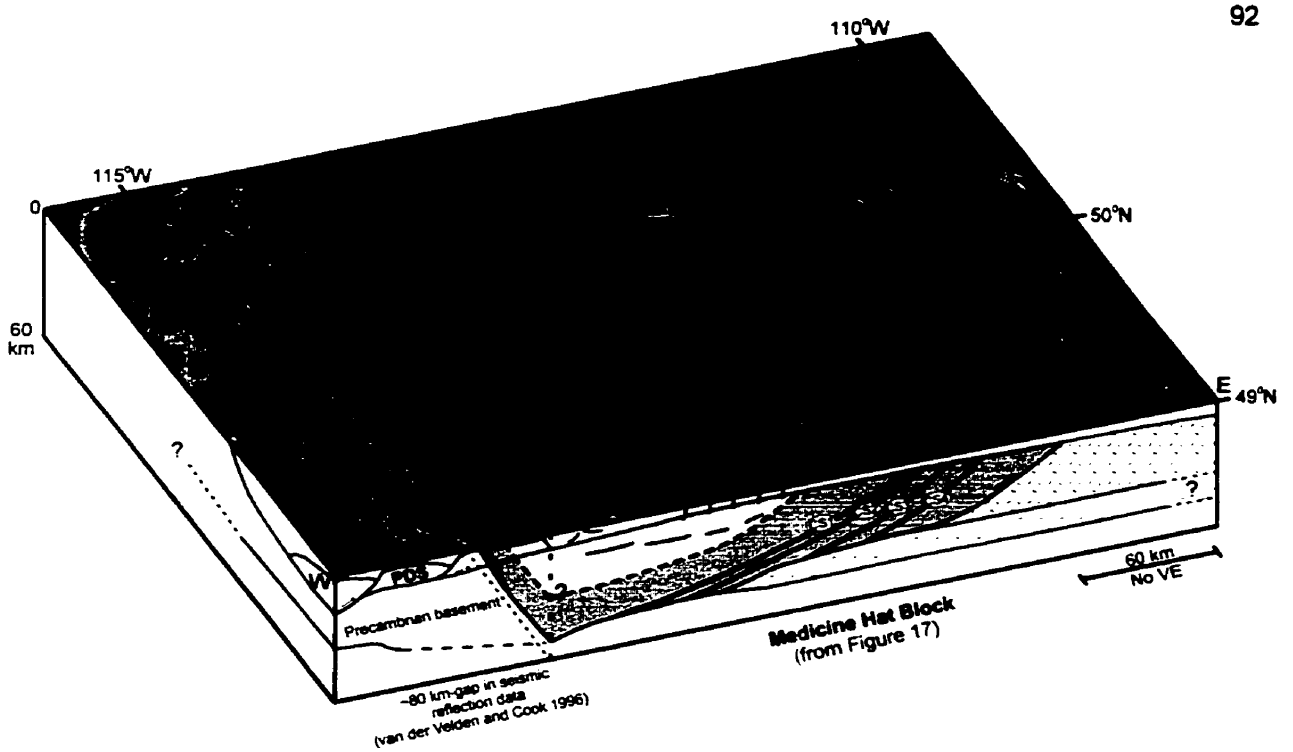


Zone 1: Phanerozoic Western Canada Sedimentary Basin

Zone 2: Imbricated Archean crust (weakly reflective)

Zone 3: Imbricated Archean crust (highly reflective)

Zone 4: Relatively undeformed Archean crust

Zone 5: Early Proterozoic (layered lower crust)

Zone 6: Upper mantle

Mid-Proterozoic (~1.5 Ga) extensional crustal-scale ramp, reactivated in Mesozoic

Lithoprobe SALT seismic reflection lines 30, 29 and 31

Discordance between magnetic fabrics

ST: Southern Rocky Mountain Trench

CD: Cordilleran deformational front

PDS: Proterozoic and Paleozoic deformed strata

Figure 44. Schematic block diagram of the MHB crustal structure illustrating the geometric relationship between magnetic anomaly trends and strikes of basement fabrics established from the seismic reflection data. The ramp subcrops 15 km east of line 31, where it is interpreted to trend northwest-southeast. Crustal surfaces CS1 and CS2 correspond to north-trending magnetic anomalies, whereas CS3 and CS4 correspond to northwest-trending anomalies. The discordance between the magnetic anomalies appears to take a western bend suggesting the presence of an oblique ramp in the middle to upper crust. An 80-km gap between the SALT lines and the southern Cordillera seismic reflection survey to the west occurs, where the western MHB limit probably lies. Note that the seismic reflection profile interpretation drawn along the 49° parallel is derived from the SALT lines and not extrapolated to the south.

## 5.2 Significance of geochronological and seismic refraction studies to Medicine Hat Block crustal geometry

Geometric relationships preserved in the MHB crust are significant to determine relative timing of ancient deformational events within the crust, but geochronological studies of drillcores and xenoliths from mafic Eocene dykes and sills add a further timing constraint on these tectonic events. When crustal xenolith localities are projected along linear northwest magnetic anomalies (~80 to 110 km to northwest) from their sampling site in the Sweetgrass Hills igneous complex (Figures 2 and 3), they fall along a segment in the middle of line 31 that corresponds to a highly imbricated crust (zone 3) underlain by layered lower crust (zone 5; Figure 17). More specifically, Archean tonalite gneisses (X1) are projected within the highly imbricated upper to middle crust, whereas Early Proterozoic paragneisses (X2) and mafic granulites (X3) are projected within the layered lower crust (Figure 17). Thus, in at least one locality, the MHB crust appears to consist of older Archean rocks overlying younger Proterozoic rocks. According to Davis et al. (1995), the lower crustal xenoliths (X2 and X3) may represent Archean crust that was metamorphosed under granulite conditions in the Early Proterozoic, or they may represent Early Proterozoic crust that was added to the base of the Archean crust at around 1.85 to 1.70 Ga.

Deep Probe/SAREX seismic refraction experiments have revealed the presence of an extensive lower crustal intermediate velocity layer (7.2 km/s) beneath the MHB, Great Falls Tectonic Zone and Wyoming Province, that is up to 25 km in thickness under the Wyoming Province (Buryanik et al. 1997; Henstock et al. 1998). Beneath the eastern portion of the MHB, this lower crustal intermediate velocity layer is estimated to be 8 km in thickness (Figure 22). The origin of this anomalous layer has been interpreted to be the result of injection of mafic melts in the Early Proterozoic (Davis et al. 1995; Henstock et al. 1998). Eaton et al. (1999) maintain that the MHB crust was overthrusted onto Loverna Block crust along a south-dipping subduction zone within the Vulcan structure. On the basis of this information and the geometric relationships presented in this research, delamination and underthrusting of the Loverna Block crust and injection of mafic melts in the lower crust of the MHB are believed to have occurred in the Early Proterozoic. These are most likely preserved within reflection zone 5 along the SALT seismic reflection profile (Figures 17 and 44). The delamination and underthrusting of the Loverna Block crust beneath the MHB crust may correspond to ~1.81 to 1.75 Ga

paragneiss xenoliths (X2), and the injection of mafic melts are compatible with ~1.75 to 1.70 Ga mafic granulite xenoliths (X3).

### 5.3 Role of the Great Falls Tectonic Zone

Determination of the MHB-Wyoming Province boundary strictly on the basis of magnetic signature is uncertain. Part of the difficulty arises from the fact that the magnetic signature of the Wyoming Province has been strongly affected by Late Cretaceous high-angle reverse faults, locally with vertical displacements in excess of 3 km (O'Neill and Lopez 1985). Nonetheless, the north and northwest fabrics of the MHB are continuous across the northern portion of the Great Falls Tectonic Zone on most filtered and unfiltered potential-field maps presented in Chapter 3. In addition, it appears that the Wyoming Province potential-field fabric is characterized by north- and northwest-trending anomalies that may correspond to the potential-field signature observed within the MHB (Figures 3, 8, 10, 11,12 and 13). If so, the MHB and Wyoming Province may have been tectonically related prior to the formation of the Great Falls Tectonic Zone. Because the nature of the Great Falls Tectonic Zone has been interpreted on the basis of surface geological mapping and corresponding potential-field anomalies, and because of the evidence for the potential-field continuity of the MHB across a portion of the Great Falls Tectonic Zone, the role of the Great Falls Tectonic Zone as a primary tectonic boundary (crustal suture) between the MHB and Wyoming Province is believed to be less significant than previously suggested by O'Neill and Lopez (1985).

The uniform extensive lower crustal intermediate velocity of 7.2 km/s beneath the MHB, the Great Falls Tectonic Zone, and the Wyoming Province is interpreted to represent injection of mafic melts, and its emplacement provides further constraints on timing and tectonic relationships. It requires that the MHB and the Wyoming Province were connected as a single basement domain prior to the injection of mafic melts around ~1.75 to 1.70 Ga. A significant result from Boerner et al. (1998)'s magnetotelluric study across the Great Falls Tectonic Zone reveals that the Great Falls Tectonic Zone lacks a pronounced two-dimensional conductive signature that can be interpreted as a plate-edge foreland basin, typical of exposed Proterozoic suture zones. Although the Great Falls Tectonic Zone represents a locus for active tectonism since the Middle Proterozoic, the evidence presented in this research and other studies (e.g., Boerner et al. 1998;

Henstock et al. 1998; Eaton et al. 1999) suggests that the Great Falls Tectonic Zone most likely represents an intracontinental zone of deformation, and not the main crustal suture between the Hearne and Wyoming Provinces.

## 5.4 Tectonic evolution of the southern Alberta basement

### 5.4.1 Introduction

The following model for the tectonic evolution of the Archean MHB incorporates geophysical and geological constraints presented here and in previous studies (e.g. Frost 1993; Mueller et al. 1993; Villeneuve et al. 1993; Davis et al. 1995; Ross et al. 1995; Buryanik et al. 1997; Henstock et al. 1998; Eaton et al. 1999).

### 5.4.2 Archean

According to geochronological data (Mueller et al. 1993; Villeneuve et al. 1993), the MHB and Wyoming granitic cratons were formed during the Archean (~3.3 to 2.6 Ga). In contrast, Loverna Block granites (~2.71 to 1.78 Ga) were either formed at different times and consist of many small terranes, or they were overprinted by Early Proterozoic magmatic events and are Archean in age (Villeneuve et al. 1993). The Archean east- and northeast-verging shortening (zones 2 and 3) preserved in the MHB crust and the geometric ramp separating relatively undeformed Archean crust (zone 4) to the east from the imbricated crust to the west (Figure 17) is interpreted to represent the remnants of an Archean collisional orogen involving two Archean domains (Archean granitic domains 1 and 2 in Figures 45A and 45B). This Archean collisional orogen may have been widespread, extending along the western margin of an Archean craton, which may have included the MHB and Wyoming Province. An estimate for the amount of crustal shortening cannot be calculated as individual thrust sheets cannot be discerned.

### 5.4.3 Early Proterozoic

Prior to the Early Proterozoic collisional event, the margins of the MHB may have undergone extension and relaxation to form active rifting margins. The MHB inverted crustal geometry, which displays Archean crust truncated by an Early Proterozoic layered lower crust (see Sections 3.3.4 and 5.2) is indicative of a continental-type collision in the Early Proterozoic (~1.85 to 1.75 Ga). This crustal geometry is interpreted

Figure 45. (next page) Schematic tectonic evolution of the MHB throughout the Precambrian. (A) Pre-continental collision prior to 2.6 Ga. Archean granitic domains 1 and 2 may have formed a convergent margin involving an active continent (domain 1), a passive continent (domain 2) and the subduction of oceanic lithosphere setting the stage for the Archean continental collision around 2.6 Ga. (B) Archean continental collision at around 2.6 Ga. Archean granitic domain 1 collided with Archean granitic domain 2 along a southwest-dipping suture (ramp). Domain 1 corresponds to reflection zones 2 and 3, whereas domain 2 corresponds to reflection zone 4, separated by the crustal-scale southwest-dipping ramp (Figures 17, 21 and 44). (C) Early Proterozoic continental collision at around 1.8 Ga. The MHB crust overthrusts the lower crust of the Loverna Block along a former south-dipping subduction zone (Eaton et al. 1999). Hanging wall reflection zones 2, 3 and 4 are truncated by footwall reflection zone 5, which partly corresponds to the delaminated lower crust and reflection Moho of the Loverna Block (Figures 17 and 44). (D) Post-Early Proterozoic continental collision at around 1.75 to 1.70 Ga. Part of reflection zone 5 and perhaps reflectivity of zone 6 is attributed to post-collisional injection of mafic material in the lower crust of the MHB.

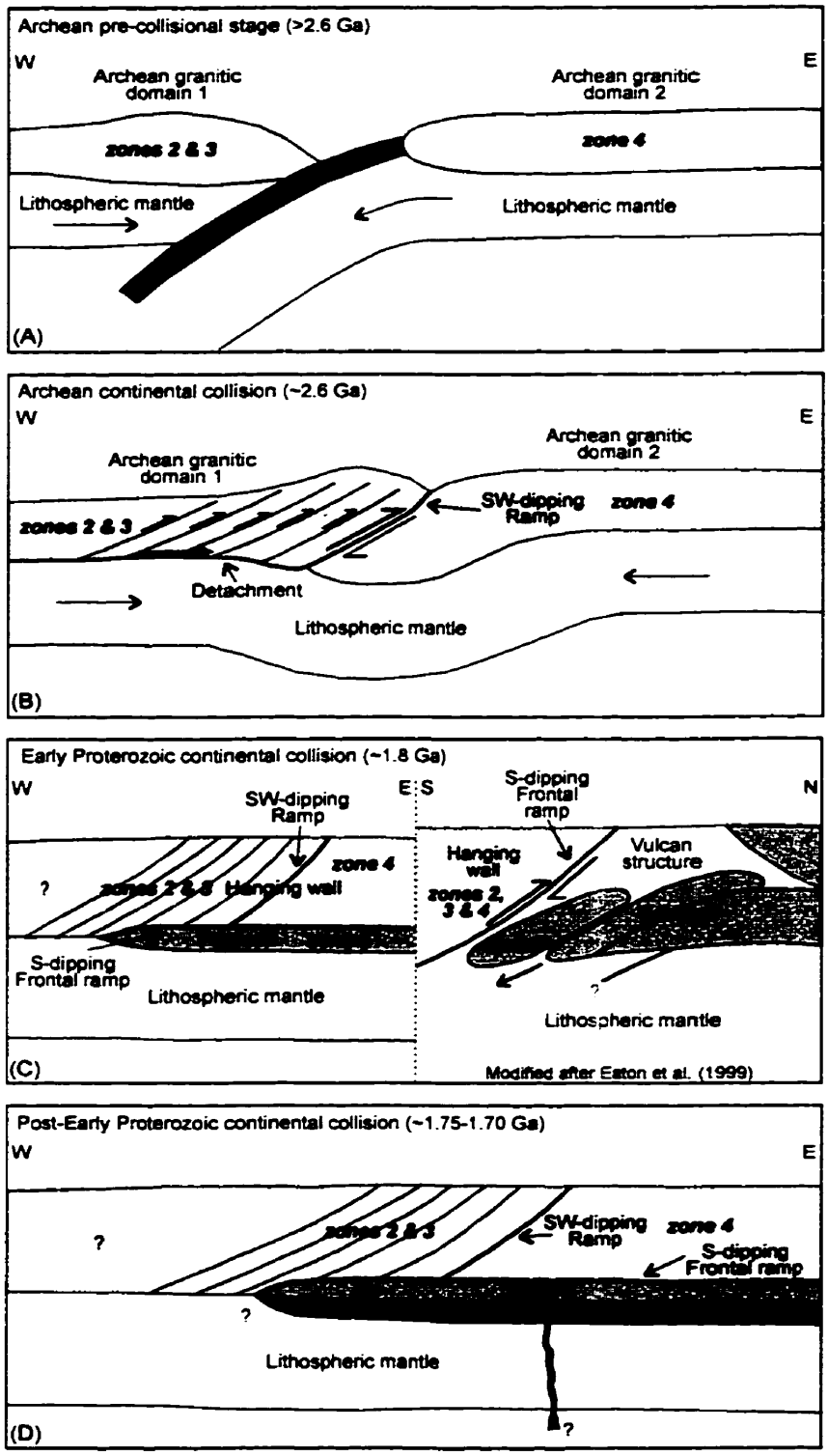
Archean pre-collisional stage (>2.6 Ga)
W
E
Archean granitic domain 1
Archean granitic domain 2
zones 2 & 3
zone 4
Lithospheric mantle
Lithospheric mantle
(A)
Archean continental collision (~2.6 Ga)
W
E
Archean granitic domain 1
Archean granitic domain 2
zones 2 & 3
SW-dipping Ramp
zone 4
Detachment
Lithospheric mantle
(B)
Early Proterozoic continental collision (~1.8 Ga)
W
E
S
N
SW-dipping Ramp
S-dipping Frontal ramp
zone 4
Hanging wall
Vulcan structure
zones 2, 3 & 4
?
zones 2 & 3 Hanging wall
S-dipping Frontal ramp
Lithospheric mantle
Lithospheric mantle
(C)
Modified after Eaton et al. (1999)
Post-Early Proterozoic continental collision (~1.75-1.70 Ga)
W
E
?
zones 2 & 3
SW-dipping Ramp
zone 4
S-dipping Frontal ramp
?
Lithospheric mantle
(D)
Medicine Hat Block crust
Loverna Block crust
Mafic melts
Oceanic crust

to be associated with the juxtaposition of the MHB crust with the Loverna Block crust in the Early Proterozoic (Figure 45C). This model is consistent with the interpretation of Eaton et al. (1999), who propose that the Vulcan structure represents the Early Proterozoic suture between the Wyoming and Hearne Provinces, where the MHB was thrusted over the lower crust of the Loverna Block along a south-dipping subduction zone (Figure 45C). The layered lower crust of zone 5 is interpreted to correspond partly to this south-dipping zone of Eaton et al. (1999), who suggested it is the delaminated lower crust and reflection Moho of the Loverna Block. If this is the case, the horizontal reflections of zone 5, as well as the reflectivity of zone 6 along the west-east line 31, represent an along-strike profile of the south-dipping subduction zone that thrusted Archean MHB crust (hanging wall) over the Archean to Early Proterozoic Loverna Block crust (footwall). The geometric cutoff between reflection zones 3 and 5 (Figure 17) represents the boundary associated with the Vulcan structure (Figures 45C and 45D). In addition, zone 5 and perhaps zone 6 reflectivity are interpreted to be partly enhanced by post-collisional injection of mafic melts in the lower crust that may have been triggered in the last stages of the continental tectonic assembly of the western Canadian Shield (Figure 45D). The MHB crust preserves no geometric evidence for its tectonic involvement in the Early Proterozoic crustal shortening associated with the Trans-Hudson orogen and Hearne Province to the northeast (see Ross et al. 1995). Hence, the boundary between the MHB and Trans-Hudson orogen to the east most likely is not compressional. The resultant continent, named Laurentia, was subjected to Middle Proterozoic to Early Cambrian rifting and passive margin formation that established the limits of the present North American craton (Hoffman 1989).

### 5.5 Relationship of extensional faulting to Medicine Hat Block

According to the extensive seismic reflection profile along the Alberta basement corridor (SALT, CAT and PRAISE), extensional faulting of the Western Canada Sedimentary Basin (WCSB) only occurs in the Peace River Arch area and the southern Alberta region (Hope et al. 1999). Furthermore, the work presented here, together with available studies on extensional faulting of the WCSB in southern Alberta, show that faulting in southern Alberta appears to be concentrated in the western half of the MHB and roughly east of Fault 1 (Figures 5, 6 and 41). Although this study lacks seismic reflection data elsewhere, the distribution of extensional faults within the MHB gives

pause to question the role and character of the lithosphere during periods of tectonism in southern Alberta. Could the rigid crust of the MHB have influenced and concentrated the distribution of Phanerozoic extensional faults in southern Alberta? The geographic extent of the MHB roughly corresponds with Montania, a paleotopographic high persistently active from Belt deposition (~1.4 Ga) through the Paleozoic, first described by Deiss (1941). Provenance studies on arkosic units of the Late Proterozoic Windermere Supergroup and the basal Devonian using U-Pb geochronology indicate that the northern and northwestern margins of Montania are of 1.74-1.86 Ga and 2.88-3.21 Ga, which correspond to Rimbey belt and MHB ages, respectively (Figures 1 and 2; Ross 1995). Hence, the MHB appears to have acted as a topographic/isostatic high from the Middle Proterozoic through the Paleozoic. The presence of the MHB as a rigid topographic high may have been instrumental in the development and distribution of extensional faults during the Phanerozoic in southern Alberta.

# CHAPTER 6. CONCLUSIONS

The detailed study of the Lithoprobe SALT seismic reflection dataset in combination with numerous geophysical data has helped to uncover significant aspects of the Archean Medicine Hat Block (MHB) crustal structure, as well as its tectonic and temporal relationship with adjacent crustal domains throughout the Precambrian. In light of the geometric constraints established from the seismic reflection data, gravity modeling and bandpass filtering of potential-field data, in addition to the published geochronological and seismic refraction studies, the MHB crust is interpreted to have undergone at least two episodes of crustal deformation in the Precambrian: (1) Late Archean formation of the MHB crust by continental collision of two Archean domains along a crustal-scale ramp; and (2) Early Proterozoic crustal shortening associated with the formation of the Vulcan structure, the delamination of the Loverna Block crust and post-collisional injection of mafic melts beneath the MHB crust. The Early Proterozoic crustal shortening within the MHB crust is coeval with the development of the Trans-Hudson orogen to the east and the formation of the east Alberta orogen to the north, denoting a remarkable period of micro-continental amalgamation in the assembly of the western Canadian Shield.

The subsurface structural analysis of the WCSB in southern Alberta revealed the presence of five significant faults that occur from ~52 km to ~140 km east of the Cordilleran triangle zone. The westernmost fault (Fault 1) is interpreted as a west-dipping compressional fault (an inverted down-to-the-west extensional fault), whereas the remaining faults (Fault 2 to 5) are down-to-the-west extensional faults. The seismic reflection expression of these faults shows a break in reflections for the lower sedimentary section with folding of the upper sedimentary section. The near-basement and Lower Paleozoic strata (Cambrian and Devonian) are interpreted to be cut by master extensional faults, whereas overlying Mississippian, Jurassic and Cretaceous strata are interpreted to deform in a more distributed fashion, accommodating the formation of extensional forced folds above the master extensional faults.

Horizontal uppermost Upper Cretaceous (Belly River Group and younger) strata are undisturbed by Fault 5, which constrains the age of the youngest extension to pre-Belly River (Campanian) age. West of Fault 5, forced folding of Belly River Group strata and younger (Faults 1 to 4) indicates that extension and foreland basin development

was continuous, possibly through the Paleocene, in response to thrust loading of the Cordilleran orogen. The faults show evidence for multiple reactivations throughout the Paleozoic and Mesozoic including onlap features interpreted as growth strata and thickness changes across the faults. The regional strike of the extensional faults appears to be northwest-southeast, which agrees with basement fabric trends inferred from the magnetic signature of the Archean MHB. The similarity between basement fabric trends and the strike of extensional faulting suggests that basement structure may have reactivated and controlled the positioning of the extensional faults observable on the SALT dataset and in the vicinity (Fort MacLeod and Lethbridge regions).

Extensional faulting had a significant impact in the development of the Western Canada Sedimentary Basin throughout the Phanerozoic, and hence, has major implications for hydrocarbon exploration. As an example, Fault 2 represents a significant depositional hinge for extension in Jura-Cretaceous time, as the dramatic thickening on its west side provided control of Cretaceous shorelines (e.g., conglomerates from the Viking Formation, M. Teitz, personal communication 1999). Finally, multiple reactivations of extensional faulting may be significant for reservoir enhancement and structural trapping of hydrocarbons. However, the major significance of these reactivated faults may well be their possible effect on the total basinwide fluid flow, because they can either act as lateral seals or vertical conduits. The seismic reflection method provides the location and orientation of these faults. Other methods will have to be used to assess their hydrodynamic properties.

## REFERENCES

Allmendinger, R.W., Nelson, K.D., Potter, C.J., Barazangi, M., Brown, L.D., and Oliver, J.E., 1987. Deep seismic reflection characteristics of the continental crust. Geology, 15, p.304-310.

Bally, A.W., Gordy, P.L., and Stewart, G.A., 1966. Structure, seismic data, and orogenic evolutionof the southern Canadian Rocky Mountains. Canadian Society of Petroleum Geology Bulletin, 14, p.337-381.

Beaumont, C., 1981. Foreland basins. Geophysical Journal Royal Astronomical Society, v.65, p.291-329.

Beaumont, C., Quinlan, G.M., and Stockmal, G.S., 1993. The evolution of the western Interior Basin: causes, consequences, and unsolved problems. Geological Association of Canada Special Paper 39, p.97-117.

Boerner, D.E., Kurtz, R.D, Craven, J.A., and Jones, F.W., 1995. Electromagnetic results from the Alberta basement Lithoprobe Transect. In 1995 Alberta Basement Transects Workshop, G.M. Ross, editor. Lithoprobe Secretariat, University of British Columbia, Lithoprobe Report 47, p.35-45.

Boerner, D.E., Craven, J.A., Kurtz, R.D., Ross, G.M., and Jones, F.W., 1998. The Great Falls Tectonic Zone: suture or intracontinental shear zone? Canadian Journal of Earth Sciences, 35, p.175-183.

Bond, G.C. and Kominz, M.A., 1984. Construction of tectonic subsidence curves for the early Paleozoic miogeocline, southern Canadian Rocky Mountains: implications for subsidence mechanisms, age of break-up and crustal thinning. Geological Society of America Bulletin, v.95, p.155-173.

Bond, G.C. and Kominz, M.A., 1991. Disentangling middle Paleozoic sea level and tectonic events in cratonic margins and interior basins of North America. Journal of Geophysical Research, v.96, p.6619-6639.

Bradley, D.C. and Kidd, W.S.F., 1991. Flexural extension of the upper continental crust in collisional foredeeps. Geological Society of America Bulletin, v.103, p.1416-1438.

Buryanik, M.J.A., Bouzidi, Y., Phadke, S., and Kanasewich, E.R., 1997. Seismic velocity models and depth migration imaging of the Alberta basement. In 1997 Alberta Basement Transects Workshop, G.M. Ross (ed.), Lithoprobe Secretariat, University of British Columbia, Lithoprobe Report 59, p.9-14.

Burwash, R.A., 1957. Reconnaissance of subsurface Preambrian of Alberta. American Association of Petroleum Geologists Bulletin, v.41, p.70-103.

Burwash, R.A., Baadsgaard, H., and Peterman, Z.E., 1962. Precambrian K-Ar dates from the western Canada Sedimentary Basin. Journal of Geophysical Research, 67, p.1617-1625.

Burwash, R.A., McGregor, C.R., and Wilson, J., 1994. Chapter 5: Precambrian basement beneath the Western Canada Sedimentary Basin. *In:* Geological Atlas of the Western Canada Sedimentary Basin. G.P. Mossop, and I. Shetsen (comps.). Canadian Society of Petroleum Geologists and Alberta Research Council, Alberta Geological Survey, Calgary, p.50.

Carlson, R.W., and Irving, A.J., 1994. Depletion and enrichment history of subcontinental lithospheric mantle: An Os, Sr, Nd, and Pb isotopic study of ultramafic xenoliths from the northwestern Wyoming Craton. Earth and Planetary Science Letters, 126, p.457-472.

Chapman, T.J. and Meneilly, A.W., 1991. The displacement patterns associated with a reverse-reactivated, normal growth fault. *In:* The Geometry of Normal Faults. A.M. Roberts, G. Yielding, and B. Freeman (eds.). Geological Society Special Publication, no.56, p.183-192.

Christensen, N.I. and Mooney, W.D., 1995. Seismic velocity structure and composition of the continental crust: A global view. Journal of Geophysical Research, 100, p.9761-9788.

Clowes, R.M. (ed.), 1997. Chapter 3: Scientific program and achievements – Lithoprobe Phase IV, 3.7 Alberta Basement Transect. Lithoprobe Phase V Proposal – Evolution of a continent revealed. Published by the Lithoprobe Secretariat, The University of British Columbia, Vancouver, British Columbia, p.3.79-3.98.

Clowes, R.M. and Kanasewich, E.R., 1972. Digital filtering of deep crustal seismic reflections. Canadian Journal of Earth Sciences, 9, 4, p.434-451.

Collerson, K.D., Hearne, B.C., MacDonald, R.A., Upton, B.G.J., and Park, J.G., 1988. Granulite xenoliths from the Bearpaw Mountains, Montana: constraints on the character and evolution of lower continental crust. Terra Cognita, 8, p.270.

Cook, F.A., Varsek, J., and Clark, E., 1991. Proterozoic craton to basin transition in western Canada and its influence on the evolution of the Cordillera. Canadian Journal of Earth Sciences, 28, p.1148-1158.

Cooley, J.W., and Tukey, J.W., 1965. An algorithm for the machine calculation of complex Fourier series. Mathematical Computers, 19, p.297-301.

Davis, W.J., Berman, R., and Kjarsgaard, B., 1995. U-Pb geochronology and isotopic studies of crustal xenoliths from the Archean Medicine Hat Block, northern Montana and southern Alberta: Paleoproterozoic reworking of the Archean crust. In 1995 Alberta Basement Transects Workshop, G.M. Ross, editor. Lithoprobe Secretariat, University of British Columbia, Lithoprobe Report #47, p.330-335.

Dawson, G.M., 1875. Report on the geology and resources of the region in the vicinity of the forty-ninth parallel from the Lake of the Woods to the Rocky Mountains. Montreal.

Dawson, G.M. and McConnell, R.G., 1883. Report on the region in the vicinity of the Bow and Belly Rivers. Geological Survey of Canada.

de Graciansky, P.C., Darbeau, G., Lemoine, M., and Tricart, P., 1989. The inverted margin of the French Alps and foreland basin inversion. *In:* Inversion Tectonics. M.A. Cooper and G.D. Williams (eds.). Geological Society Special Publication, no.44, p.87-104.

Deiss, C., 1941. Cambrian geography and sedimentation in the central Cordilleran region. Geological Society of America Bulletin, 52, p.1085-1116.

Dobrin, M.B., 1976. Introduction to geophysical prospecting. Third Edition, McGraw-Hill Book Company Inc., New York, 630 pp.

Dobrin, M.B., and Savit, C.H., 1988. Introduction ot geophysical prospecting. Fourth Edition, McGraw-Hill Book Company Inc., New York, 867 pp.

Dowling, D.B., 1910. Southern Alberta Plains. Geological Survey of Canada, Memoir 93.

Eaton, D.W. and Ross, G.M., 1996. SALT and VAULT: Summary of data acquisition and processing over the Vulcan Low. *In:* 1996 Alberta Basement Transects Workshop. G.M. Ross (ed.). Lithoprobe Report #51, Lithoprobe Secretariat, University of British Columbia, p.1-10.

Eaton, D.W., Lemieux, S., and Ross, G.M., 1997. Regional seismic perspectives on the evolution of the Peace River Arch. *In:* 1997 Alberta Basement Transects Workshop. G.M. Ross (ed.). Lithoprobe Report #59, Lithoprobe Secretariat, University of British Columbia, p.91-111.

Eaton, D.W., Ross, G.M., and Clowes, R.M., 1999. Seismic-reflection and potential-field studies of the Vulcan structure, western Canada: A Paleoproterozoic Pyrenees?. Journal of Geophysical Research, in press.

Frost, C.D., 1993. Nd isotopic evidence for the antiquity of the Wyoming province. Geology, 21, p.351-354.

Gordy, P.L., Frey, F.R., and Norris, D.K., 1977. Geological guide for the CSPG 1977 Waterton-Glacier Park Field Conference. Canadian Society of Petroleum Geologists, Calgary, 93pp.

Hacquebard, P.A., 1977. Rank of coal as an index of organic metamorphism for oil and gas in Alberta. In: G. Deroo, T.G. Powell, B. Tissot, and R.G. Mc Grossan (eds.), The origin and migration of petroleum in the Western Canada Sedimentary Basin, Alberta: Geological Survey of Canada Bulletin 262, p.11-22.

Hanmer, S., 1990. Snowbird tectonic zone, N. Saskatchewan; geological window onto a 3000 km long geophysical anomaly. *In:* 1990 Trans-Hudson Orogen Transect. Z. Hajnal and J. Lewry (eds.). Lithoprobe Report #12, Lithoprobe Secretariat, University of British Columbia, p.38-39.

Hartman, R.R., Tesky, D.J., and Friedberg, L.L., 1971. A system for rapid digital aeromagnetic interpretation. Geophysics, vol. 36, p.891-918.

Hellwege, K.H. (ed. in chief), 1982. Landolt-Bornstein Numerical data and functional relationships in science and technology, New Series, Group V: Geophysics and Space Research, vol.1, Physical properties of rocks, Subvolume b, Springer-Verlag, Berlin, p.38-72.

Henstock, T.J., Levaner, A., Snelson, C., Keller, R., Miller, K.C., Harder, S.H., Gorman, A.R., Clowes, R.M., Buryanik, J.A., and Humphreys, E.D., 1998. Probing the Archean and Proterozoic Lithosphere of western North America. GSA Today, 8 (7), 1-5, p.16-17.

Hiebert, S.N., 1992. Deformational styles near the leading edgr of the fold-and-thrust belt, Pincher Creek, Alberta. M.Sc. thesis, unpublished, The University of Calgary, Calgary, Alberta.

Hiebert, S.N. and Spratt, D.A., 1996. Geometry of the thrust front near Pincher Creek, Alberta. Bulletin of Canadian Petroleum Geology, vol.44, no.2, p.195-201.

Hoffman, P.F., 1988. United Plates of America, the birth of a craton: Early Proterozoic assembly and growth of Proto-Laurentia. Annual Reviews of Earth and Planetary Science, 16, p.543-603.

Hoffman, P.F., 1989. Precambrian geology and tectonic history of North America. In: The geology of North America – an overview, (ed.) A.W. Bally and A.R. Palmer, Geological Society of America, The Geology of North America, v.A, p.447-512.

Hoffman, P.F., 1990. Subdivision of the Churchill Province and extent of the Trans-Hudson orogen. In: Lewry, J.F. and Stauffer, M.R. (eds.), The Early Proterozoic Trans-Hudson Orogen of North America, GAC Special Paper 37, p.15-39.

Hope, J., Eaton, D.W., and Ross, G.M., 1999. Lithoprobe seismic transect of the Alberta Basin: Compilation and overview. Bulletin of Canadian Petroleum Geology, vol.47, no.4, p.331-345.

Irish, E.J.W., 1967. Lethbridge (82H), Alberta-Geology (preliminary series); Geological Survey of Canada, Map 20-1967, scale 1:253 440.

Kalkreuth, W. and McMechan, M., 1988. Burial history and thermal maturity, Rocky Mountain Front Ranges, Foothills, and Foreland, east-central British Columbia and adjacent Alberta, Canada. The American Association of Petroleum Geologists Bulletin, v.72, no.11, p.1395-1410.

Kanasewich, E.R., Clowes, R.M. and McCloughan, C.H. 1969. A buried Precambrian rift in western Canada, Tectonophysics, 8, p.513-527.

Kane, M.F. and Godson, R.H., 1985. Features of a pair of long-wavelength (>250 km) and short-wavelength (<250 km) Bouguer gravity maps of the United States. In: W.J. Hinze (ed.), The utility of regional gravity and magnetic anomaly maps. Society of Exploration Geophysicists, Tulsa, Oklahoma, p.46-61.

Kovaric, D.N., Brady, J.B., Cheney, J.T., Grove, M., Jacob, L.J., and King, J.T., 1996. $^{40}Ar/^{39}Ar$ evidence for reheating events affecting basement rocks in the Tobacco Root, Ruby and Highland Mountains, southwestern Montana. Geological Society of America, Abstracts with Programs, 28, A493.

Krogh, T.E., 1982. Improved accuracy of U-Pb zircon ages by the creation of more concordant systems using an air abrasion technique. Geochimica et Cosmochimica Acta, v.46, p.637-649.

Lash, G.G., 1987. Geodynamic evolution of the lower Paleozoic central Appalachian foreland basin. *In:* Sedimentary basins and basin-forming mechanisms. C. Beaumont and A.J. Tankard (eds.). Canadian Society of Petroleum Geologists Memoir 12, p.413-424.

Lebel, D., 1996. Raley (82H/6), Alberta-Geology (preliminary); Geological Survey of Canada, Open File Map 3363, scale 1:50 000.

Leckie, D.A., 1989. Upper Zuni sequence: Upper Cretaceous to Lower Tertiary. *In:* Chapter 11. Zuni sequence: The foreland basin. Western Canada Sedimentary Basin: A case history. B.D. Ricketts (ed.). Canadian Society of Petroleum Geologists, Geological Survey of Canada, Calgary, p.269-284.

Lemieux, S., Cook, F.A., .J., and Ross, G.M., 2000. Crustal geometry and tectonic evolution of the southern Alberta basement, the Archean Medicine Hat Block, western Canadian Shield. In review by the Canadian Journal of Earth Sciences.

Lemieux, S., 1999. Seismic reflection expression and tectonic significance of Late Cretaceous extensional faulting of the Western Canada Sedimentary Basin in southern Alberta. Bulletin of Canadian Petroleum Geology, vol.47, no.4, p.375-390.

Lerand, M.M., 1983. Sedimentology of the Blood Reserve sandstone in southern Alberta. Canadian Society of Petroleum Geologists Guidebook.

Lillie, R.J., Johnson, G.D., Yousuf, M., Zamin, A.S.H., and Yeats, R.S., 1987. Structural development within the Himalayan foreland fold-and-thrust belt of Pakistan. *In:* Sedimentary basins and basin-forming mechanisms. C. Beaumont and A.J. Tankard (eds.). Canadian Society of Petroleum Geologists Memoir 12, p.379-392.

Magara, K. 1976. Thickness of removed sedimentary rocks, paleoporepressure and paleotemperature, southwestern part of the western Canada basin. American Association of Petroleum Geologists Bulletin, v.60, p.554-565.

Mandler, H.A.F. and Clowes, R.M., 1998. The HSI bright reflector: further evidence for extensive magmatism in the Precambrian of western Canada. Tectonophysics, 00, p.1-11.

Monger, J.W.H., 1989. Chapter 2: Overview of Cordilleran geology. *In:* Western Canada Sedimentary Basin: A case history. B.D. Ricketts (ed.). Canadian Society of Petroleum Geologists, Geological Survey of Canada, Calgary, p.9-32.

Mossop, G.P. and Shetsen, I. (comps.), 1994. The Geological Atlas of the Western Canada Sedimentary Basin. P. Canadian Society of Petroleum Geologists and Alberta Research Council, Alberta Geological Survey, Calgary, 510 pp.

Mueller, P.A., Shuster, R.D., Wooden, J.L., Erslev, E.A., and Bowes, D.R., 1993. Age and composition of Archean crystalline rocks from the southern Madison Range, Montana: Implications for crustal evolution in the Wyoming craton. Geological Society of America Bulletin, 105, p.437-446.

Mueller, P.A., Shuster, R.D., D'Arcy, K.A., Heatherington, A.L., Nutman, A.P., and Williams, I.S., 1995. Source of the northeastern Idaho Batholith: isotopic evidence for a Paleoproterozoic terrane in the northwestern United States. The Journal of Geology, 103, p.63-72.

Mueller, P.A., Heatherington, A., Wooden, J., Mogk, D., and Nutman, A., 1996. Proterozoic evolution of the northwestern Wyoming Craton. Geological Society of America, Abstracts with Programs, 28, A314.

Okulitch, A.V., Lopez, D.A., and Jerzykiewicz, T. (comps.), 1996. Geology, Lethbridge, Alberta-Saskatchewan-Montana. Geological Survey of Canada, Map NM – 12 – G, scale 1:1 000 000 (National Earth Science Series, Geological Atlas).

O'Neill, J.M., and Lopez, D.A., 1985. Character and regional significance of the Great Falls Tectonic Zone, east-central Idaho and west-central Montana. American Association of Petroleum Geologists Bulletin, 69, p.437-447.

Pollard, D.D., Muller, O.H., and Dockstader, D.R., 1975. The form and growth of fingered sheet intrusions. Geological Society of America Bulletin, 86, p.351-363.

Press, F., and Siever, R., 1986. Earth. Fourth Edition, W.H. Freeman and Company, New York, 656 pp.

Roddick, J.C., Loveridge, W.D., and Parrish, R.R., 1987. Precise U/Pb dating at the subnannogram Pb level. Chemical Geology, v.66, p.111-121.

Ross, G.M., 1991. Tectonic setting of the Windermere Supergroup revisited. Geology, v.19, p.1125-1128.

Ross, G.M., 1995. Detrital mineral U-Up geochronology and provenance of Neoproterozoic and Devonian arenites, southeastern British Columbia: mapping the shoulders of Montania. In: 1995 Alberta Basement Transects Workshop. G.M. Ross (ed.). Lithoprobe Report #47, Lithoprobe Secretariat, University of British Columbia, p.53-96.

Ross, G.M., 1997. Assembly of the southwestern Laurentian craton. In: 1997 Alberta Basement Transects Workshop. G.M. Ross (ed.). Lithoprobe Report #59, Lithoprobe Secretariat, University of British Columbia, p.23-34.

Ross, G.M. and Stephenson, R.A., 1989. Crystalline basement: the foundation of Western Canada Sedimentary Basin. Chapter 3 in B.D. Ricketts (ed.) Western Canada Sedimentary Basin: A case history, Canadian Society of Petroleum Geologists, p.33-46.

Ross, G.M., Parrish, R.R., Villeneuve, M.E., and Bowring, S.A., 1991. Geophysics and geochronology of the crystalline basement of the Alberta basin, western Canada. Canadian Journal of Earth Sciences, 28, p.512-522.

Ross, G.M., Milkereit, B., Eaton, D., White, D., Kanasewich, E.R., and Burianyk., 1995. Paleoproterozoic collisional orogen beneath the Western Canada Sedimentary Basin imaged by Lithoprobe crustal seismic-reflection data. Geology, 23, p.195-199.

Ross, G.M., Mariano, J., Dumont, R., Kjarsgaard, B.A., and Teskey, D., 1997. Was Eocene magmatism widespread in the subsurface of southern Alberta? Evidence from new aeromagnetic anomaly data. *In:* Exploring for minerals in Alberta: Geological Survey of Canada, Canada-Alberta agreement on mineral development (1992-1995). R.W. Macqueen (ed.). Geological Survey of Canada Bulletin 500, p.235-246.

Ross, G.M. and Eaton, D.W., 1999. Basement reactivation in the Alberta Basin: Observational constraints and mechanical rationale. Bulletin of Canadian Petroleum Geology, vol.47, no.4, p.391-411.

Rudnick, R.L., and Fountain, D.M., 1995. Nature and composition of the continental crust: A lower crustal perspective. Reviews of Geophysics, 33, p.267-309.

Russell, L.S. and Landes, R.W., 1940. Geology of the Southern Alberta Plains. Geological Survey of Canada, Department of Mines and Resources, Mines and Geology Branch, Bureau of Geology and Topography, Memoir 221, p.1-128.

Sheriff, R.E., 1991. Encyclopedic dictionary of exploration geophysics. Society of Exploration Geophysicists, Tulsa, 376 pp.

Skuce, A.G., Goody, N.P., and Maloney, J., 1992. Passive-roof duplexes under the Rocky Mountain foreland basin, Alberta. American Association of Petroleum Geologists Bulletin, v.76, p.67-80.

Stockmal, G.S. and Beaumont, C., 1987. Geodynamic models of convergent margin tectonics: the southern Canadian Cordillera and the Swiss Alps. *In:* Sedimentary basins and basin-forming mechanisms. C. Beaumont and A.J. Tankard (eds.). Canadian Society of Petroleum Geologists Memoir 12, p.393-412.

Thomas, M.D., Sharpton, V.L. and Grieve, R.A.F., 1987. Gravity patterns and Precambrian structure in the North Central Plains, Geology, 15, p.489-492.

Ulrych, T.J., 1968. Effect of wavelength filtering on the shape of the residual anomaly. Geophysics, vol.33, p.1015-1018.

van der Velden, A.J. and Cook, F.A., 1996. Structure and tectonic development of the southern Rocky Mountain Trench. Tectonics, 15, 3, p.517-544.

Vasudevan, K., Cook, F.A., Ross, G.M., and Kelsh, L., 1995. Structure of the Medicine Hat Block, Taber area, southern Alberta-insights from reprocessing of industry seismic reflection data. In 1995 Alberta Basement Transects Workshop, G.M. Ross, editor. Lithoprobe Secretariat, University of British Columbia, Lithoprobe Report 47, p.9-21.

Villeneuve, M.E., Ross, G.M., Parrish, R.R., Theriault, R.J., Miles, W., and Broome, J., 1993. Geophysical subdivision, U-Pb geochronology and Sm-Nd isotope geochemistry of the crystalline basement of the Western Canada Sedimentary Basin, Alberta and northeastern British Columbia. Geological Survey of Canada, Bulletin 447, 86 pp.

White, R.J. (ed.), 1960. Oil fields of Alberta: A reference volume, The Alberta Society of Petroleum Geologists, p.90-91.

Williams, G.D., Powell, C.M., and Cooper M.A., 1989. Geometry and kinematics of inversion tectonics. *In:* Inversion Tectonics. M.A. Cooper and G.D. Williams (eds.). Geological Society Special Publication, no.44, p.3-15.

Williams, M.Y., Dyer, W.S., Whittaker, E.J., and Warren, P.S., 1930. Geology of the southern Alberta and southwestern Saskatchewan. Geological Survey of Canada, Memoir 163.

Withjack, M.O., Olson, J., and Peterson, E., 1990. Experimental models of extensional forced folds. American Association of Petroleum Geologists Bulletin, v.74, p.1038-1054.

Wright, G.N., McMechan, M.E., and Potter, D.G., 1994. Chapter 3: Structure and architecture of the Western Canada Sedimentary Basin. In: Geological Atlas of the Western Canada Sedimentary Basin. G.P. Mossop and I. Shetsen (comps.). Canadian Society of Petroleum Geologists and Alberta Research Council, Alberta Geological Survey, Calgary, p.25-40.